DEUTERIUM NMR INVESTIGATIONS OF A MODEL MEMBRANE CONTAINING PHYTANIC ACID AND PHYTOL

by

JUNSHI YUE

M.Sc., SHANGHAI INSTITUTE OF ORGANIC CHEMISTRY,
ACADEMIA SINICA, SHANGHAI CHINA, 1982

THESIS SUBMITTED IN PARTIAL FULFILLMENT OF
THE REQUIREMENTS FOR THE DEGREE OF
DOCTOR OF PHILOSOPHY
in the Department
of
CHEMISTRY

SIMON FRASER UNIVERSITY

JAN 1991

APPROVAL

Name: JUNSHI YUE

Degree: DOCTOR OF PHILOSOPHY

Title of thesis: **DEUTERIUM NMR INVESTIGATION OF A MODEL MEMBRANE CONTAINING PHYTOL AND PHYTANIC ACID**

Examining Committee: Chairman: Dr. D. Sutton

Dr. R. J. Cushley
Senior Supervisor

Dr. A. C. Oehlschlager
Supervisory Committee

Dr. R. Cornell
Supervisory Committee

Dr. D. H. Boal
Internal Examiner
Department of Physics

Dr. E. E. Burnell
External Examiner
Department of Chemistry
University of British Columbia

Date Approved: Jan. 28, 1991

PARTIAL COPYRIGHT LICENSE

I hereby grant to Simon Fraser University the right to lend my thesis, project or extended essay (the title of which is shown below) to users of the Simon Fraser University Library, and to make partial or single copies only for such users or in response to a request from the library of any other university, or other educational institution, on its own behalf or for one of its users. I further agree that permission for multiple copying of this work for scholarly purposes may be granted by me or the Dean of Graduate Studies. It is understood that copying or publication of this work for financial gain shall not be allowed without my written permission.

Title of Thesis/Project/Extended Essay

Deuterium NMR investigations of a model membrane containing phytanic acid and phytol

Author: _____
(signature)

Junshi Yue
(name)

Jan. 28, 1991
(date)

ABSTRACT

The phase behavior of model membranes containing branched chain compounds (phytol, phytanic acid) has been studied using deuterium nuclear magnetic resonance spectroscopy (^{2}H NMR) and differential scanning calorimetry (DSC). The model membrane systems were 50 wt% dispersions of 1-palmitoyl(stearoyl)-2-[$^2H_{31}$]palmitoyl-sn-glycero-3-phosphocholine (PC-d_{31}) containing phytol or phytanic acid in deuterium depleted water (DDW) and 15 wt% dispersions of 1,2-dipalmitoyl-sn-glycerol-[α,β-$^2H_4$] phosphocholine (DPPC-d_4) containing phytol or phytanic acid in DDW or "Tris buffer" (25 mM, pH 7.4, in DDW). Either branched chain compound broadens the gel to liquid crystalline phase transition of the phospholipid membrane and reduces the onset temperature of the transition, indicating that the branched chain compound causes significant disruption of the gel phase. The pretransition is clearly observed in the ^{2}H NMR temperature studies of DPPC-d_4. Order parameters, S_{CD}, for various chain positions have been calculated. At 50^{0}C there is no significant change in the profile of S_{CD} versus phospholipid acyl chain position, induced by either branched chain compound. Either branched chain compound (20 mol%) causes an approximate 9% increase in the mean order parameter $\langle S_{CD} \rangle$. In the liquid crystalline phase, phytol induces more random movement of the head group while phytanic acid causes a

conformational change of the choline group which can be explained by the negative charge density due to the ionization of the acid on the membrane surface. The effect of branched chain compounds on the lateral diffusion of phospholipid has been studied using a DANTE pulse sequence. Deuterium spin-lattice relaxation times (T_1) and spin-spin relaxation times (T_{2e}, the decay of the quadrupolar echoes) have been measured over a wide temperature range. 20 Mol% phytol increases T_1 in the plateau region (carbons 3-10 on sn-2 chain) by 11% at the same reduced temperature. The increase of T_1 by branched chain compounds is essentially due to the phase transition temperature depression. T_{2e} depends very much on the method of sample preparation and the morphology of the resulting liposomes. The presence of 20 mol% phytanic acid results in orientation of the DPPC bilayer in the magnetic field as shown by ^{2}H and ^{31}P NMR. The sample must be carried through several freeze-thaw cycles in the presence of Tris buffer in order that the phospholipid magnetic field ordering occurs. Possible explanations for the effect of phytol and phytanic acid on the dynamic structure of both hydrophilic and hydrophobic regions of phospholipids in the bilayer are suggested.

DEDICATION

To Bicheng and Bizheng

ACKNOWLEDGEMENTS

I am grateful to my supervisor, Dr. R. J. Cushley, for his guidance, advice and encouragement during the course of this study. I also wish to thank Dr. A. C. Oehlschlager, Dr. B. L. Funt and Dr. R. Cornell for their efforts and time as members of my supervisory committee.

I also wish to thank Dr. J. C. Irwin (Physics Department, SFU) for the use of his DSC facility and Dr. K. K. Nair (Biological Sciences Department, SFU) for the use of his Phase Contrast Microscope.

Thanks also due to the present and past members of Dr. Cushley's group for their cooperation, discussion and fellowship. In particular Drs. W. D. Treleaven and J. T. Thewalt provided assistance with many aspects of this study.

Financial support from Simon Fraser University, Chemistry Department and from Dr. Cushley is gratefully acknowledged.

Finally, I wish to thank my husband, Dr. Z. Z. Wu, for his encouragement during the course of this study.

TABLE OF CONTENTS

LIST OF TABLES

LIST OF FIGURES

LIST OF ABBREVIATIONS

^{2}H NMR, deuterium nuclear magnetic resonance;
^{31}P NMR, phosphorus-31 nuclear magnetic resonance;
CSA, chemical shift anisotropy;
DSC, differential scanning calorimetry;
EFG, electric field gradient;
ESR, electron spin resonance;
QELS, quasi-elastic light scattering;
PC, phosphatidylcholine;
PE, phosphatidylethanolamine;
egg PC, egg phosphatidylcholine;
DMPC, 1,2-dimyristoyl-sn-glycero-3-phosphocholine;
DPPC, 1,2-dipalmitoyl-sn-glycero-3-phosphocholine;
SPPC, 1-stearoyl-2-palmitoyl-sn-glycero-3-phosphocholine;
POPC, 1-palmitoyl-2-oleoyl-sn-glycero-3-phosphocholine;
POPG, 1-palmitoyl-2-oleoyl-sn-glycero-3-phosphoglycerol;
lysoPC, lysophosphatidylcholine;
PC-d_{31}, 1-palmitoyl(stearoyl)-2-[$^{2}H_{31}$]palmitoyl-sn-glycero-3-phosphocholine;
DPPC-d_{4}, 1,2-dipalmitoyl-sn-glycero-[α,β-$^{2}H_{4}$]phosphocholine;
CDI, 1,1'-carbonyldiimidazole;
DDW, deuterium depleted water;
DMSO, dimethylsulfoxide;
EDTA, ethylenediaminetetraacetic acid;
LCAT, lecithin:cholesterol acyl transferase;
PIPES, piperazine-N,N'-bis[2-ethanesulfonic acid];
THF, tetrahydrofuran;

I. Introduction

Membranes are basic structural units of living systems, forming the boundaries of cells and intracellular organelles, providing a framework for many physiological processes. Biological membranes contain a wide variety of chemical species, of which lipids, proteins and carbohydrates are the major ones (Harrison and Lunt, 1980). Model membranes, prepared from lipids, are well-suited subjects of investigation in order to elucidate the physical properties of biological membranes. Considerable interest has focussed on the structures and properties of the lipid bilayer and the lipid-protein interactions in the bilayer. Glycerophospholipids are the most commonly found membrane lipids, of which phosphatidylcholine (PC) is the most extensively used in model membrane studies. When phospholipids are shaken in an aqueous phase, large multilamellar liposomes (>2000 Å in diameter), composed of concentric bilayers, are formed spontaneously (Bangham and Horne, 1964). The treatment of these liposomes with ultrasonic radiation leads to the formation of vesicles which are sealed unilamellar structures with an average diameter of ≈250 Å (Sheetz and Chan, 1972), (Figure 1). Both multilamellar liposomes and vesicles are commonly used in the investigation of membrane structure. In cellular membrane the long-chain hydrocarbon attached to the

Figure 1: Schematic structures of liposomes and vesicles.

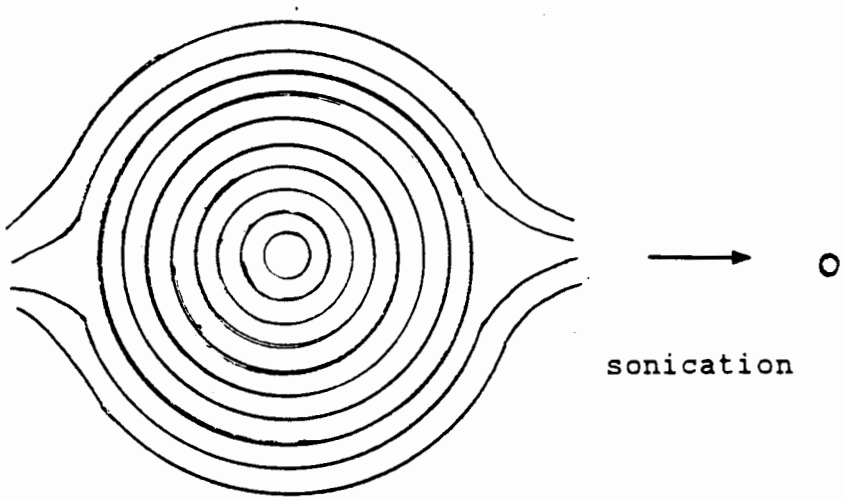

d ≈ 10,000Å
τ ≈ 1sec

multilamellar liposomes

d ≈ 250Å
τ ≈ 10^{-6}sec

vesicles

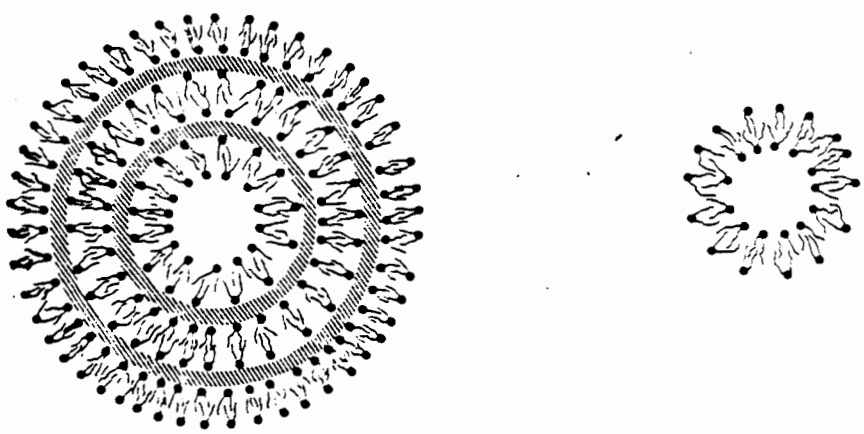

τ = correlation time for tumbling

sn-1 position of glycerol is usually a saturated acyl chain, while the hydrocarbon attached to the *sn*-2 position can be saturated, cis-unsaturated, or sometimes branched. Most model membrane studies were carried out on the lipids with linear acyl chains, however, the lipids with branched acyl chains have gained more attention lately (Dufourc et *al.*, 1984; Silvius et *al.*, 1985; Nuhn *et al.*, 1986; Lewis et *al.*, 1987a; Gutknecht, 1987, 1988).

Recently, several studies have appeared on membrane lipids containing multi-methyl branched chains joined to glycerol through either ether linkage (Aoki and Poilter, 1985; van Boeckel et *al.*, 1984) or ester linkage (Debose et *al.*, 1985; Pownall et *al.*, 1987). The membrane lipids of higher organisms contain almost exclusively linear acyl and alkyl hydrocarbon chains, the membrane lipids of a variety of prokaryotes contain large amounts of branched acyl chains (Kanada, 1977). For example, 2,3-di-*O*-phytanyl-*sn*-glycerol occurs in archaebacterial membranes and is one of the features distinguishing archaebacteria from eubacteria and eukaryotes. DeBose et *al.* (1985) and Pownall *et al.* (1987) have investigated the effect of branched chain phospholipids on enzyme activity. The authors have found that PCs with branching in both acyl chains were unreactive to phospholipase A_2 and human lecithin:cholesterol acyltransferase.

Amphipathic isoprenoid compounds characterized by long branched chains are an important series of biologicals. These

include retinol (vitamin A), D-α-tocopherol (main constituent of vitamin E), vitamin K, ubiquinone (coenzyme Q) and phytanic acid. As well, the esterified form of phytol is the side chain which anchors the chlorophyll molecule to the thylakoid membrane.

We have been interested in the effects of three isoprenoids, phytol, α-tocopherol (Vitamin E) and phytanic acid, upon membranes. The physiology of these compounds is well understood. The most important one of the above three compounds is Vitamin E, which functions as an antioxidant, protecting unsaturated lipids from free radical attack (Tappel, 1962; Sebrell *et al.*, 1972; Scott, 1978). Phytanic acid has been found to be a factor in the progression of Refsum's disease. An accumulation of phytanic acid up to 50% of the total fatty acid content has been found in the tissues, and up to 200 mg per 100 ml in the blood, of patients with this disease (Kahlke, 1964). The patients are unable to α-oxidize phytanic acid or similar branched chain fatty acids (Steinberg *et al.*, 1967). The relationship between accumulation of phytanic acid and the neuropathological changes is unclear yet. It has been speculated that the high degree of branching in this acid could lead to changes in the characteristics of myelin or other membranes, and it might be a causative factor in the degeneration of the nervous system which eventually leads to death (MacBrinn and O'Brien, 1968). Gutknecht (1987,1988) has recently reported the effects of

Figure 2: Structure of isoprenoid compounds and deuterated phospholipid used in the study.

phytol

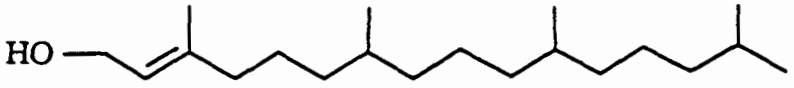

phytanic acid

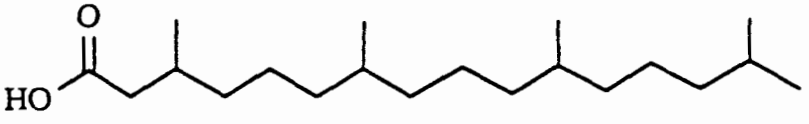

1-palmitoyl(stearoyl)-2-[D_{31}]-palmitoyl-sn-glycero-3-physphocholine ($PC\text{-}d_{31}$)

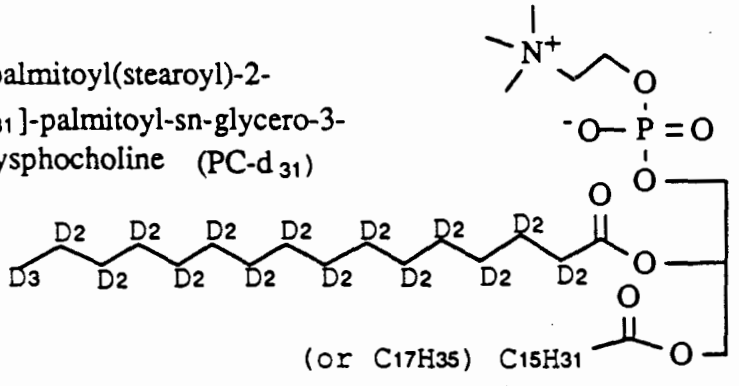

1,2-dipalmitoyl-sn-[$\alpha,\beta\text{-}D_4$]phosphatidylcholine ($DPPC\text{-}d_4$)

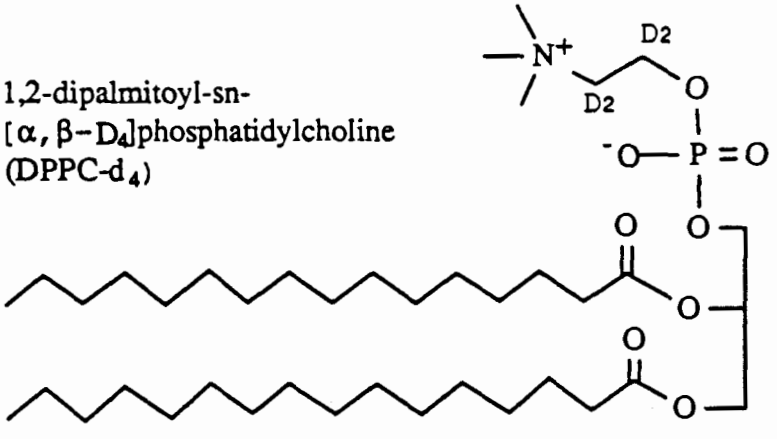

long-chain fatty acids on the proton/hydroxide conductance through phospholipid bilayer membranes, and the author has suggested that the fatty acids act as simple (A^- type) proton carriers, this increases the proton conductance of planar bilayers. His results elucidate that phytanic acid has a twice greater effect than the similar linear fatty acids do. The mechanism of fatty acid toxicity is suggested to be partially due to the increased proton conductance.

Moreover, a number of observations have been made linking a common effect owing to the isoprenoid side chain compounds, which suggests that these compounds may play a structural role in membranes. For instance, succinic-cytochrome c reductase, which has been inactivated by its extraction from porcine liver, is reactivated not only by Vit.E, but also by 6-O-acetyl-α-tocopherol, phytanic acid and phytol (Weber et al., 1958). Numerous studies on the effect of α-tocopherol on phospholipid membranes have been reported. However many of them are restricted to a qualitative discussion and some of the results are quite conflicting (see reviews in Wasssall et al., 1986). For example, the permeability of the bilayer was reported to be increased (Cushley and Forrest, 1977; Srivastava et al., 1983) and decreased (Diplock et al., 1977; Stillwell and Bryant, 1983) by the incorporation of α-tocopherol. Another conflicting example regards the interactions between projecting methyl groups of the phytyl chain of α-tocopherol and the 'pockets' present in the

polyunsaturated phospholipids of membranes. Diplock and Lucy (1973) and Maggio et *al*. (1977) suggested the existance of such interactions. Erin et *al*. (1984) have shown the formation of a complex between α-tocopherol and fatty acid using ultraviolet absorption and fluorescence spectra. The equilibrium constant for the formation is very high if the fatty acid is unsaturated. Skrypin et *al*. (1984) have found by using differential scanning calorimetry (DSC) that α-tocopherol protects the 1,2-dipalmitoyl-sn-glycero-3-phosphocholine (DPPC) bilayer from the destructive action of linoleic acid. However, Urano et *al*. (1987) have suggested that no special interaction exists between projecting methyl of α-tocopherol and the 'pockets' of the unsaturated phospholipid using ^{13}C NMR T_1 measurements. In spite of the extensive studies of the effects of α-tocopherol on membrane structure in the past decades, little attention has been paid to the effects of phytol and phytanic acid on membrane structure, although they have a similar side chain structure to α-tocopherol and are physiologically important in themselves.

Preliminary investigations on the effects of phytol, α-tocopherol and phytanic acid on the structure and function of egg yolk lecithin (EYL) model membranes have been carried out previously in this laboratory (Cushley et *al*., 1976, 1977, 1979). Using ESR, ^{31}P NMR and ^{13}C NMR, the authors found that branched compounds induce a low order, high fluidity and high

permeability of EYL bilayer.

For the evaluation of membranes' detailed organization on a molecular level, magnetic resonance techniques have become an important tool. This is particularly true for deuterium NMR which has proved to be a powerful technique in studying structure and dynamic properties of membranes (Seelig and Seelig, 1980; Jacobs and Oldfield, 1981; Davis, 1983; Bloom and Smith, 1985). Due to the low natural abundance of the deuterium isotope, preparation of deuterated phospholipid is required for ^{2}H NMR measurement. Employing specifically deuterated phospholipids enables the investigation to be focused on any part of the lipid bilayer system. Due to the strong quadrupolar interaction, the ^{2}H NMR spectrum for multilamellar bilayers is simple, and the orientation of the C-D bond with respect to the axis of molecular motion can be measured directly. This is the advantage of ^{2}H NMR over the conventional proton or carbon NMR, since the ^{1}H and ^{13}C NMR spectra for multilamellar membranes are usually very complicated, caused by the strong dipolar interactions. Furthermore, quadrupolar and dipolar interactions are expected to be the two contributions to the relaxation in deuterated systems. Because of the large quadrupole moment of the deuteron and small nuclear gyromagnetic ratio, the quadrupolar interaction is expected to dominate the relaxation processes. The interaction of a quadrupole moment and the electric field gradient is time dependent due to the molecular reorientation

(Seelig, 1977). Thus, the advantage of ^{2}H NMR over other NMR techniques is that ^{2}H NMR easily detects anisotropic motions, so it can directly measure the order of molecules in membranes, and that ^{2}H NMR relaxation time is dominated by quadrupolar interaction, so it measures the dynamic properties of the membrane.

Almost the same information can be obtained from Electron Spin Resonance (ESR) using spin labels, which is a more sensitive method. The ESR order parameter is easily determined from the anisotropy of hyperfine splitting, while the correlation time can be deduced from the linewidth (Seelig, 1976). The ESR spectrum of spin labelled membranes is influenced by the amplitude of anisotropic motion of the nitroxide group and by the geometry of the oxazolidine ring of the nitroxide (Taylor and Smith, 1983). However, the attachment of a bulky nitroxide spin label causes severe steric interaction and the order parameter may not reflect the order in the natural membrane. Compared with the spin label ESR technique, deuterium-labelling takes a great advantage of the identity of the van der Waals radii between ^{1}H and ^{2}H; in other words, deuterium substitution does not alter membrane structure. Therefore ^{2}H NMR is a sterically non-perturbing probe technique.

The investigation in this thesis has focussed on the studies of the dynamic structures of membranes incorporated with phytanic acid or phytol by using ^{2}H NMR technique. The

phospholipids used in model membrane systems are phosphocholine with two saturated acyl chains, PC-d_{31} and DPPC-d_4, as shown in Figure 2. The reasons of choosing these two PCs are that DPPC is stable and the most common phospholipid used in model membrane studies, and that the DPPC membrane has a gel-liquid crystalline phase transition temperature at 42^{0}C. Thus we can easily investigate the system over a wide temperature range and in different phases.

The gel-liquid crystalline phase transition is a first-order thermotropic transition. At the transition temperature the hydrocarbon chains of the phospholipid undergo a transition from an ordered crystalline-like state to a more disordered liquid-like state. In the gel phase the hydrocarbon chains are fully extended, tilted with respect to the plane of bilayer, and packed in a quasi-hexagonal lattice; whereas in the liquid crystalline phase the hydrocarbon chains melt assuming a liquid-like conformation, the average orientation of the chains is perpendicular to the plane of bilayer, and the chains are packed in a regular hexagonal lattice. Certain phospholipids, e.g., phosphatidylethanolamine (PE) may form a different structure other than a lamellar-bilayer structure in the liquid crystalline phase. In fact, the bilayer structure is the most important one, because it represents the natural membrane. Natural membranes contain a complex mixture of lipids, sterols and proteins. Their phase transition is not as sharp as those of synthetic phospholipid. However, the

hydrocarbon chains in natural membranes are believed to be generally in a liquid-like state at physiological temperatures (Harrison and Lunt, 1980).

Deuterium NMR is the major technique in this study. Although phosphorus NMR is less informative, it is used in some cases. Differential scanning calorimetry is another tool to measure the phase behavior of the model membranes. The effects of branched chain compounds have been studied as three aspects: (1) on the hydrophobic region of the bilayer, (2) on the hydrophilic region, (3) on the diffusion properties of phospholipids in bilayer. Chapters IV, V and VI of the thesis present the results and discussion of these three aspects respectively. Chapter III is the experiment part, chapter II is a brief review of the theory of the techniques used in the investigation, and chapter VII is the summary.

II. Theory

This Chapter presents a concise survey of the theories related to the measurements and calculations employed in this thesis.

1. ^{2}H NMR

The general NMR theory can be found in the books of Slichter (1978) and Harris (1983). The application of ^{2}H NMR to lipid membranes is discussed in the reviews by Seelig (1977) and Davis (1983).

A. *General theory and the powder pattern*

The Nuclear Magnetic Resonance technique measures transitions between states of nuclear apin orientation in a magnetic field. The deuterium nucleus (nuclear spin I=1) has a non-spherically symmetric charge distribution, which results in an electric quadrupolar moment. The total Hamiltonian for a deuterium nucleus in a magnetic field is composed of two parts: H_M and H_Q. The magnetic Hamiltonian H_M describes the interaction of the nuclear magnetic moment μ_M with the magnetic field B_0. The quadrupole Hamiltonian H_Q describes the electrostatic interaction of the nuclear quadrupole moment

with the electric field gradient at the position of the nucleus.

Due to H_M, the energy level of deuterium nuclei in a magnetic field B_0 is split into three Zeeman energy levels:

$$E_M = -g\beta_N B_0 m$$
$$= -\gamma_D \hbar B_0 m \qquad (m = 0, \pm 1) \qquad (1)$$

where β_N is the nuclear magneton, g is the nuclear g-factor, m is the magnetic quantum number and $\gamma_D = g\beta_N/\hbar$ is the gyromagnetic ratio of deuterium. According to the selection rules, only $\Delta m = \pm 1$ transitions are allowed, which will give one absorption line in the NMR spectrum with frequency ν_0.

$$\nu_0 = \Delta E/h = \gamma_D B_0/2\pi \qquad (2)$$

Considering a single crystal containing only one type of deuterium spin, the principal axes of the electric field gradient are X, Y, Z and the components V_{XX}, V_{YY}, V_{ZZ} are in the order of: $V_{ZZ} \geq V_{XX} \geq V_{YY}$. In the principal axis set (Slichter, 1978):

$$H_Q = \frac{eQ}{4I(2I-1)} [V_{ZZ}(3I_z^2 - I^2) + (V_{XX} - V_{YY})(I_x^2 - I_y^2)] \qquad (3)$$

where I^2, I_x^2, I_y^2 and I_z^2 are the operators of the nuclear angular moment. Defining $V_{ZZ} = eq$ and $\eta = (V_{XX} - V_{YY})/V_{ZZ}$, equation

(3) becomes

$$H_Q = \frac{e^2qQ}{4I(2I-1)}\left[(3I_z^2-I^2) + \eta(I_x^2-I_y^2)\right] \qquad (4)$$

The quadrupolar effects manifest themselves as a perturbation of the Zeeman interaction. As a result of first order approximation, the energy levels of the total Hamiltonian are

$$\begin{aligned} E_m &= E_M + E_Q \\ &= -g\beta_N B_0 m + \frac{eQ}{4I(2I+1)} V^{(2,0)}[3m^2-I(I+1)] \\ &= \begin{cases} g\beta_N B_0 + eQV^{(2,0)}/4 & (m=-1) \\ -eQV^{(2,0)}/2 & (m=0) \\ -g\beta_N B_0 + eQV^{(2,0)}/4 & (m=1) \end{cases} \end{aligned} \qquad (5)$$

where e is the elementary charge of the proton, Q is the scalar quadrupole moment and $V^{(2,0)}$ is the irreducible component of the electric field gradient along the direction of B_0 at the position of the nucleus. From eq(5), the three equally spaced Zeeman energy levels are shifted due to the quadrupolar coupling. Transitions between $\Delta m = \pm 1$ will give two separated lines with ν_0 at the center (see Figure 3), the separation of the lines is called the quadrupole splitting:

$$\Delta\nu_Q = (3/2)(eQ/h)V^{(2,0)}. \qquad (6)$$

Figure 3: The energy levels and relative absorption lines of deuterium nucleus.

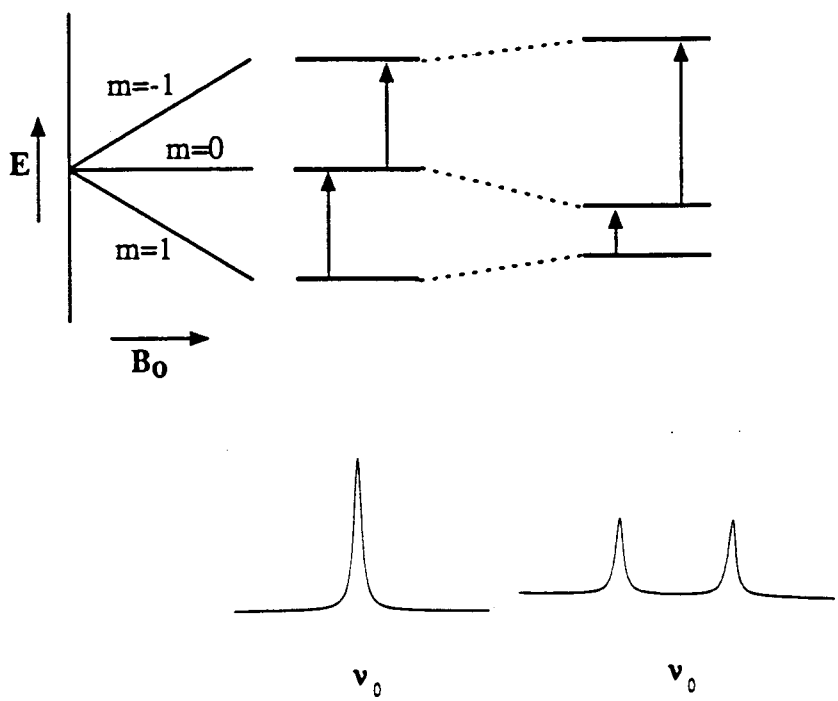

If the B_0 direction is defined using spherical polar angles (θ,Φ) in the electric field gradient principal axis system, we can calculate the transformed element by applying the Wigner rotation matrix $D^{(2)}(\alpha\beta\gamma)$, Choosing the Euler angles $\alpha = \Phi$, $\beta = \theta$, $\gamma = 0$, we find:

$$V^{(2,0)} = \Sigma_{p=0,\pm1,\pm2} D_{p,0}^{(2)} V_P^{(2,p)}$$
$$= V_{ZZ}[(3\cos^2\theta-1) + \eta\sin^2\theta\cos2\Phi]/2 \qquad (7)$$

where $V_P^{(2,p)}$ are the five irreducible components of the electric field gradient in the principal axis coordinate system and $D_{p,0}^{(2)}$ are the five elements of the rotation matrix $D^{(2)}(\alpha\beta\gamma)$. By substituting eq(7) into eq(6), we have

$$\Delta\nu_Q = (3/2)(e^2qQ/h)[(3\cos^2\theta-1)/2 + \eta\sin^2\theta\cos2\Phi/2] \qquad (8)$$

where (e^2qQ/h) is referred to as the static quadrupolar coupling constant, which is 168 kHz (Burnett and Muller, 1971; Davis and Jeffrey, 1977) for a paraffinic C-D bond. In the case of a C-D bond, the asymmetry parameter $\eta \leq 0.05$, therefore neglecting η, eq(8) becomes:

$$\Delta\nu_Q = (3/2)(e^2qQ/h)[(3\cos^2\theta-1)/2]. \qquad (9)$$

For a polycrystalline powder sample, where the nuclear sites are randomly oriented with respect to B_0, each

orientation will give an unique doublet and the NMR spectrum is the so-called "powder pattern" which is the sum of lines for all θ (see Fig.4a). The splitting of the principal peaks of the powder pattern corresponds to θ = 90^0, thus

$$\Delta\nu_Q = (3/4)(e^2qQ/h). \qquad (10)$$

B. Spectra of membranes and the order parameter (S_{CD})

From the biological point of view, the most important structure of the phospholipid liquid crystalline phase is the bilayer. We define a director Z', usually the bilayer normal, around which the acyl chain and head group undergo rapid rotational motions. As the motion is anisotropic, $V^{(2,0)}$ is not averaged to zero and therefore gives rise to a quadrupole splitting. Also, the rate of motion is much faster than the time scale of NMR, so only an average result is observed. If β is the angle between the C-D bond and the director Z', and β' is the instantaneous angle between Z' and B_0, from eq(9) the quadrupole splitting is:

$$\Delta\nu_Q = \frac{3}{2}\left(\frac{e^2qQ}{h}\right)\left(\frac{3\cos^2\theta-1}{2}\right)$$

$$\Delta\nu_Q = \frac{3}{2}\left(\frac{e^2qQ}{h}\right)\left(\frac{3\cos^2\beta'-1}{2}\right)\left\langle\frac{3\cos^2\beta-1}{2}\right\rangle. \qquad (11)$$

Figure 4: ^2H NMR powder pattern spectra:

(a) The spectrum is from a calculation of a sum of Lorentzian lines of such an intensity distribution that the nuclear sites are randomly oriented with respect to B_0. Spectral width = 200 kHz, quadrupolar splitting = 29.1 kHz, line broadening = 160 Hz.

(b) Experimental spectrum of 5,5-DPPC-d_2*/H_2O dispersion recorded at 45°C using 90^0_y-τ-90^0_x-t pulse sequence. 90^0 pulse = 6.5 μs, τ = 50 μs, t = 250 ms; sweep width = ±100 kHz; data size = 4K in complex; line broadening = 50 Hz; number of acquisitions = 8,000.

* 5,5-DPPC-d_2 is a kind gift from Dr. R.S. Chana.

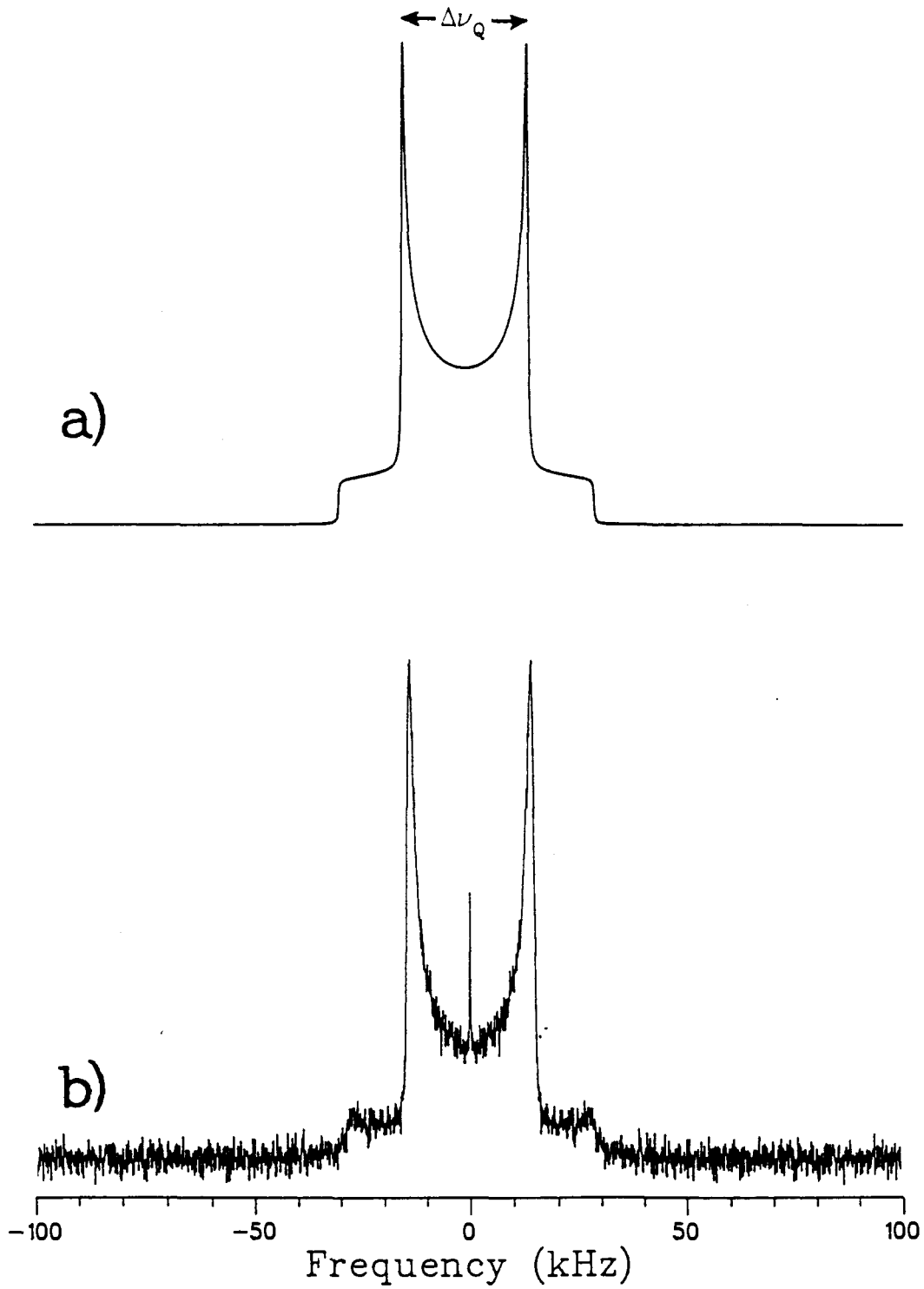
$\Delta\nu_Q$
a)
b)
−100
−50
0
50
100
Frequency (kHz)

For $\beta'=90^0$, we obtain

$$\Delta\nu_Q = (3/4)(e^2qQ/h)S_{CD} \qquad (12)$$

where $S_{CD} = \langle(3\cos^2\beta-1)/2\rangle$, is a measure of the time average of the angular fluctuations of the C-D bonds with respect to the director axis Z', and is defined as the orientational order parameter for a C-D bond, the angular brackets denote a time average. The ^2H NMR spectra from measurement of a model membrane and from the calculation of a sum of Lorentzian lines (Seelig, 1977) are shown in Figure 4.

C. Deuterium relaxation

The magnetization of spin I along the Z axis in a magnetic field B_0 is M_0, at thermal equilibrium. Following an rf pulse in the x-y plane the nuclear spin system returns to equilibrium by relaxation processes. The relaxation is treated as a first-order process with characteristic time constants which are referred to as relaxation times. For spin I=1/2 system, two relaxation times T_1 (the spin-lattice relaxation time) and T_2 (the spin-spin relaxation time) are enough to describe the relaxation process. With time constant T_1, the magnetization M_z returns back to M_0, whereas with T_2 magnetizations both M_x and M_y decay to zero. In a classical approach, the motion of magnetization is described by the

Bloch equations (Farrar and Becker, 1971):

$$dM_x/dt = \gamma(M_y B_0 + M_z B_1 \sin\omega t) - M_x/T_2 \qquad (13)$$

$$dM_y/dt = \gamma(M_z B_1 \cos\omega t - M_x B_0) - M_y/T_2 \qquad (14)$$

$$dM_z/dt = -\gamma(M_x B_1 \sin\omega t + M_y B_1 \cos\omega t) - (M_z - M_0)/T_1 \qquad (15)$$

For deuterium (I=1), the classical Bloch equations are insufficient to determine the relaxation times and the best way to deal with the dynamics of the spin system is in terms of a 3 X 3 density matrix $\rho(t)$. The expectation of **M** is simply equal to $T_r(\rho\mathbf{M})$ (Slichter, 1978). The density matrix is expanded in terms of the unit operator and a set of eight orthonormal, Hermitian operators P_i, where i=1,2···8:

$$\rho(t) = C_0 1_{op} + \Sigma_i C_i(t) P_i \qquad (16)$$

In the presence of a Hamiltonian **H**, the equation of motion is

$$dC_i/dt = -\Sigma_j Q_{ij} C_j \qquad (17)$$

where $Q_{ij} = -Q_{ji} = -iT_r\{P_i[P_j,H]\}$, Hamiltonian **H** is also expressible in P_i. Different sets of the orthonormal, Hermitian operators may be chosen (Vega and Pines, 1977; Jeffrey, 1981; Bloom, 1987). According to Bloom (1987); a

common operator set is given as following:

$$P_1 = I_x/\sqrt{2},\ P_2 = I_y/\sqrt{2},\ P_3 = I_z/\sqrt{2},$$

$$P_4 = (3I_z^2 - 2)/\sqrt{6},\ P_5 = (I_xI_z + I_zI_x)/\sqrt{2},\ P_6 = (I_yI_z + I_zI_y)/\sqrt{2},$$

$$P_7 = (I_x^2 - I_y^2)/\sqrt{2},\ P_8 = (I_xI_y + I_yI_x)/\sqrt{2}.$$

Five relaxation times have been chosen to characterize the time dependence of $C_i(t)$. They are T_{1Z} (time constant of the return of Zeeman order, related to C_3), T_{1Q} (time constant of the decay of quadrupolar order, related to C_4), T_{2D} (time constant of the decay of double-quantum coherence, related to C_7 and C_8) and two other spin-spin relaxation time, T_{2a} and T_{2b} (related to C_1, C_2, C_5 and C_6). In an NMR experiment, the observed signals are proportional to $T_r(\rho I_x)$ and $T_r(\rho I_y)$ which are associated with C_1 and C_2. To determine these relaxation times special pulse sequences and techniques may be employed (Jacobsen and Schaumberg, 1976; Vold and Vold, 1977). The relaxation theory for a spin I=1 system and the various pulse sequences for measuring these relaxation times in membrane systems are discussed in the paper of Jeffrey (1981).

The measurement of deuterium relaxation times offers the advantage that the dominant relaxation pathway is quadrupolar relaxation. The interaction of a quadrupole moment and the electric field gradient is time dependent due to the molecular reorientation (Seelig, 1977). Usually, T_1 ($=T_{1Z}$) and T_2 ($1/T_2 = 1/2T_{2a} + 1/2T_{2b}$) are measured. The relaxation times are expanded

in terms of spectral densities, which are related to the motions of deuterium sites in different frequency ranges. Following the general relaxation theory (Abragam, 1961), the simplest case of deuterium relaxation is that of a fast-tumbling spherical molecule in an isotropic liquid:

$$1/T_1 = (3/80)(e^2qQ/\hbar)^2(1+\eta)[J(\omega_0)+4J(2\omega_0)] \quad (18)$$

$$1/T_2 = (1/160)(e^2qQ/\hbar)^2(1+\eta)[9J(0)+15J(\omega_0)+6J(2\omega_0)] \quad (19)$$

where $J(\omega)$ is the spectral density.

In ordered media such as the membrane system, the deuterium relaxation is complicated. The relaxation rate is related to not only the correlation time but also the order of the media. Assuming that motional fluctuations with respect to the director can be described by a single correlation time τ_c, and that the motion is in the extreme narrowing limit ($\omega_0^2\tau_c^2<<1$), the expression for T_1 is (Brown, 1979; Brown et al., 1979; Brown and Davis, 1981):

$$1/T_1 = (3/8)(e^2qQ/\hbar)^2(1-S_{CD}^2)\tau_c \quad (20)$$

Experimentally, $T_1>>T_2$ is found in the membrane system. This fact implies that there must exist motions with correlation time $\tau_1 \leq \omega_0^{-1}$, which are responsible for T_1 relaxation, and that other motions with correlation time $\tau_2 >> \omega_0^{-1}$, which are dominant in T_2 relaxation (Davis, 1979; Bloom

and Sternin, 1987).

In the case of a multilamellar system, the dependence of T_2 on the orientation is obvious (Jeffrey, 1981; Volke,1984). T_{2e} is experimentally measured from the decay of the quadrupole echo signals. Thus, T_{2e} is an orientationally averaged value. In order to describe the relationship between T_{2e} and the correlation time, the second moment of a spectrum is introduced.

The nth moment of a spectrum with lineshape $f(\omega)$ is defined by: (Davis, 1983)

$$M_n = \int_0^\infty \omega^n f(\omega)\, d\omega \;/\; \int_0^\infty f(\omega)\, d\omega \qquad (21)$$

For the second moment, the equation is

$$M_2 = (1/5)(\Delta\omega_Q)^2 = (4\pi^2/5)(\Delta\nu_Q)^2 \qquad (22)$$

Due to the rotation of the molecule-fixed principal axes about the axis Z' having spherical polar angles (β,α) in the principal axis coordinate system, the apparent second moment of a powder pattern changes by $(1/5)(3e^2qQ/4\hbar)^2[(1 + \eta^2/3) - (S_{CD}+\eta\sin^2\beta\cos2\alpha)^2]$. Neglecting η, we have

$$\Delta M_2 = (1/5)(3e^2qQ/4\hbar)^2(1-S_{CD}^2) \qquad (23)$$

for the fast motion limiting case, $\Delta M_2\tau_c^2 << 1$,

$$1/T_{2e} = \Delta M_2 \cdot \tau_c \qquad (24)$$

while for the slow motion limiting case, $\Delta M_2 \tau_c^2 >> 1$, giving:

$$T_{2e} = p \cdot \tau_c \qquad (25)$$

where p is a constant for a given spin system (Pauls *et al.*, 1985). To distinguish the two limiting regions of τ_c, a quadrupolar CPMG pulse sequence 90^0_y-$[\tau$-90^0_x-$\tau]_n$-t is employed, the decay constant of echoes appearing at time $2n\tau$ is the relaxation time $T_2^{q\text{-}CPMG}$ (Bloom and Sternin, 1987; Blicharski, 1986)

$$1/T_2^{q\text{-}CPMG} = \Delta M_2 \tau_c \, [1-(\tau_c/\tau)\tanh(\tau/\tau_c)] \qquad (26)$$

For the fast motion limiting case, $\tau_c << \tau$, $T_2^{q\text{-}CPMG}$ equals T_{2e}. While in the slow motion limiting case, using $\tau << \tau_c$, in the pulse train, we have

$$1/T_2^{q\text{-}CPMG} = \Delta M_2 \tau^2/3\tau_c + 1/T_2 \neq 1/T_{2e}. \qquad (27)$$

$1/T_2$ is the spin-spin relaxation rate due to processes having correlation times $<< (\Delta M_2)^{-1/2}$ (eq.19), thus, τ_c can be obtained from τ^2 dependence of $1/T_2^{q\text{-}CPMG}$.

D. Pulse sequences and precession diagram

The Block equations (eq.13-15) describe the motions of magnetization of a spin half system, which are composed of the Larmor precession and the relaxation. For the solution of the Block equations, precession diagrams are often used to describe the motions of magnetization in the magnetic field. For a spin half system, under a static magnetic field B_0 along Z axis, the nuclear magnetization precesses about Z axis with Larmor frequency $\omega_0 = \gamma B_0$. Applying an alternating magnetic field $B_1 \cos\omega_0 t$ along X axis introduces precession about X axis with frequency ω_1 in a coordinate system that rotates about Z axis at frequency ω_0. In such a coordinate system, the alternating magnetic field becomes static. Figure 5 illustrates the precessions of magnetization for these cases.

The precession diagrams give us a good way to understand how the pulse sequences work for different purposes. Three dimensional space is not enough for the precession of a spin one system, therefore, the space spanned by the basic operator set must be considered. Using commutation relations between the basic operators, the solutions of eq.17 can be represented by precession diagrams (Bloom, 1987). Figure 6 presents the precession diagrams under various Hamiltonian operations and Figure 7 illustrates the evolution of motions of magnetization under various pulse sequences.

Figure 5: a) Larmor precession of the magnetization in the static magnetic field (in the laboratory coordinate system).

b) 90^0 r.f. pulse along Y axis brings the magnetization **M** from Z axis to X axis in a coordinate system which is rotating around Z axis with Larmor frequency.

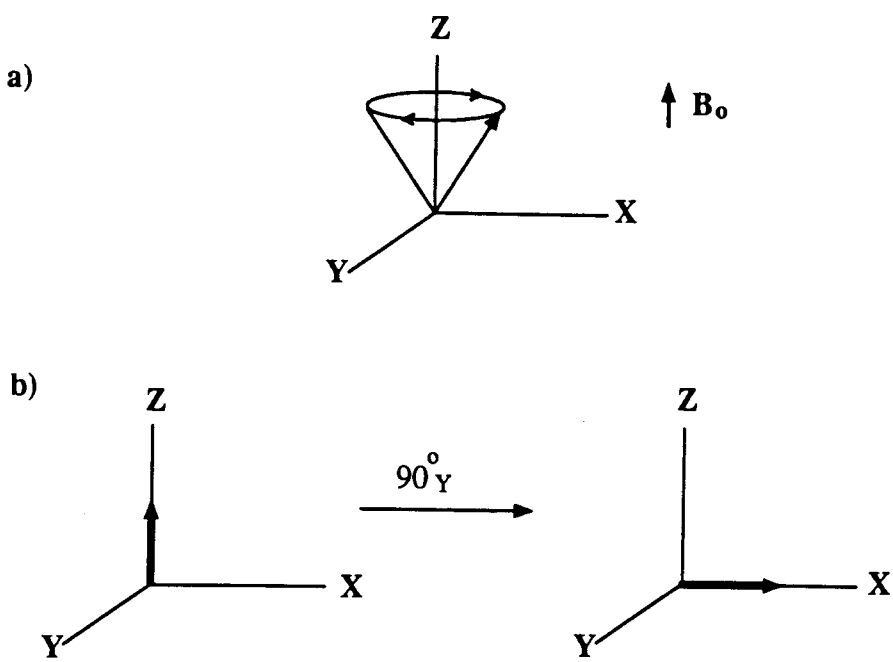

Figure 6: Precession diagram for a spin-1 under various Hamiltonian operations.
The diagrams in the first column are equivalent to the classical Larmor precession. The diagrams in the other two columns describe the evolution of the higher order components of the density matrix, which do not have classical vector analogues.

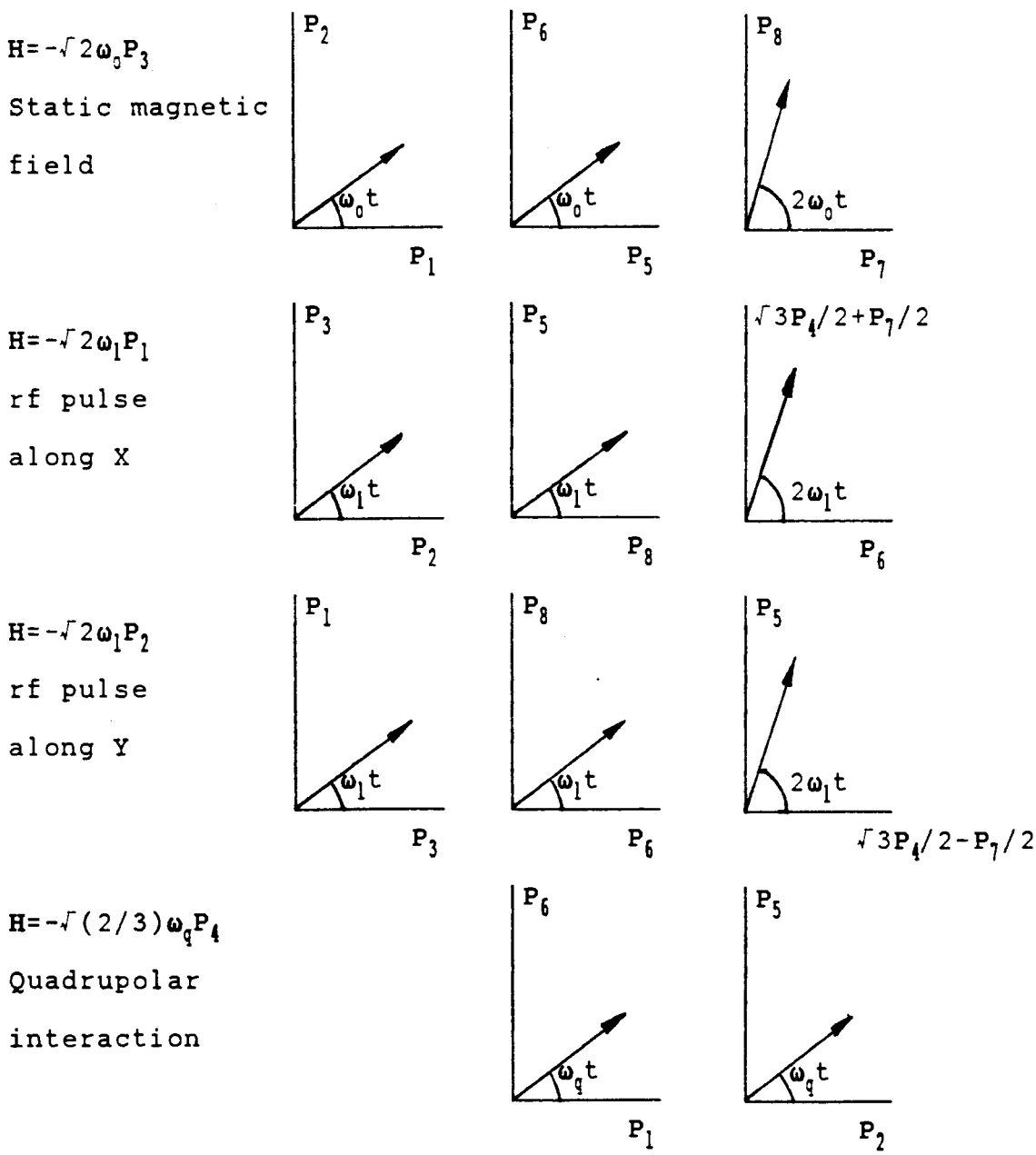

Figure 7: Precession diagrams for a spin-1 in cases of various pulse sequence.

FID

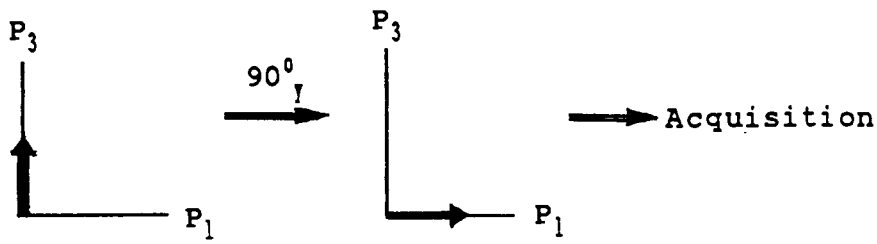

Quadrupolar Echo

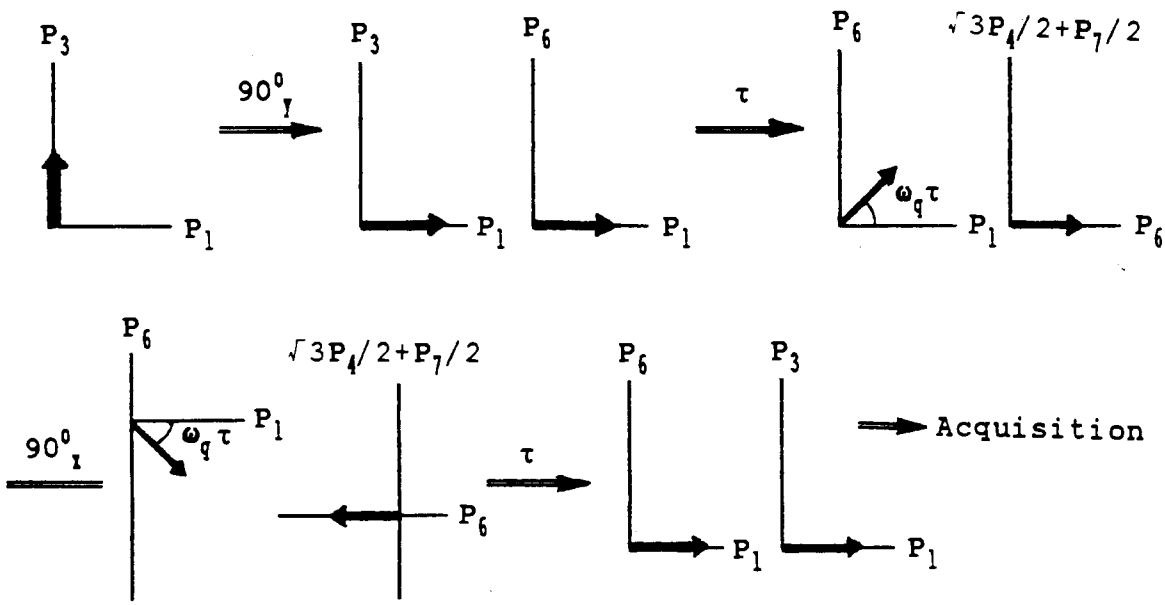

Inversion Recovery

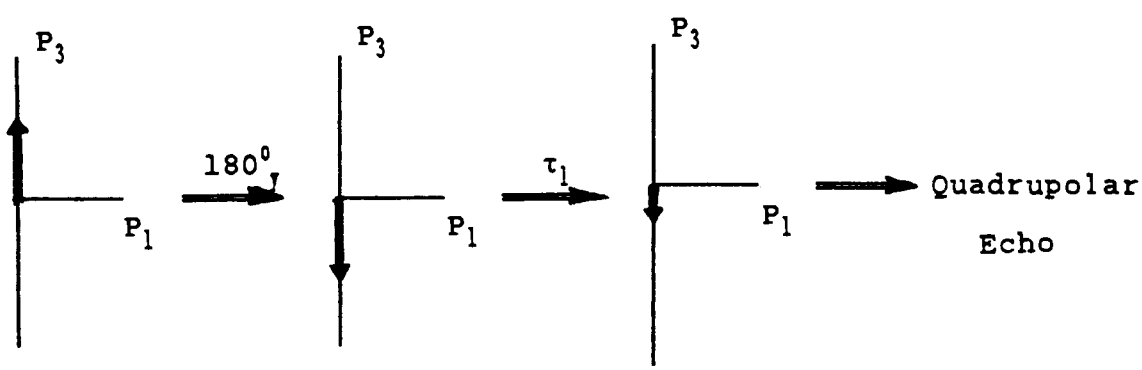

Selective Inversion Recovery

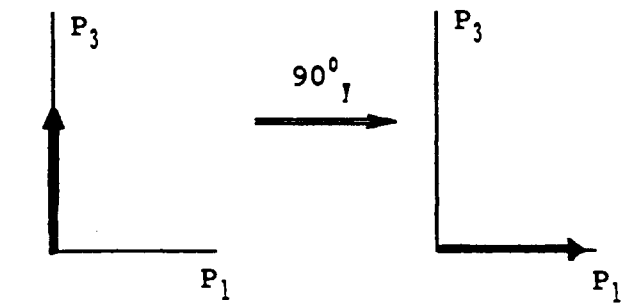

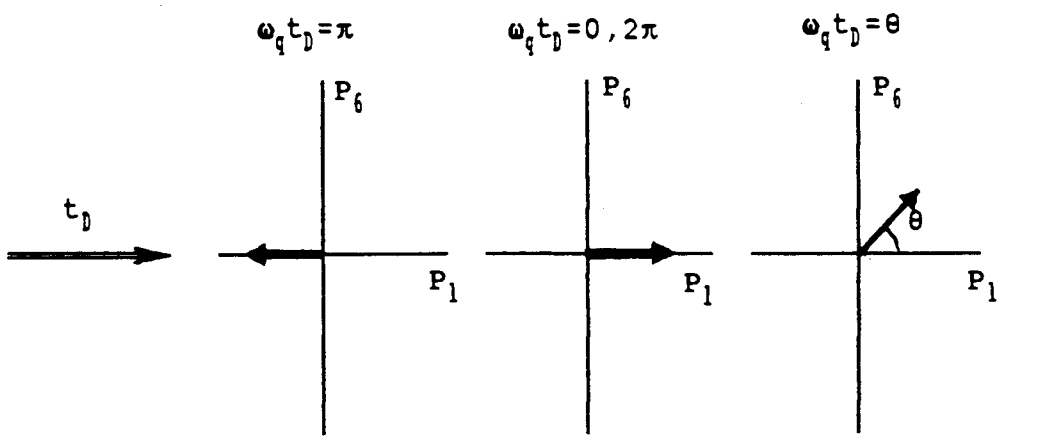

Not inverted Inverted Partialy inverted

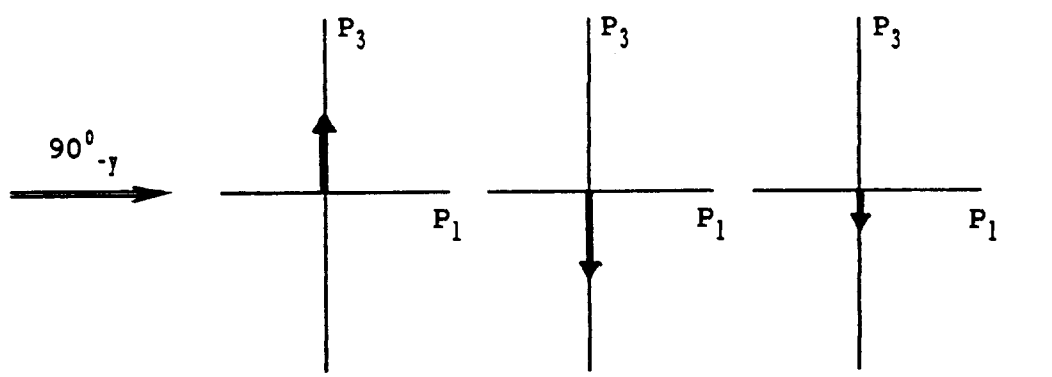

τ_1, Relaxation and Diffusion

Quadrupolar Echo

2. ^{31}P NMR

The application of ^{31}P NMR to lipid membranes can be found in the review by Smith and Ekiel (1984).

The ^{31}P chemical shift of phospholipid in the solid state depends on the orientations of the phosphodiester moiety with respect to the magnetic field. For a polycrystalline sample ^{31}P NMR spectrum is the sum of spectra for all possible orientation, which is a broad band characterized by three principal chemical shift values σ_{11}, σ_{33} and σ_{22} as two edges and one peak. ^{31}P NMR for phospholipid in membranes is an axially symmetric powder pattern due to the rapid anisotropic motion of the phospholipid molecule and/or of the phosphodiester moiety. The width of the powder pattern represents the chemical shift anisotropy (CSA), $\Delta\sigma = \sigma_{\parallel}-\sigma_{\perp}$, which is related to the orientation of the axis of motional averaging with respect to the principal components of the chemical shift tensor and also related to the order of the phosphate group, i.e., the amplitude of angular excursion during motional averaging. The lineshape of ^{31}P NMR of phospholipid in membrane is further affected by the isotropic motions.

The isotropic motions, i.e., phospholipid lateral diffusion and membrane tumbling, are two factors determining the lineshape of ^{31}P NMR spectra obtained from phospholipid in a membrane. In the case of multilamellar liposomes, the

particles are big, the tumbling of the particles and lateral diffusion are so slow compared with the width of spectrum that the motional averaging does not happen and the spectrum is an asymmetrical broad line. In the case of sonicated unilamellar vesicles, particles are much smaller and narrow symmetrical 'high resolution' NMR spectra are obtained as a result of the motional averaging. With increasing viscosity of the medium, the tumbling motion slows down and the narrow spectral line becomes broad. The lateral diffusion constant of phospholipid can be measured from the spectral simulation (Bayerl *et al.*, 1984) and from the viscosity-dependent linewidth of the spectra (Cullis, 1976; Cushley *et al.*, 1987). In certain ranges of viscosity and vesicle size the lineshape of spectra can be changed gradually from a narrow Lorentzian line to an asymmetric broad one, which was predicted by the theory of Campbell *et al.* (1979). The rate of isotropic motion for a membrane vesicle, $1/\tau_e$, has contributions from tumbling ($1/\tau_t$) and lateral diffusion ($1/\tau_{diff}$), which is expressed:

$$\begin{aligned} 1/\tau_e &= (1/\tau_t) + (1/\tau_{diff}) \\ &= (3kT/4\pi\eta r^3) + (6D_T/r^2) \end{aligned} \qquad (28)$$

where η is the viscosity, r is the radius of the vesicle and D_T is the diffusion coefficient.

3. Differential scanning calorimetry (DSC)

DSC is one of the most popular techniques for the study of phase behavior of model or biological membranes. Reviews can be found in Mabrey and Sturtevant (1978) and McElhaney (1982, 1986). DSC is a relatively simple and straightforward physical technique which measures the thermally induced phase transition. In the DSC experiment a sample and an 'inert' reference material are simultaneously heated in cells at an identical rate. In our case the sample is a very small amount of lipid multilamellar liposome sealed in a sample pan while the reference is an empty sample pan. Since equal quantities of heat are initially being applied to both cells, the temperature of both sample and reference increase linearly with time, such that their differential temperature is maintained at zero. However, if the sample undergoes a thermally induced phase transition, part of the heat is absorbed (or liberated) by the sample, which results in a temperature difference between the sample and reference cells. The instrumental control system will supply more (or less) heat to the sample cell so that the same temperature of both cells will be maintained. DSC measures the extra heat flow required to keep a sample and reference cell at the same temperature. Both pre- and main gel to liquid crystalline transitions of phospholipid liposomes are first order transitions, which give endothermal peaks in DSC thermogram.

The phase transition temperature T_m is the temperature at which the extra heat flow reaches maximum. The peak area under DSC trace when calibrated with a known standard is a direct measurement of enthalpy for the phase transition:

$$\Delta H_{cal} = \int_{T1}^{T2} (dH/dt)_{ex}(dt/dT)dT. \qquad (29)$$

For a symmetric phase transition, T_m represents the temperature at which the transition from the gel to liquid crystalline state is one-half complete. At the phase transition midpoint-temperature the change in free energy (ΔG) of the system is zero, the entropy change (ΔS) associated with the transition can be calculated:

$$\Delta G = \Delta H_{cal} - T_m \Delta S \qquad (30)$$

III. Experimental Methods

1. Materials

Palmitic acid was purchased from Fisher Scientific Co. Ten percent palladium on activated carbon, phosphorus oxychloride and trimethylamine were purchased from Aldrich Chemical Co. Egg yolk lysophosphatidylcholine (lysoPC), 1,2-dipalmitoyl-sn-glycero-3-phosphocholine (DPPC), 1,2-dipalmitoyl-sn-glycerol, phytol, 1,1'-carbonyldiimidazole (CDI), Trizma base, Trizma hydrochloride and deuterium depleted water (DDW) were purchased from Sigma Chemical Co. Sigma lysoPC (from egg yolk) contains 66 - 68% palmitic acid, 24 - 26% stearic acid, and 6 - 10% other saturated acids (Thewalt et al., 1985). 2-Bromoethanol-1,1,2,2-d_4 and deuterium oxide were purchased from MSD Isotopes. Phytanic acid was purchased from Analabs. "Baker analysed" Silica gel, 60-200 mesh, was purchased from J.T. Baker Chemical Company. The solvents were A. R. grade from Fisher or BDH. The chemicals were used as received unless otherwise stated.

2. Synthesis of [$^2H_{31}$]palmitic acid

Perdeuterated palmitic acid ([$^2H_{31}$]palmitic acid) was prepared by deuterium exchange of a melt of palmitic acid with

deuterium gas in the presence of 10% palladium on activated carbon following the general method of Hsiao *et al.* (1974). Palmitic acid was analyzed by GC-Mass Spectroscopy (Hewlett-Packed 5985 GC-MS, column DB-1) of its methyl ester and contained 1% of pentadecanoic acid and 2% of heptadecanoic acid. Deuterium gas was generated using a Varian Aerograph model 9650 hydrogen generator. A 150 ml round-bottomed flask was equipped with an inlet tube and a magnetic stir bar. The flask was charged with palmitic acid (25 g) and 10% palladium on activated carbon (5 g). The reaction mixture was heated with a silicon oil bath (195±5^{0}C) under stirring. Deuterium gas was introduced into the flask for 40 days. The reaction was monitored by mass spectroscopy. At the end of the exchange reaction, chloroform was added to the mixture, and the catalyst was filtered off. Chloroform was removed under reduced pressure to give crude perdeuterated palmitic acid (27.6 g). The crude acid (8 g) was then purified by column chromatograph on silica gel (60-200 mesh) with hexane eluent followed by chloroform eluent to provide white crystals (6 g) of [$^2H_{31}$]palmitic acid with 73.9% yield. The purified [$^2H_{31}$]palmitic acid was analyzed by mass spectroscopy to show 97.4% of deuteration level (see Appendix I for the calculation).

3. Synthesis of 1-palmitoyl(stearoyl)-2-[$^2H_{31}$]palmitoyl-sn-glycero-3-phosphocholine (PC-d_{31})

PC-d_{31} was synthesized by condensing of [$^2H_{31}$]palmitic acid and egg yolk lysoPC with 1,1'-carbonyldiimidazole (CDI) according to the published procedure (Grover and Cushley, 1979) and the modifications of Thewalt *et al.* (1985).

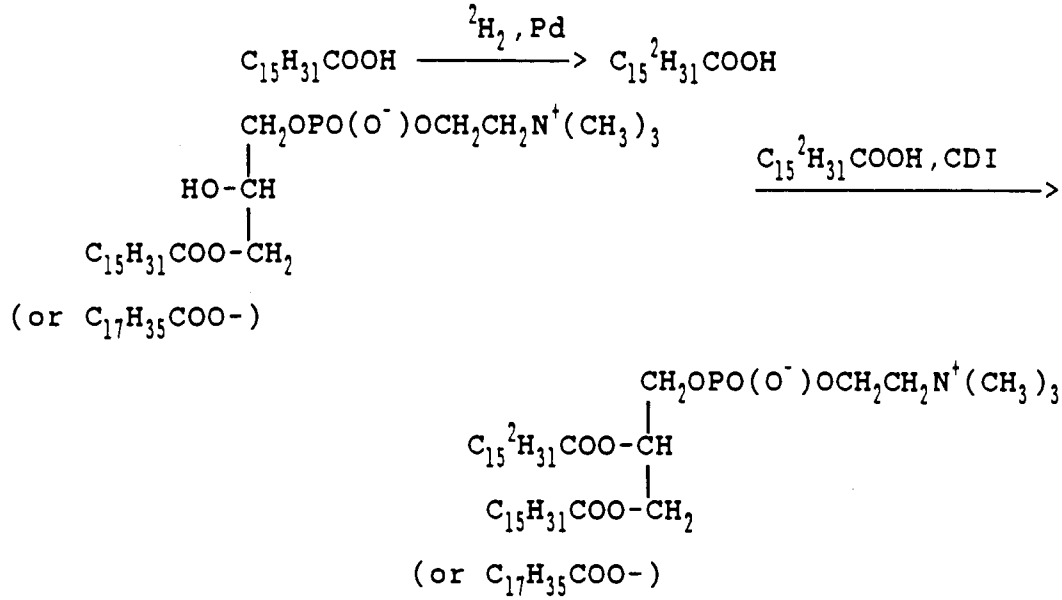

A 50 ml pear shaped flask was equipped with an inlet tube and a magnetic stir bar, and was flame dried under a stream of nitrogen. The flask was charged with [$^2H_{31}$]Palmitic acid (1.26 g, 4.4 mmol, freshly dried under high vacuum overnight at room temperature) and dry benzene (20 ml, freshly distilled from sodium) under nitrogen. To the benzene solution CDI (0.78 g, 4.8 mmol) was added from a freshly opened bottle. Carbon dioxide was immediately generated indicating formation of the palmitoylimidazole derivative. In one hour of stirring at room temperature, egg yolk lysoPC (2 g, 4.2 mmol, freshly dried under high vacuum overnight at room temperature) was added to

the mixture. The reaction mixture was kept stirring at room temperature under nitrogen, the solvent was removed by the stream of nitrogen, and the residue was further dried under high vacuum. The dried residue in sealed flask was incubated at 85^{0}C in an oil bath for 3 hr. During the incubation, the formation of imidazole crystals indicated that the palmitic acid had esterified the lysoPC. The reaction mixture was cooled to room temperature and dissolved into petroleum ether (30-60, 25 ml)/95% ethanol (4 ml). The solution was then transferred into a 150 ml Erlenmeyer flask. A precipitate was formed when cold acetone (90 ml) was added into the solution. The precipitation was repeated once, PC-d_{31} (white solid powder, 2.0 g, 65.5%) unreacted [$^2H_{31}$]palmitic acid and lysoPC were separated, by column chromatography on silica gel (60-200 mesh) with chloroform-methanol-water (70:26:4, by vol.). A thin layer chromatogram (TLC) of PC-d_{31} on silica gel with chloroform-methanol-water (65:25:4, by vol.) showed a single spot, R_f = 0.29, which was identical to that of an undeuterated authentic sample of DPPC (Sigma).

The proposed structure of PC-d_{31} was supported by Mass Spectroscopy and proton NMR. The mass spectrum showed two sets of lines centered at m - 183 (m - $^+N(CH_3)_3(CH_2)_2OPO_3^-$) = 580 and 608, corresponding to phospholipid with a mixed palmitoyl and stearoyl *sn*-1 chain. The relative intensities for these two sets were 2.85:1 which was in agreement with the composition of Sigma lysoPC. The proton NMR spectrum of PC-d_{31} in $CDCl_3$

Figure 8: ^{1}H and ^{2}H NMR spectra of PC-d_{31} in chloroform.
a) ^{1}H NMR spectrum of DPPC (from Sigma) in $CDCl_3$ solution,
b) ^{1}H NMR spectrum of PC-d_{31} in $CDCl_3$ solution,
c) ^{2}H NMR spectrum of PC-d_{31} in $CHCl_3$ solution.
Concentration: 10 mg/ 0.5 ml. Spectra were measured using a Bruker WM 400 spectrometer (^{1}H, at 400.1 MHz; ^{2}H, at 61.6 MHz). Chemical shifts were expressed in ppm downfield from TMS, using the residue solvent peak as a reference.

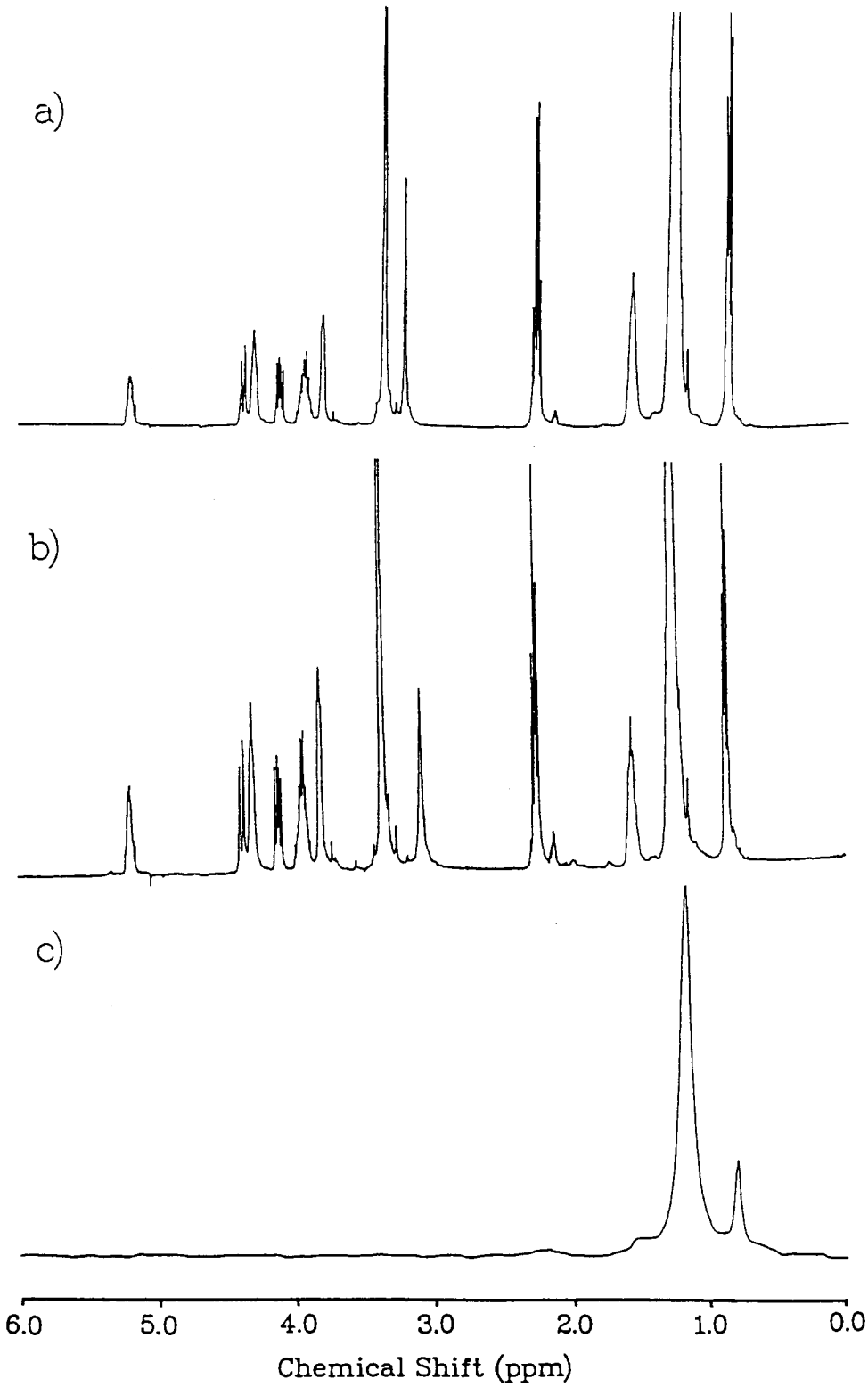
a)
b)
c)
6.0
5.0
4.0
3.0
2.0
1.0
0.0
Chemical Shift (ppm)

(Fig. 8b) is characterized by the presence of two doublets of doublets at δ = 4.12 and δ = 4.39 ppm for the CH_2OCO glycerol protons and a multiplet at δ = 3.94 ppm for the CH_2OP glycerol protons. Similar chemical shifts are obtained for Sigma DPPC (Fig. 8a), in agreement with the published spectra of 1,2-distearoyl-*sn*-glycero-3-phosphocholine (Ponpipom and Bugianesi, 1980). 1,3-Distearoyl-*sn*-glycero-3-phosphocholine shows a doublet at δ = 4.24 ppm for CH_2OCO glycerol protons (Ponpipom and Bugianesi, 1980), which is not shown in ^1H NMR spectrum of PC-d_{31}. Therefore, in PC-d_{31} the deuterated fatty acid chains were attached to the *sn*-2 position.

4. Synthesis of 1,2-dipalmitoyl-*sn*-glycero-3-[α,ß-$^2H_4$] phosphocholine (DPPC-d_4)

DPPC-d_4 was synthesized with five steps starting from 1,2-dipalmitoyl-*sn*-glycerol according to H. Eibl *et al.* (1978, 1978a, 1980). Minor modifications were made to improve the yield in our small scale synthesis.

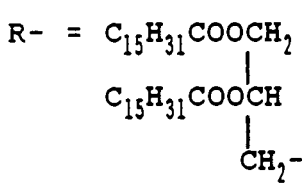

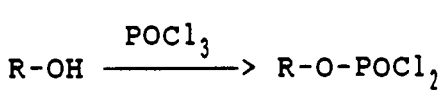

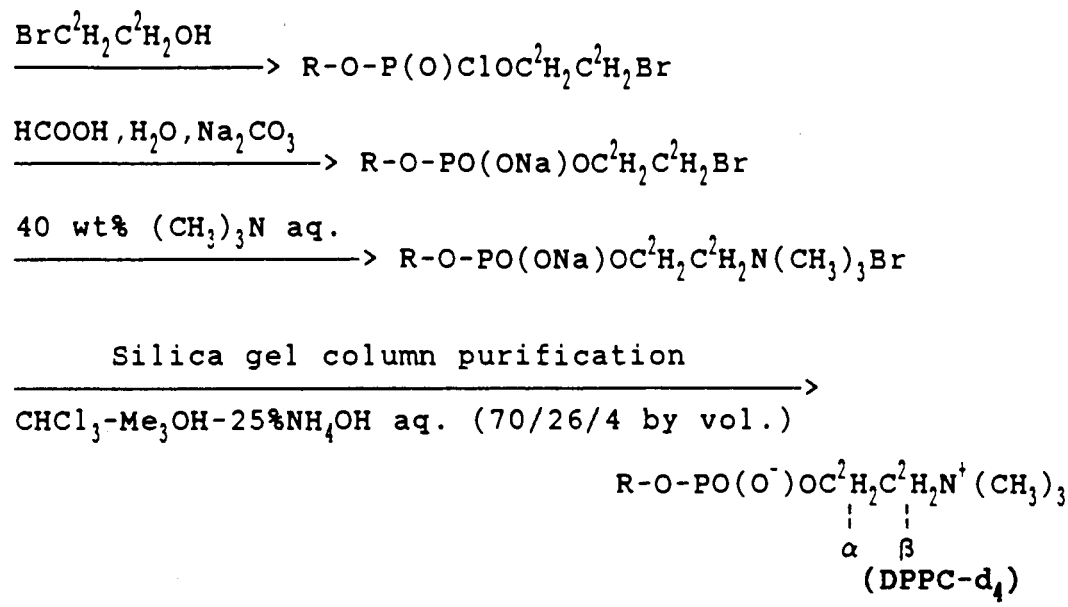

1,2-Dipalmitoyl-*sn*-glycerol was converted into 1,2-dipalmitoyl-*sn*-glycero-3-phosphoric acid dichloride. An anhydrous tetrahydrofuran (THF) (3 ml, freshly distilled from sodium and benzophenone) solution of triethylamine (0.3 g, 3 mmol, freshly distilled from sodium) was added to phosphorus oxychloride (0.45 g, 3 mmol, freshly distilled) with stirring under nitrogen at room temperature. To the above solution an anhydrous THF solution (7 ml) of 1,2-dipalmitoyl-*sn*-glycerol (1 g, 1.8 mmol, freshly dried under vacuum overnight) was added dropwise over 15 min at 5°C. The reaction mixture was stirred for 20 min, and precipitated triethylamine hydrochloride was filtered off. To the filtrate was added 2.5 ml of toluene, and the solvents were then removed under reduced pressure leaving an oily residue. To an anhydrous THF solution (4 ml) of the oily residue was added an anhydrous THF

solution (2 ml) of dried triethylamine (0.5 g, 5 mmol) followed by dropwise addition of an anhydrous THF solution (6 ml) of 2-bromoethanol-1,1,2,2-d_4 (0.35 g, 2.7 mmol) over 25 min with stirring under nitrogen. The reaction mixture was then kept at 40°C with stirring for 1 hr. The resulting phosphorous chloride ester in the above reaction mixture was hydrolyzed by adding an aqueous solution of formic acid (4M, 5 ml) at 10°C. The hydrolyzed product was extracted by hexane (10 ml), and to the hexane solution was added toluene (3 ml). The solvents were then removed under reduced pressure. A di-isopropyl ether solution (10 ml) of the residue was washed with 0.5 M Na_2CO_3 (10 ml) and methanol (10 ml). After phase separation, acetone (30 ml) was added to the upper phase to precipitate 1,2-dipalmitoyl-*sn*-glycero-3-phosphoric bromoethyl ester, which was filtered in 1 hr of storage at -18°C. This bromoethyl ester was then converted into the phosphocholine bromide (DPPC-d_4 bromide). To a chloroform solution (4.5 ml) of the bromoethyl ester were added (at 50°C) 2-propanol (7.5 ml), acetonitrile (7.5 ml) and 40% aq. trimethylamine (10.5 ml, prepared from 25% aq. and pure trimethylamine). The reaction mixture was incubated at 50°C for 12 hr, and the reaction was monitored by TLC (silica gel with chloroform-methanol-water, 65:25:4, by vol.). After the solvents were removed, the residue was dissolved in a mixture of water (20 ml), chloroform (20 ml) and methanol (26 ml) with vigorous stirring. The bottom phase, containing DPPC-d_4 bromide, was

Figure 9: ^{1}H and ^{2}H NMR spectra of DPPC-d_4 in chloroform.
a) ^{1}H NMR spectrum of DPPC (from Sigma) in $CDCl_3$ solution,
b) ^{1}H NMR spectrum of DPPC-d_4 in $CDCl_3$ solution,
c) ^{2}H NMR spectrum of DPPC-d_4 in $CHCl_3$ solution.

Concentration: 10 mg/ 0.5 ml. Spectra were measured using a Bruker WM 400 spectrometer (^{1}H, at 400.1 MHz; ^{2}H, at 61.6 MHz). Chemical shif s were expressed in ppm downfield from TMS, using the residue solvent peak as a reference.

* contaminated by DMSO.

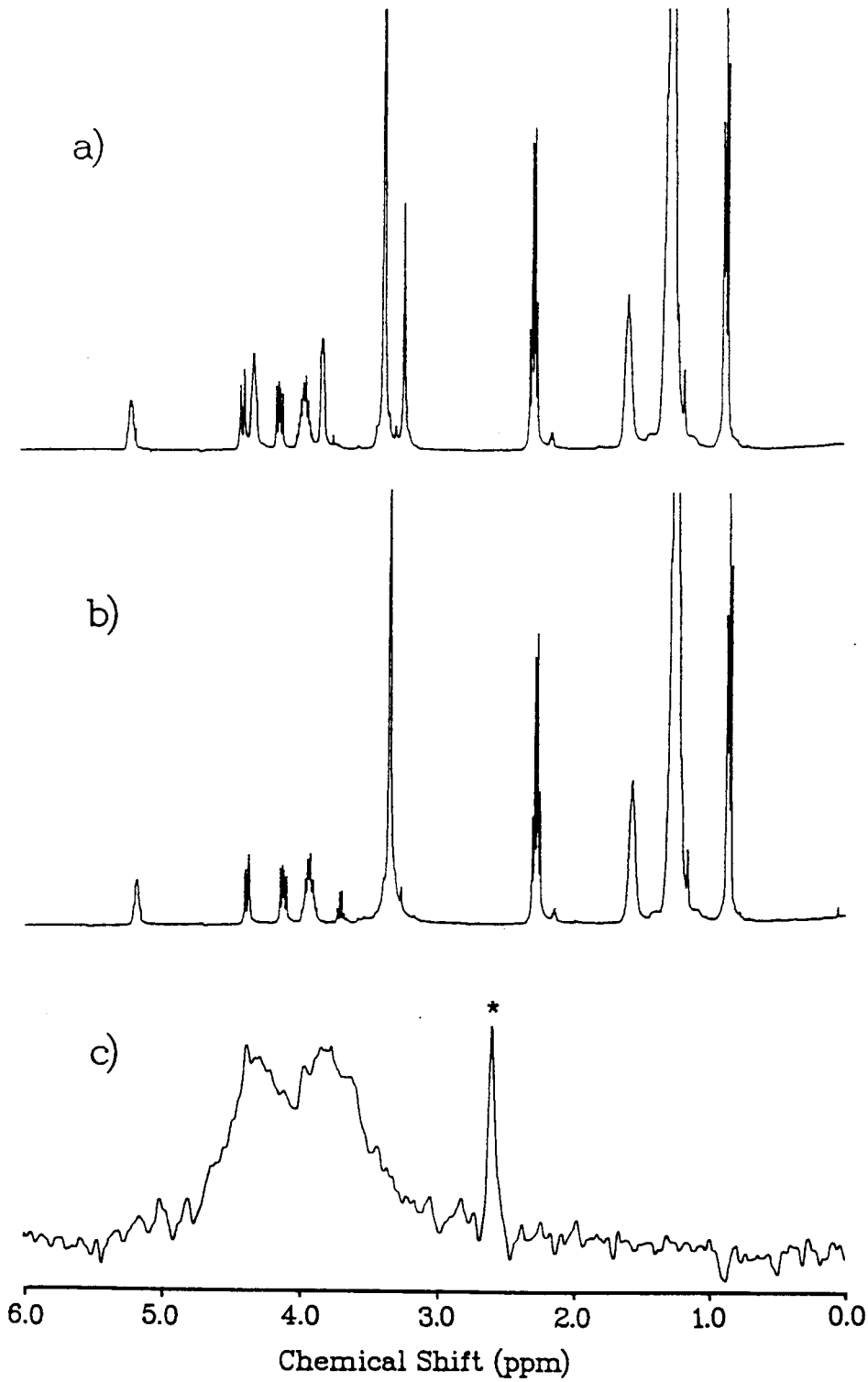
a)
b)
c)
*
6.0
5.0
4.0
3.0
2.0
1.0
0.0
Chemical Shift (ppm)

taken to dryness by evaporating the solvent under reduced pressure, and the residue was further dried under high vacuum. Crude DPPC-d_4 bromide was further precipitated in chloroform solution (5 ml) by adding cold acetone (35 ml). The DPPC-d_4 bromide precipitate was then purified by column chromatography on silica gel (60-200 mesh) with chloroform-methanol-25% ammonium hydroxide (70:26:4 by vol.) to provide the zwitterionic form of DPPC-d_4 (0.75 g, 55.6%).

TLC analysis (silica gel with chloroform/methanol/water, 65:25:4, by vol.) of the purified DPPC-d_4 showed a single spot at R_f = 0.29. The proton NMR spectrum of DPPC-d_4 was identical to that of an authentic sample of DPPC (Sigma), except for loss of signals at 4.31 and 3.81 ppm. A deuterium NMR spectrum of DPPC-d_4 showed the chemical shifts at 4.3 and 3.8 ppm (Figure 9c). Both ^1H NMR and ^2H NMR confirmed existence of the deuterated choline methylenes (>NCD_2CD_2-O-).

5. Preparation of multilamellar dispersions

Aqueous multilamellar dispersions of deuterated phospholipid (PC-d_{31} or DPPC-d_4) and deuterated phospholipid incorporated with branched chain compounds (phytol or phytanic acid) were prepared according to the following two methods.

A. Method I: Preparation of 50 wt% dispersions.

The general procedure was employed to prepare 50 wt% dispersions of 20 mol% phytol:PC-d_{31} in DDW. PC-d_{31} (≈150-200 mg) was dissolved in a chloroform solution of phytol (purified on a silica gel column, eluted with ether-hexane (3:4 by vol.)) to bring the mole ratio of phospholipid:phytol to 4:1. The solution was evaporated to a thin film in a test tube using a stream of dry nitrogen, and the film was further dried under high vacuum overnight. Deuterium depleted water (DDW) , equal in weight to total lipid, was added to make 50 wt% dispersions. The sample was mixed to homogeneity at a temperature above the gel to liquid crystalline phase transition temperature (45^{0}C) using a spatula and a vortex mixer. The sample was sealed in an NMR tube and heated to 50^{0}C for two hours to ensure that the hydration of the phospholipid had reached equilibrium. The sample was stored at -18^{0}C until used for the NMR experiments.

The procedures for preparation of 50 wt% dispersions of PC-d_{31}, 5 mol% phytol:PC-d_{31}, 5 mol% phytanic acid:PC-d_{31} and 20 mol% phytanic acid:PC-d_{31}, and 40 wt% dispersions of DPPC-d_4, all in DDW, were similar, except that the amount of DPPC-d_4 used was ≈80 mg.

B. Method II: Preparation of 15 wt% dispersions

DPPC-d_4 (70-80 mg) was used to make ≈30 wt% dispersions in DDW or Tris buffer[1] in DDW (pH 7.4) according to method I. Then another 3.5 ml of DDW (or Tris buffer) was added stepwise in portions of 0.5, 1, 1 and 1 ml. For each step the dispersions were vortexed to homogeneity. Five freeze-thaw cycles (liquid nitrogen/45°C) and vortex mixing at 45°C were applied to the dispersions. Then, the dispersions were centrifuged at 45,000 rpm for 3 hr at 25°C, in a Ti 75 rotor. The resulting pellet (≈0.5 ml) was collected and transferred to an NMR tube. The sample was sealed and stored at -18°C until used for the NMR experiments. Samples made in this way are referred to as ≈15 wt% dispersions in the text.

Particle sizes of the multilamellar dispersions were determined using a Zeiss Phase Contrast Microscope, calibrated by a standard stage scale. Mean diameters were calculated by counting 200-300 particles.

6. Preparation of phospholipid unilamellar vesicles

Unilamellar vesicles of DPPC and DPPC containing 20 mol%

---

[1]25 mM tris(hydroxymethyl)aminomethane / tris(hydroxymethyl)aminomethane hydrochloride in DDW, pH 7.4.

of phytol (phytanic acid) were prepared by sonication. DPPC (≈300 mg) was dispersed in 5 ml of water using method I, above. The homogenous suspension was sonicated until the suspension became clear (2 hrs; 50% duty cycle) under nitrogen using a Heat Systems model W-375 sonicator at a power output control setting 4. The temperature was maintained above the phase transition of DPPC (45-50^{0}C). The solution was centrifuged on a clinical centrifuge for 10 min to remove multilamellar dispersions of DPPC and titanium particles, and then filtered through a 0.22 μm Milipore filter. The procedures for preparation of unilamellar vesicles of 20 mol% phytol:DPPC and of 20 mol% phytanic acid:DPPC were similar to the above except that the sonication time was 50 min. The vesicle samples were examined by TLC to make sure that no lysoPC was formed during sonication. The vesicle samples were stored in a water bath at 45-48^{0}C prior to NMR experiments.

Particle size of the unilamellar vesicles was measured by Quasi-Elastic Light Scattering using a Nicomp Model 270 Submicron Particle Sizer. The scattering angle was 90^0. The autocorrelation function was analysed using 64 channels and evaluated by a Gaussian analysis. Mean diameter ± standard deviation was obtained from the Guassian analysis. Usually 10 repeated runs were taken for each of the samples, and mean diameter and standard deviation were averaged values from ten runs.

7. Nuclear magnetic resonance spectroscopy

A. ^2H NMR

^2H NMR experiments were performed at 38.8 MHz using a Nalorac 5.9 T superconducting magnet and a home-built spectrometer. The temperature of all the experiments was controlled to an accuracy of ±0.5°C, with a nitrogen or air flow, by a solid state temperature controller built by the SFU Electronic Shop. Samples were allowed to equilibrate for 20-30 min at a given temperature. Normally, spectra were recorded as a function of temperature. Sometimes when a relatively low temperature spectrum was recorded following a relatively high temperature run, the sample needed to be cooled down lower than the desired temperature then heated up to that temperature in order to avoid hysteresis effects. Spectra were measured using the quadrupolar echo pulse sequence 90^0_y-τ-90^0_x-t (Davis *et al.*, 1976) and a broadband probe with a horizontally mounted coil. The 90^0 pulse was 6.5 μs or 7.5 μs depending on the size of the coil. The spectral parameters are given in the Figure legends. Data collection was accomplished with a Nicolet Explorer IIIA digital oscilloscope. For the experiments of acyl chain deuterated PC the spectra were recorded in one channel mode. Fourier transforms were performed using a Nicolet BNC-12 computer. After modification

of the instrument, a Vaxstation I microcomputer was used as the data acquisition and processing system (Sternin, 1988). In the new system a CYCLOPS phase alternating pulse sequence was used to eliminate the imperfections due to phase and length of the rf pulse (Hoult and Richards, 1975; Rance and Byrd, 1983). Quadrature detection was used in the modified system, however most of the spectra presented in this thesis were symmetrized by zeroing the out of phase channel and reflecting the spectra about the carrier frequency, resulting in an increase in the signal to noise ratio of $\sqrt{2}$. The frequency of the spectrometer was adjusted to be at the center of the symmetrical powder pattern. The symmetrized spectra were compared with the non-symmetrized spectra to ensure that no distortion was induced by the folding process.

Prior to Fourier transformation the FID data points were shifted, so that the initial point in the data set was at the top of the echo, thus eliminating distortion of the spectra (Davis, 1983). In the VAX system, the FID data points went through a phase correction routine before they were shifted. Spectral moments were calculated on either the Nicolet BNC-12 computer or Vaxstation I microcomputer according to the following equation:

$$M_n = \int_0^\infty \omega^n f(\omega)\, d\omega \;/\; \int_0^\infty f(\omega)\, d\omega \qquad (21)$$

where $f(\omega)$ is the spectral intensity at frequency ω. Phase transitions were measured from the M_1 curves with the

following definitions: T_s = transition onset temperature, the intersection determined from extrapolation of gel phase M_1 and transition region M_1; T_f = transition completion temperature, the intersection of transition region M_1 and liquid crystalline phase M_1. Depaking was performed on an IBM 4341 computer to calculate the "aligned" ^2H NMR spectrum from the "random" powder pattern spectrum using a program by Sternin (1982). Data were transferred between the Nicolet or Vaxstation I and the main frame via an interface routine written by Dr. I. Gay (Chemistry, SFU) or via Kermit. Generally six iterations were performed for calculating the depaked spectra. Order parameters S_{CD} were calculated from the quadrupolar splitting of the "aligned" spectra using the following equation (Seelig, 1977):

$$\Delta\nu_Q = (3/2)(e^2qQ/h)S_{CD} \qquad (31)$$

where $\Delta\nu_Q$ is the quadrupolar splitting in the depaked spectra.

Spin-lattice relaxation time, T_1, was measured at 38.8 MHz using the inversion-recovery quadrupolar echo sequence 180^0_y-τ_1-90^0_y-τ-90^0_x-t. Either the FID echo height (below the phase transition temperature) or the spectral peak intensity (above the phase transition temperature) was used to calculate T_1 from the expression

$$A(\tau_1) = A(\infty)\ [1 - 2\exp(-\tau_1/T_1)] \qquad (32)$$

where $A(\infty)$ is the intensity at the longest τ_1 value. The delay time, t, was adjusted to be longer than $5T_1$. The details are given in the Figure legends and table notations. Transverse relaxation time, T_{2e}, was determined from the initial slope of the semi-log plot of $A(2\tau)$ *versus* 2τ using the expression

$$A(2\tau) = A(0)\ \exp(-2\tau/T_{2e}) \qquad (33)$$

where A(0) is the maximum echo intensity. The range of τ values employed depended on the samples and on the temperatures at which measurements were taken. The details are given in the Figure legends and table notations.

B. ^{31}P NMR

^{31}P NMR spectra were acquired at 102.2 MHz on the home-built spectrometer. The spectra were collected without proton decoupling using a broad band probe. The simulated spectra were generated using a computer program obtained from Dr. Burnell. Burnell *et al.* (1980) were able to simulate experimental spectra of DOPC vesicles for different temperatures and viscosities of the medium or different sizes.

8. Diffusion study of PC in the presence of branched chain compounds

Diffusion measurements of PC-d_{31}, with or without incorporation of branched chain compounds, were performed on the multilamellar liposome samples by ^2H NMR using $T_2^{q\text{-}CPMG}$ pulse program (Bloom and Sternin, 1987) and a modified DANTE pulse program (see Chapter II). The lateral diffusion coefficients, $D_\parallel$, for DPPC in the presence of branched chain compounds were calculated for vesicle samples from the simulation of their ^{31}P NMR spectra.

9. Differential scanning calorimetry (DSC)

DSC was performed over the heating range from -30°C to 60°C on a Dupont Instruments Series 99 Thermal Analyzer fitted with a 910 DSC accessory. Both temperature and enthalpy measurements were calibrated with gallium as the standard (T_m = 29.8°C, ΔH = 19.2 cal/g). DSC traces were measured with 1 - 2 mg samples of 50 wt% phospholipid multilamellar dispersions in hermetically sealed sample pans. For enthalpy measurements ≈5 mg of sample was employed. Each sample was heated at a rate of 5°C/min. The temperature of maximum heat absorption was defined as T_m. T_s and T_l were determined by the intersections of the extrapolated endothermic peak and the baseline. The

weight of phospholipids in the sample pan was determined with two methods: (1) from the difference between the sample weight and the water weight, (2) phosphorus analysis. In method one water weight was calculated from the ice melting peak, assuming that 11 moles of water are tightly bound to 1 mole of PC (Ruocco and Shipley, 1982), and that this fraction of the water is not seen in the 0^0C DSC peak (Ladbrooke and Chapman, 1969). In some cases method two was utilized, *i.e.*, the amount of phospholipid in the sample pan was determined by phosphorus analysis as described by Ames (1966). Good agreement between these two methods was observed.

The entropy change ΔS of the phase transition was calculated using the equation

$$\Delta S = \Delta H/T_m \qquad (34)$$

where ΔH is the transition enthalpy determined from the area under the endothermic peak. The peak areas were measured by planimetry.

IV. The Effects of Branched Chain Compounds on Acyl Chain Perdeuterated Phosphatidylcholine Membranes

1. Differential scanning calorimetry

The effects of phytanic acid and of phytol on the thermotropic phase transition of PC-d_{31} were studied with Differential Scanning Calorimetry (DSC). Phospholipid multilamellar dispersions (≈50 wt% in DDW) of PC-d_{31} and PC-d_{31} containing various amounts of phytanic acid or phytol were prepared at 50°C. PC-d_{31} was synthesized by condensing [$^2H_{31}$]palmitic acid to the *sn*-2 position of egg yolk lysoPC. [$^2H_{31}$]palmitic acid is 97% pure, with the remaining 1% of perdeuterated pentadecanoic acid and 2% of perdeuterated heptadecanoic acid. The *sn*-1 position is palmitoyl/stearoyl ≈ 3:1. The properties of PC-d_{31} closely resemble those of DPPC (Thewalt *et al.*, 1985). The DSC trace of PC-d_{31} (the curves in both Figure 10a and 11a) shows a pretransition onset at 30.5°C, a main gel to liquid crystalline phase transition onset T_s at 39.3°C, and a completion temperature T_l at 43.0°C. Figures 10 and 11 show that concentrations of phytanic acid and phytol as low as 1 mol% introduce a visible perturbation in PC-d_{31}, both pre- and main transition temperatures decrease (the curves 10b and 11b). As the concentration of branched chain compound increases further, the pretransition of PC-d_{31}

Figure 10: Differential scanning calorimetry trace of multilamellar dispersions of 50 wt% PC-d_{31} (a) and PC-d_{31} incorporated with different concentrations of phytanic acid: 1 mol% (b); 5 mol% (c); 10 mol% (d) and 20 mol% (e).
Scanning rate was 5^0C/min over the range of -30 to 60^0C.

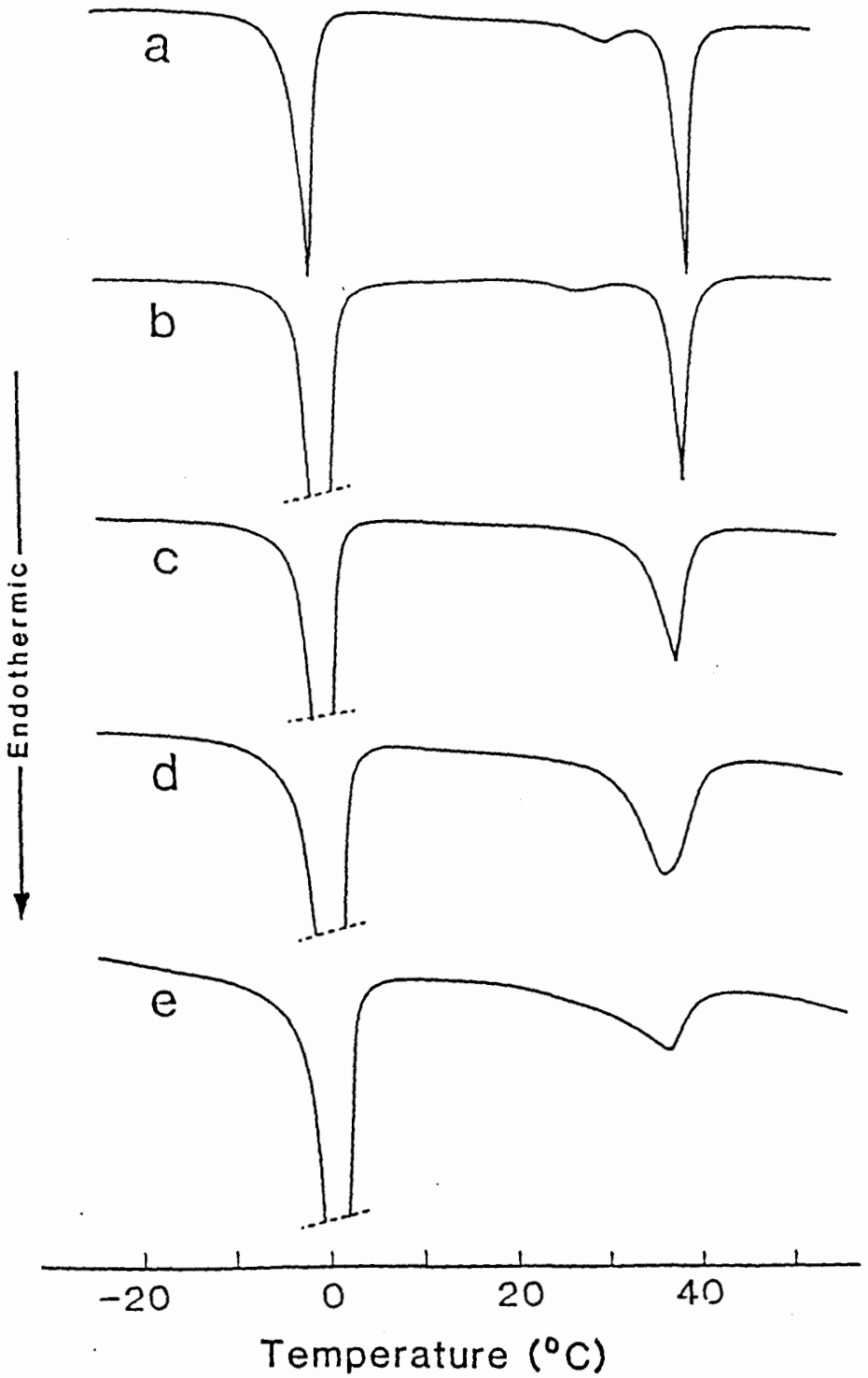
a
b
c
d
e
Endothermic
−20
0
20
40
Temperature (°C)

Figure 11: Differential scanning calorimetry trace of multilamellar dispersions of 50 wt% PC-d_{31} (a) and PC-d_{31} incorporated with different concentrations of phytol: 1 mol% (b); 5 mol% (c); 10 mol% (d) and 20 mol% (e).
Scanning rate was 5^0C/min over the range of -30 to 60^0C.

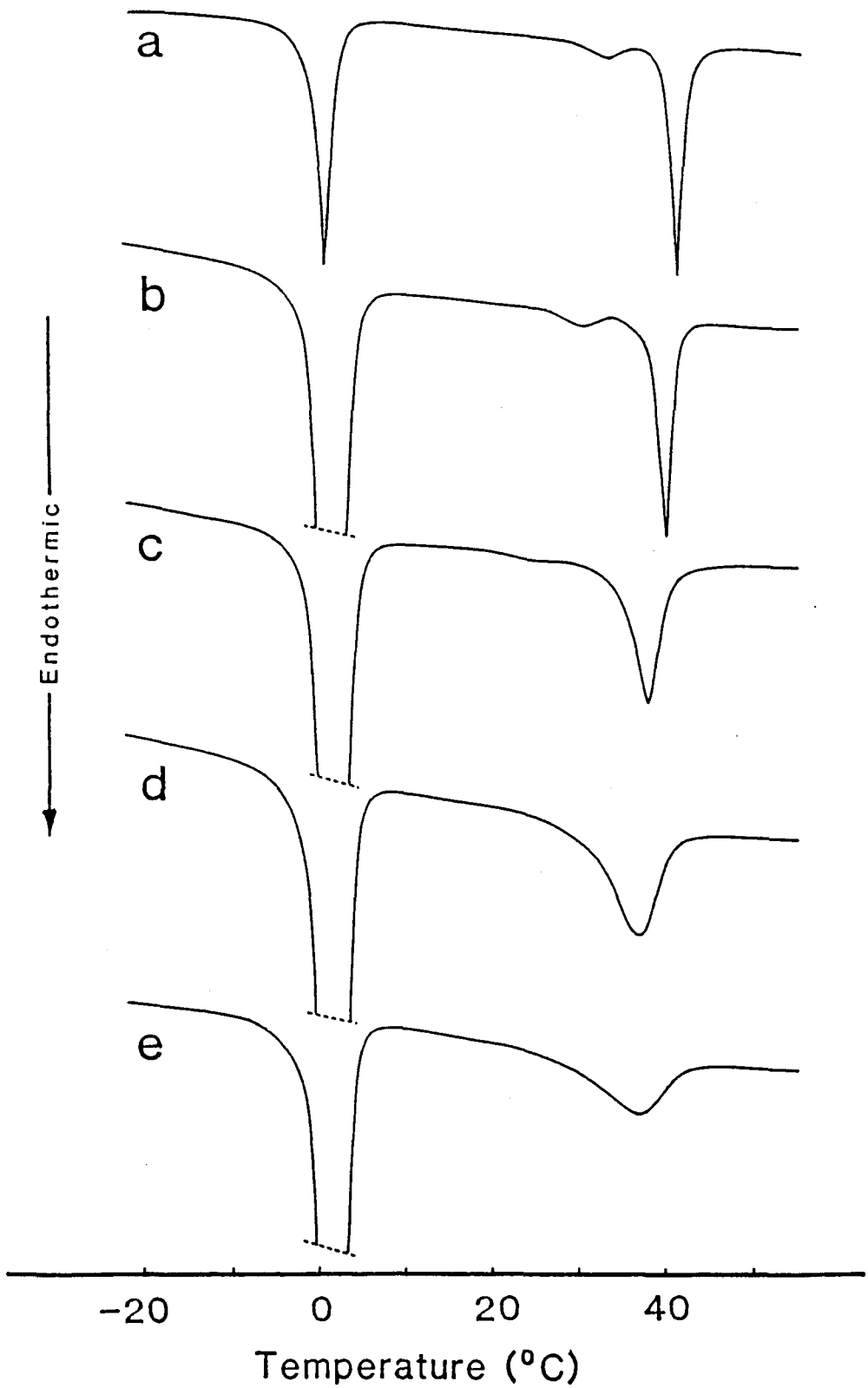
a
b
c
d
e
Endothermic
-20
0
20
40
Temperature (°C)

is eliminated and the main transition is further broadened and shifted to lower temperature. For example, the values of T_s for 20 mol% phytanic acid and for 20 mol% phytol have been lowered to 28.3°C and 27.3°C, respectively, from the T_s of 39.3°C for PC-d_{31}. In both cases the half height width of the transition has been broadened to 8°C from 1.7°C for PC-d_{31}.

Table I summarizes the thermodynamic parameters obtained from the DSC measurement. As shown in Figure 10, Figure 11 and Table I, the phase behavior of PC-d_{31} is very sensitive to the incorporated branched chain compounds. Especially for the pretransition, 1 mol% of phytanic acid reduces the onset of the pretransition by 5°C while 5 mol% of phytanic acid eliminates the pretransition. Furthermore, phytol exhibits a slightly weaker effect on the pretransition of PC-d_{31} than that of phytanic acid. The pretransition is still detected at 5 mol% incorporation of phytol as shown in Figure 11c.

The rationale for the effect of the incorporation of a branched chain compound on the pretransition is attributed to steric hindrance in the phospholipid head group region. Comparison of the phase behavior between PC and phosphatidylethanolamine (PE) might help one to understand the effect on the pretransition. PC possesses both a pre- and a main transition, whereas PE has only a main transition at temperatures 20-25°C higher than PC. PC has a larger head group than PE has, the pretransition has been suggested to be a consequence of steric hindrance in the head group region of

Table I: Thermodynamic Parameters Relating to the Phase Transition of PC-d_{31} Multilamellar Dispersions

Phytanic Acid in PC-d_{31} (mol%)	Transition Temperature (DSC) pre- (onset) (^{0}C)	main T_s (^{0}C)	main T_m (^{0}C)	main T_l (^{0}C)	Enthalpy of Transition pre- (kcal/mole)	Enthalpy of Transition main (kcal/mole)	Entropy of Transition main (cal/mole^{0}K)
0	30.5	39.5	41.4	43.0	1.5	8.8	28
1	25.4	38.4	40.2	41.8	1.2	8.6	28
5		35.2	38.5	41.0		8.3	27
10		32.2	36.5	41.2		7.8	25
20		28.3	36.3	40.0		7.4	24
Phytol in PC-d_{31} (mole)							
1	26.6	38.1	40.1	41.9	1.3	8.6	27
5	19.5	34.1	37.8	40.8	0.6	9.2	30
10		30.8	37.1	40.8		8.8	28
20		27.3	37.1	41.8		7.9	25

T_s = onset temperature of gel to liquid crystalline phase transition
T_m = temperature of maximum heat absorption
T_l = completion of transition

PC (Chapman et al., 1974). Once either phytol or phytanic acid is incorporated into PC membranes, their molecules are situated in the lipid phase with the phytyl chains parallel to the phospholipid acyl chains, with the hydroxy or carboxyl groups located in the hydrophilic region. Consequently, incorporation of phytol or phytanic acid makes the phospholipid head group region less crowded, leading to elimination of the pretransition.

The concentration effects of phytanic acid and of phytol on the main transition of PC-d_{31} studied by DSC may be also found in Figure 12. The effects of phytol and phytanic acid are qualitatively similar: with increasing concentration of phytanic acid or phytol both ΔH and T_m are diminished (Figure 12a,b), whereas the half-height width of the transition peak is increased (Figure 12c). This observation is similar to that reported recently for another branched chain compound, i.e., of α-tocopherol (Vitamin E) (Ortiz, 1987).

Klausner et al. (1980) have used the direction of shifts in the midpoint of the phase transition curve to determine whether a free fatty acid partitions into the gel or liquid crystalline phase. According to ideal solution theory, the following equation is obtained (Klausner et al., 1980):

$$T_{mid} = T_0 \left(\frac{\Delta H}{\Delta H + RT_0 \, Ln\gamma}\right) \qquad (35)$$

where γ is the ratio of the mole fraction of solvent in the gel phase to that in the liquid crystalline phase, T_0 is the phase transition temperature of pure solvent, ΔH is the phase transition enthalpy and T_{mid} is the midpoint temperature of the phase transition. If the midpoint decreases in the presence of a solute, this indicates that the solute tends to partition into the liquid crystalline phase. We assume that Klausner's theory is applicable to our phospholipid system containing branched chain compounds, and that T_m is close to the midpoint of the phase transition. On the basis of the diminution of T_m, we conclude that either phytol or phytanic acid preferentially partitions into the liquid crystalline phase. As shown in Table I, the onset temperature T_s decreases rapidly with increasing concentration of branched chain compounds, while the completion temperature T_l decreases, but to a much lesser degree (maximum 3^0C). The diminution of T_s and T_l broadens the main transition. Such a broadening effect may be explained by the preference of the branched chain compounds for the liquid crystalline phase, which introduces a heterogeneity of the distribution of branched chain compound in phospholipid during the melting process.

The ΔH values of DPPC/water dispersions have been reported to be in the range of 1.6-2.3 kcal/mole and 8.7-9.7 kcal/mole for pre- and main transition, respectively (Phillips et al., 1969; Albon and Sturtevant, 1978; Silvius and Lyons,

Figure 12: Changes in main phase transition temperature (T_m), transition enthalpy (ΔH) and half-height width ($\Delta t_{1/2}$) of PC-d_{31} incorporated with phytol(o) and phytanic acid(•).

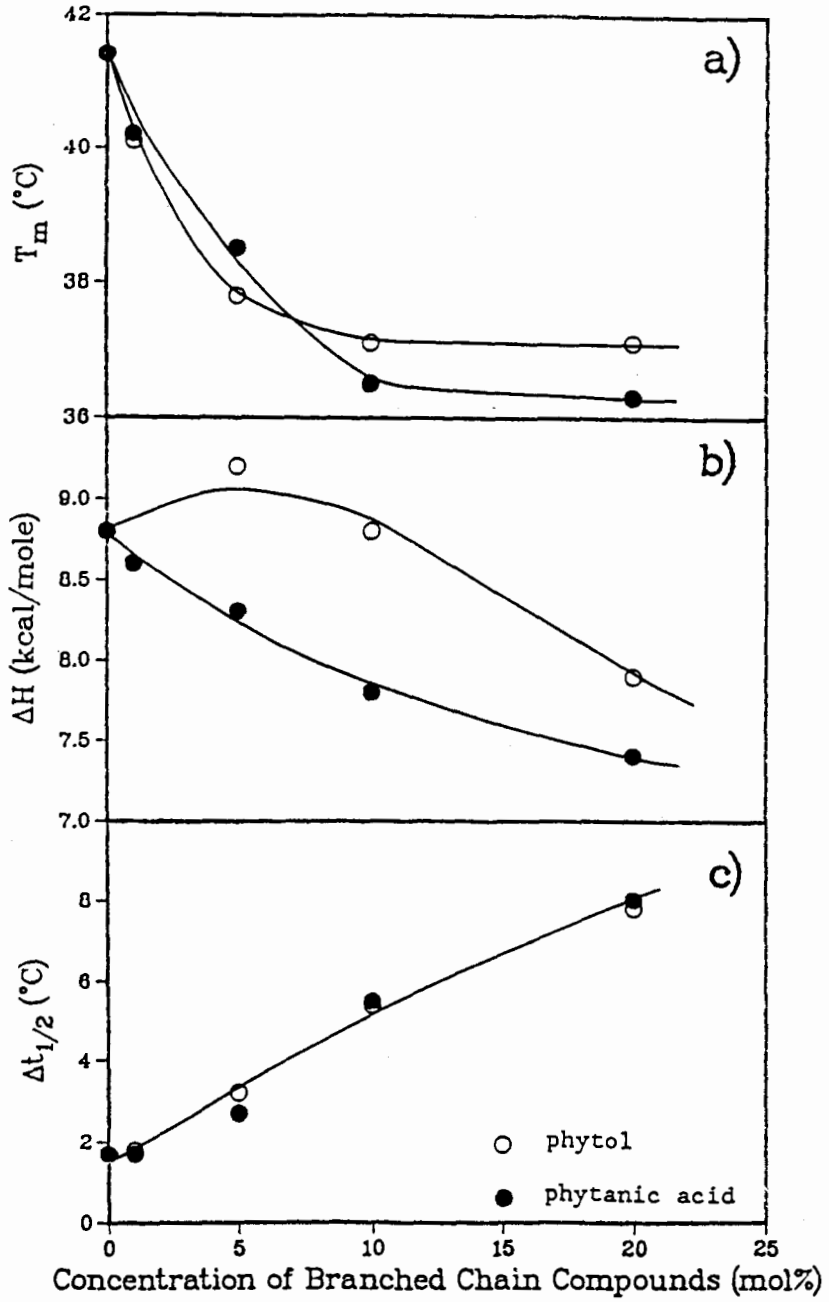

1985). ΔH for 1-stearoyl-2-palmitoyl-*sn*-glycero-3-phosphocholine (SPPC) has also been reported in the range of 7.3-8.3 kcal/mole (Stumpel *et al.*, 1983; Chen and Sturtevant, 1981). Our ΔH values for pre- and main transition of PC-d_{31} are 1.5 and 8.8 kcal/mole, respectively, which are in a good agreement with the above reported values. The main gel to liquid crystalline phase transition is a chain melting transition, and the transition enthalpy depends on the number of gauche conformations and the distance between hydrocarbon chains in the gel phase. The incorporation of phytanic acid or phytol increases the number of gauche conformations, which is supported by our ^2H NMR results (see discussion of ^2H NMR spectral moments). The monolayer surface areas of phytanic acid and phytol are 61 $Å^2$ and 55 $Å^2$ per molecule, respectively (Gaines, 1966), while the areas of one hydrocarbon chain of DPPC in the liquid crystalline and in gel phase are only 23.5 $Å^2$ and 19.5 $Å^2$, respectively (Ruocco and Shipley, 1982). Obviously, the branched chain compounds are too large to fit into the lattice arrangement of phospholipid acyl chain packing. ΔH decreases as concentration of phytanic acid increases, which implies that phytanic acid incorporated into PC-d_{31} not only acts as a defect in the gel phase structure, but also destroys the hexagonal packing arrangement. A higher concentration of phytol is necessary to achieve the same effect, as shown in Figure 12b, which is consistent with the fact of the smaller surface area of phytol than phytanic acid.

Table II: The Cooperative Unit for the Main Transition of PC-d_{31} in the Presence of Branched Chain Compounds

Phytanic acid in PC-d_{31} (mol%)	T_m (°C)	$\Delta t_{1/2}$ (°C)	CU
0	41.4	1.7	46
1	40.2	1.7	46
5	38.5	2.7	30
10	36.5	5.5	15
20	36.5	8.0	11
Phytol in PC-d_{31}			
1	40.1	1.8	44
5	37.8	3.2	23
10	37.1	5.4	14
20	37.1	7.8	11

The DSC data may be described in terms of the cooperative unit. The cooperative unit (in molecules), CU, equals $\Delta H_{vH}/\Delta H_{cal}$, where $\Delta H_{vH} \approx 6.9\ T_m^2\ /\ \Delta t_{1/2}$. ΔH_{vH} is the standard enthalpy change in a two-state phase change (Mabrey and Sturtevant, 1978). CU is a measure of the degree of intermolecular cooperation between phospholipid molecules in a bilayer. Since the CU value is very sensitive to the

presence of impurities and the measurement of CU is also limited by an instrument, the CU values which we measured may not be comparable with the values reported by others. The comparison within this study, however, is still valuable. Table II lists the results of our calculations. The trend of the CU values indicates a monotonic reduction in intermolecular interactions of phospholipid by phytanic acid and phytol. As shown in Table I, the enthalpy of the pretransition decreases rapidly with increasing concentration of branched chain compounds, the cooperative property of the pretransition is more affected by the branched chain compounds than that of main transition.

2. Deuterium nuclear magnetic resonance

A. Results

Representative ^2H NMR spectra for 50 wt% multilamellar dispersions (in DDW) of PC-d_{31}, 20 mol% phytol:PC-d_{31} and 20 mol% phytanic acid:PC-d_{31} were recorded as a function of temperature, as shown in Figure 13. Table III lists the quadrupolar splittings ($\Delta\nu_Q$) for the three samples at all temperatures studied.

At -5°C, the spectrum for PC-d_{31} (Figure 13a) has a broad component with edges at ±63 kHz and a central component of high intensity with $\Delta\nu_Q$ ≈17 kHz (Table III). The broad component is characteristic of C^2H_2 groups of which the lineshape provides evidence that a large fraction of the chains are static on the ^2H NMR time scale, while the narrow component corresponds to the C^2H_3 moiety undergoing significant motion. At 20°C, a gel-state spectrum is obtained for PC-d_{31} (Figure 13b) which is characterized by decreased intensity of the ±63 kHz edge and a monotonic increase in intensity toward the narrow component. Such a spectrum is not a simple powder pattern and straightforward analysis of this type of spectrum is not possible (Davis, 1983). The spectra for PC-d_{31} show the same overall gel state pattern from 20 to 37°C with an abrupt change to liquid crystalline state spectrum occurring at

Figure 13: Temperature dependent ^2H NMR spectra of multilamellar dispersions of
(a-f) PC-d_{31}
(g-l) 20 mol% phytanic acid:PC-d_{31}
(m-r) 20 mol% phytol:PC-d_{31}.

Spectral parameters: pulse width = 6.5 μs (flip angle = 90^0); τ, the interval between pulses in quadrupolar echo sequences, = 75 μs; t, the delay between echo sequence, = 1 s; sweep width = ±250 kHz; data size = 2K; line broadening = 200 Hz, number of acquisitions = (a,i,q)2000, (j,k,l)500, (m,r)1500, others,1000.

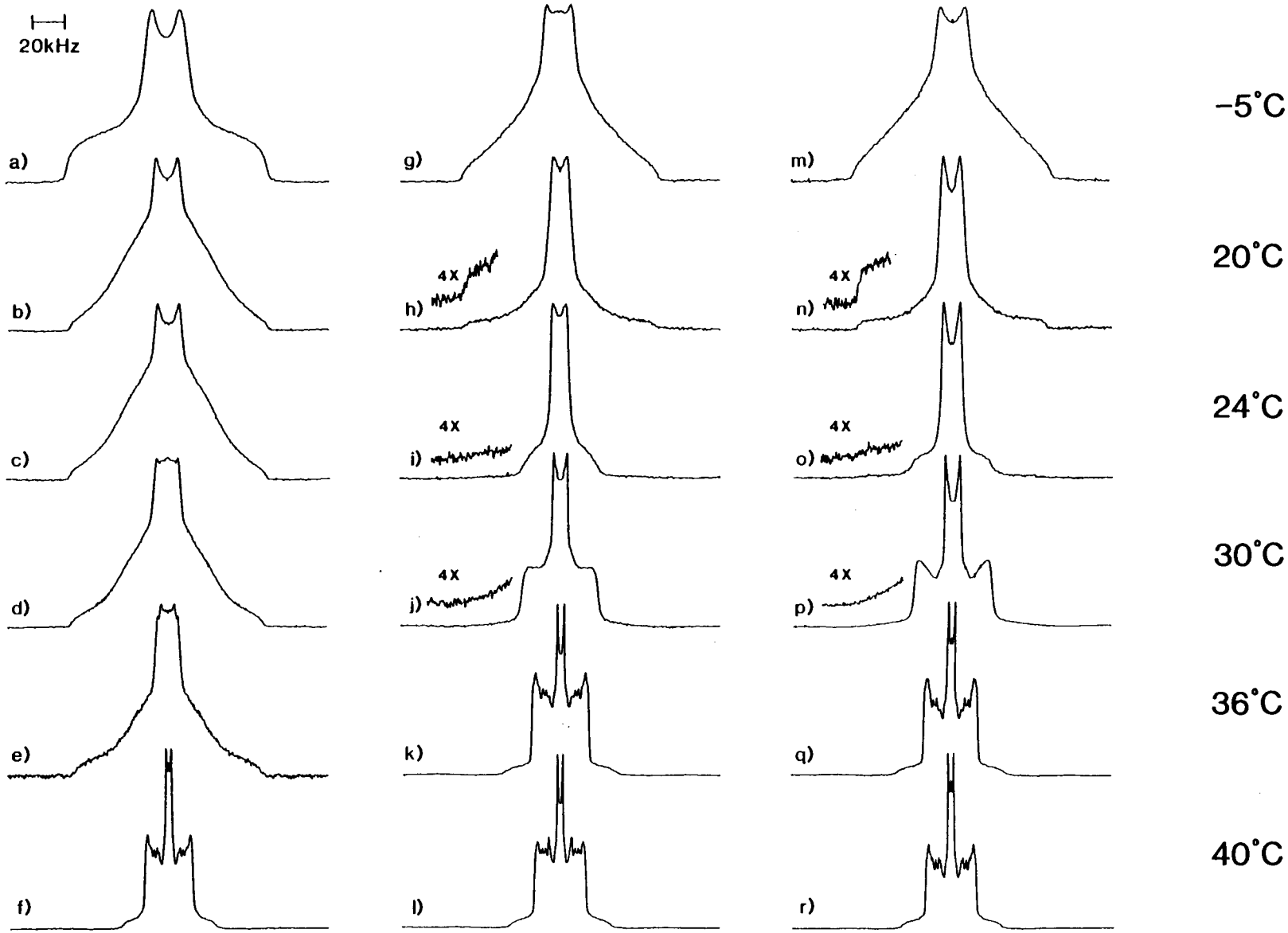
20kHz
a)
b)
c)
d)
e)
f)
g)
h)
i)
j)
k)
l)
m)
n)
o)
p)
q)
r)
4X
-5°C
20°C
24°C
30°C
36°C
40°C

Table III: Quadrupolar Splitting (kHz) of ^2H NMR Powder Patterns of PC-d_{31} Multilamellar Dispersions in the Presence of Branched Chain Compounds

PC-d_{31}			20 mol% Phytanic acid:PC-d_{31}			20 mol% Phytol:PC-d_{31}		
T(°C)	Narrow[a] peaks	Broad[b] component	T(°C)	Narrow[a] peaks	Broad[b] component	T(°C)	Narrow[a] peaks	Broad[b] component
-5	17.0	126	-5	≈8,15.5	126	-5	15.5	126
20	13.5	125	0	≈8,15.2	125	0	≈10,15.0	125
						5	≈10,14.5	125
24	13.4	125	10	≈8,14.6	123	10	13.0	123
27.5	13.2	124	12	8.3,13.4	122	15	11.0	123
30	8.5,13.2	124	20	8.4	122	20	10.2	120
32.5	8.0,12.6	122	24	8.2	120	24	10.2	120
						26	10.0	120
35	7.9,12.6	122	27.5	8.4	120	28	8.8	46.5,120
36	7.9,12.2	122	30	8.2	45.0,120	30	8.8	47.0,120
37	7.7,12.1	120	32	7.3	42.7,118	32	6.9	42.5
38	3.8	120	34	5.4	38.4	34	5.3	37.4
39	3.5	29.6	36	4.3	35.0	36	3.9	33.4
			38	3.4	31.8	38	3.5	31.3
40	3.3	28.5	40	3.3	30.5	40	3.4	30.5
42	2.9	27.5	42	2.9	29.9	42	3.2	29.0
45	2.5	25.8	45	2.8	28.3	45	3.0	28.0
50	2.3	24.8	50	2.4	27.0	50	2.6	27.5
55	2.0	23.9	55	2.3	26.0	55	2.3	25.9

[a] measured from the separation of the top of the peaks.
[b] measured from the edge of the broad component.

38-39°C (Figure 14). Above 39° an axially symmetric powder pattern is observed as the characteristic of PC-d_{31} in the liquid crystalline phase (Figure 13f). The liquid crystalline phase spectrum possesses well-defined sharp edges ($\Delta\nu_Q$ = 28 kHz) associated with a plateau in the variation of the order parameter, S_{CD}, with the deuterium position along the phospholipid acyl chain.

In the presence of 20 mol% phytol or phytanic acid the gel spectra occur at a much lower temperature, -5°C, than for PC-d_{31} alone (Figure 13g,m). In addition, inside the inner doublet (≈17 kHz) there is evidence, more pronounced with phytanic acid, of a second doublet, splitting ≈8-10 kHz. The equivalent situation for PC-d_{31} alone does not occur until ≈30°C (Figure 13d). The behavior of PC-d_{31} dispersions containing 20 mol% branched chain compounds is distinctly different from PC-d_{31} dispersions over the temperature range 20-30°C. At 20°C (Figure 13h,n) a gel-state spectrum is still observed but with significantly reduced intensity of the sloping, featureless component seen for PC-d_{31}. The lineshape of ^{2}H NMR spectra for 20 mol% phytol(or phytanic acid) depends on the delay time τ of the quadrupolar echo pulse sequence at 20-24°C. Figure 15 illustrates such a lineshape change for 20 mol% phytanic acid:PC-d_{31}. The spectrum of τ = 75 μs, which is the same as Figure 13h, has a much lower intensity for the broad component than that of τ = 20 μs.

Figure 14: ^{2}H NMR spectra of multilamellar liposomes of PC-d_{31} at temperatures near the gel to liquid crystalline phase transition.

Spectral parameters are the same as in Figure 13 except that the number of acquisition is 1000.

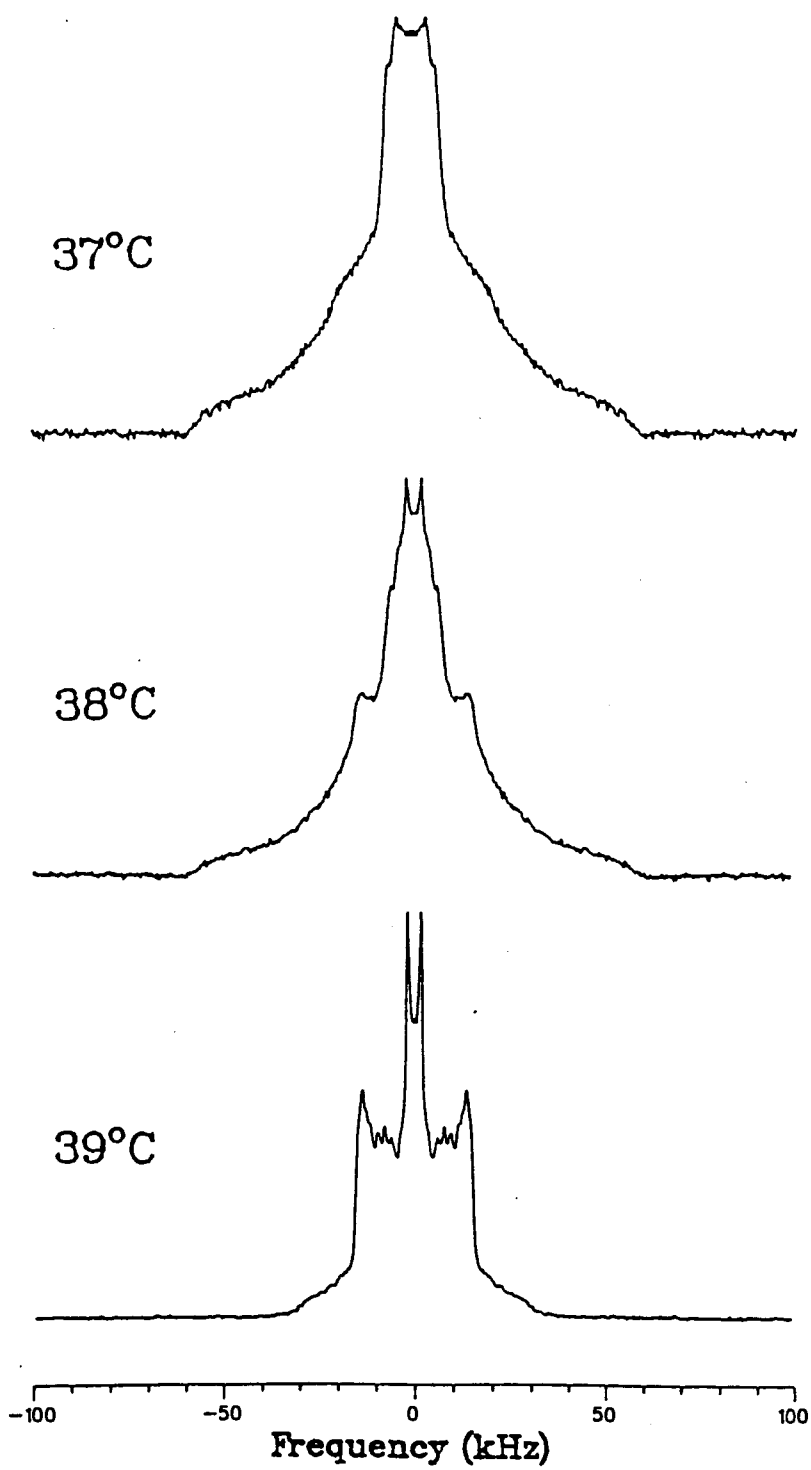
37°C
38°C
39°C
−100
−50
0
50
100
Frequency (kHz)

Figure 15: ^2H NMR spectra of 20 mol% phytanic acid: PC-d_{31} at 20°C with different τ values.

Spectral parameters are same as in Figure 13 except for the number of acquisition: 500 (τ=20μs) and 1000 (others).

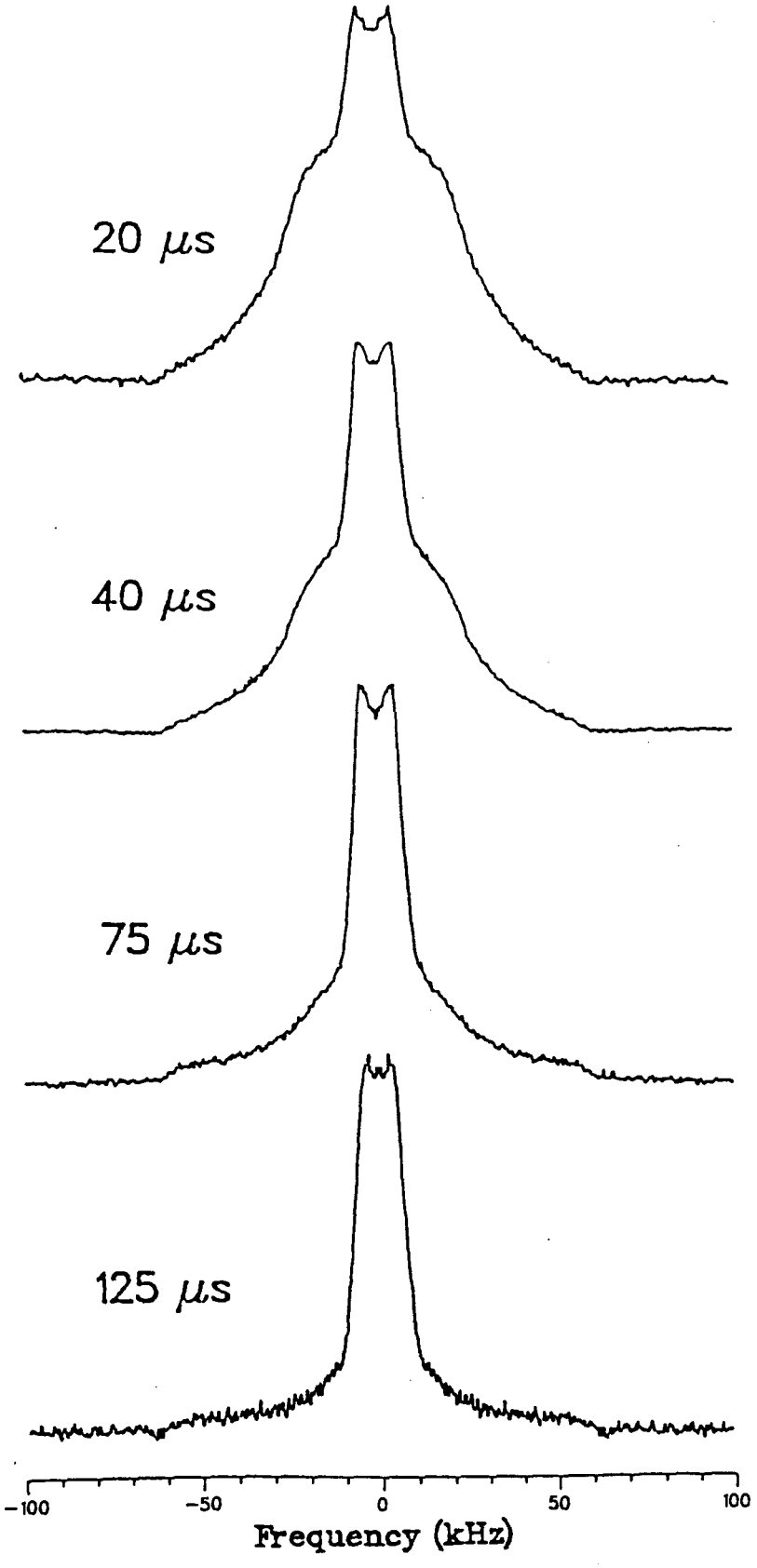
20 μs
40 μs
75 μs
125 μs
−100
−50
0
50
100
Frequency (kHz)

^{2}H NMR spectra for 20 mol% phytol(or phytanic acid):PC-d_{31} do not show an abrupt change from a gel state spectrum to a liquid crystalline spectrum. Instead, a number of gradual temperature dependent changes are exhibited. The inner C^{2}H$_3$ doublet dominates and narrows, the gel features and ±63 kHz edge gradually disappear and a new broad feature appears $\Delta\nu_Q \approx 46$-48 kHz. The significant reduction in the intensity of the broadest components compared with PC-d_{31} is attributed to T_{2e} spectral distortion (see Discussion). Over the temperature range of 20-30°C the narrow doublet splitting for 20 mol% phytanic acid:PC-d_{31} is always less than for 20 mol% phytol:PC-d_{31} at any given temperature (Table III). As temperature increases further, the characteristic liquid crystalline spectrum appears (Figure 13k,l) for the samples containing branched chain compounds but at lower temperatures than that for PC-d_{31} alone.

The temperature-dependent ^{2}H NMR spectra of 5 mol% phytol (or phytanic acid):PC-d_{31}, represented in Figure 16, also show a gradual change from a gel state to a liquid crystalline state but over a narrower temperature range than that for 20 mol% branched chain compound.

Spectral moment analysis gives a more quantitative interpretation. The first moments M_1 calculated from the ^{2}H NMR spectra for PC-d_{31}, 5 mol% phytanic acid:PC-d_{31} and 20 mol% phytanic acid:PC-d_{31} dispersions are plotted versus temperature

Figure 16: Temperature dependent ^2H NMR spectra of multilamellar dispersions of 5 mol% phytanic acid:PC-d_{31}(a-d) and 5 mol% phytol:PC-d_{31}(e-h).

Spectral parameters are the same as in Figure 13 except for number of acquisitions = (e,f)1800, others 1500.

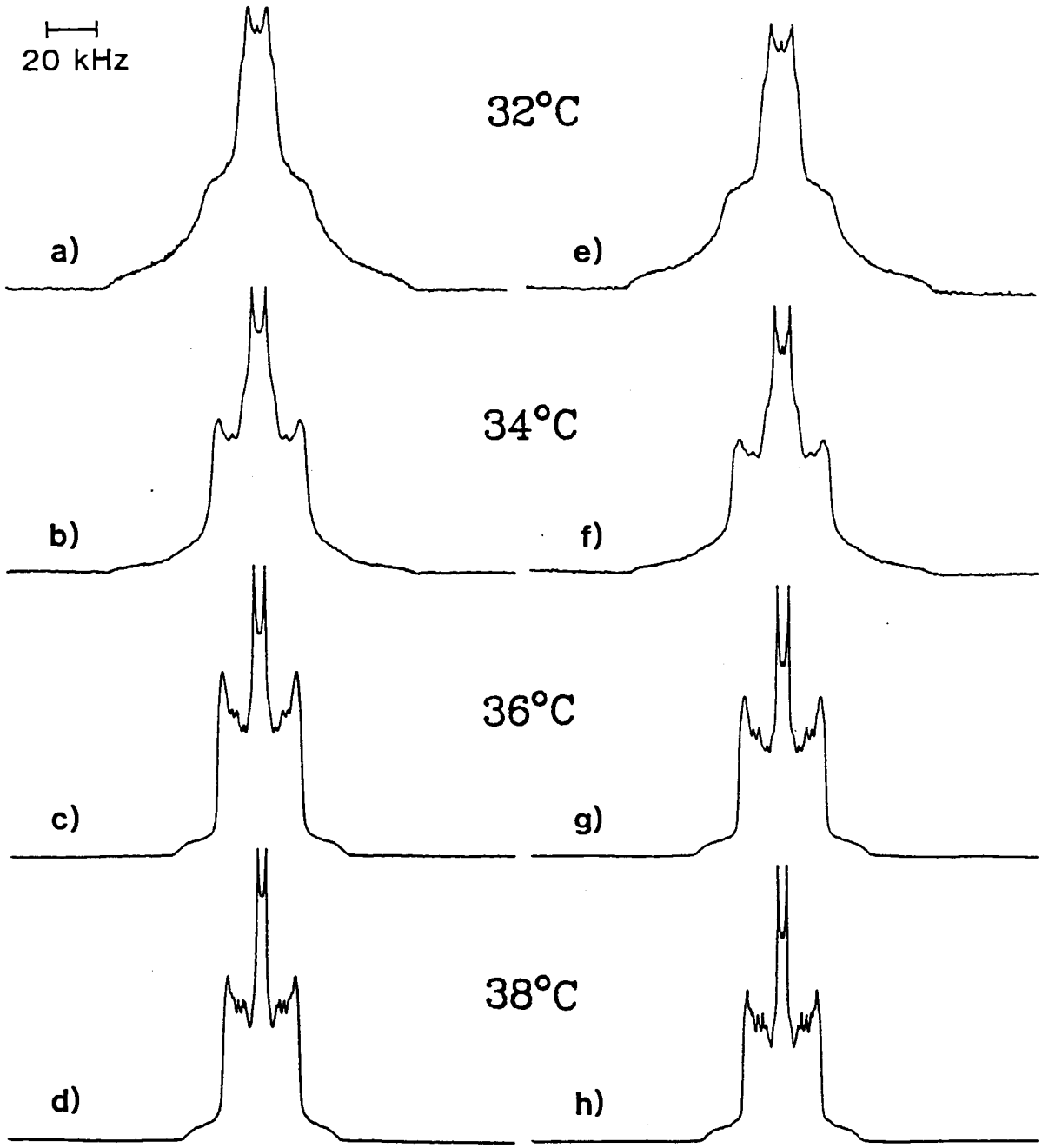
20 kHz
32°C
34°C
36°C
38°C
a)
b)
c)
d)
e)
f)
g)
h)

in Figure 17. In the phase transition region the first moment depends on the delay time τ between the two 90^0 pulses of the quadrupolar echo pulse sequence. The values plotted in Figure 17 were obtained by extrapolation to zero delay of M_1 measured as a function of τ. Figure 18 shows the extrapolation of M_1 for 20 mol% phytanic acid:PC-d_{31} at different temperatures. The uncertainty of the data is approximately 1% except in the transition temperature region where the uncertainty is approximately 5%.

Figure 17 shows that, for PC-d_{31} the first moment M_1 drops very rapidly from a gel to a liquid crystalline value at the main transition temperature over a range of approximately 1.5^0C. Also seen on the M_1 plot is an inflection point at 30.5^0C which reflects the pre-transition of PC-d_{31}. The M_1 transition range (T_l-T_s) increases with increasing phytanic acid concentration: 34-38^0C for 5 mol% phytanic acid:PC-d_{31} and 28-39^0C for 20 mol% phytanic acid:PC-d_{31}. Upon addition of phytanic acid the pretransition disappears.

A plot of M_1 versus temperature for 5 and 20 mol% phytol: PC-d_{31} (Figure 19) shows an almost identical observation to that for phytanic acid. The only significant difference appears at 20 mol% concentration at temperature range less than 25^0C, in which M_1 for phytol is greater than one for phytanic acid.

Figure 17: Variation of the first moment (M_1) with temperature for the ^2H NMR spectra of (•) PC-d_{31}, (♦) PC-d_{31} + 5 mol% phytanic acid and (o) PC-d_{31} + 20 mol% phytanic acid.

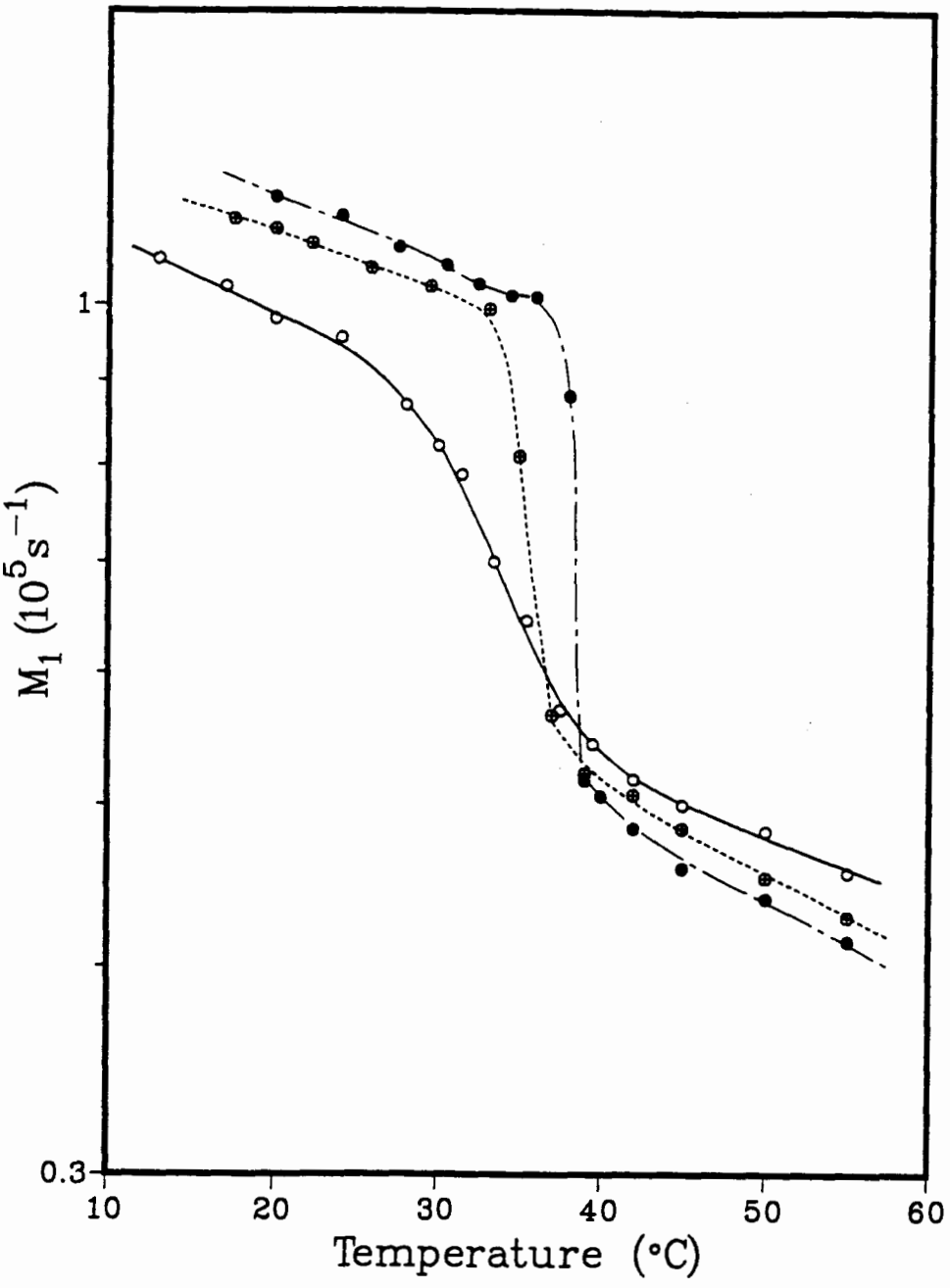

Figure 18: The extrapolation plot of M_1 as a function of pulse decay, τ for dispersions of PC-d_{31} containing 20 mol% of phytanic acid.

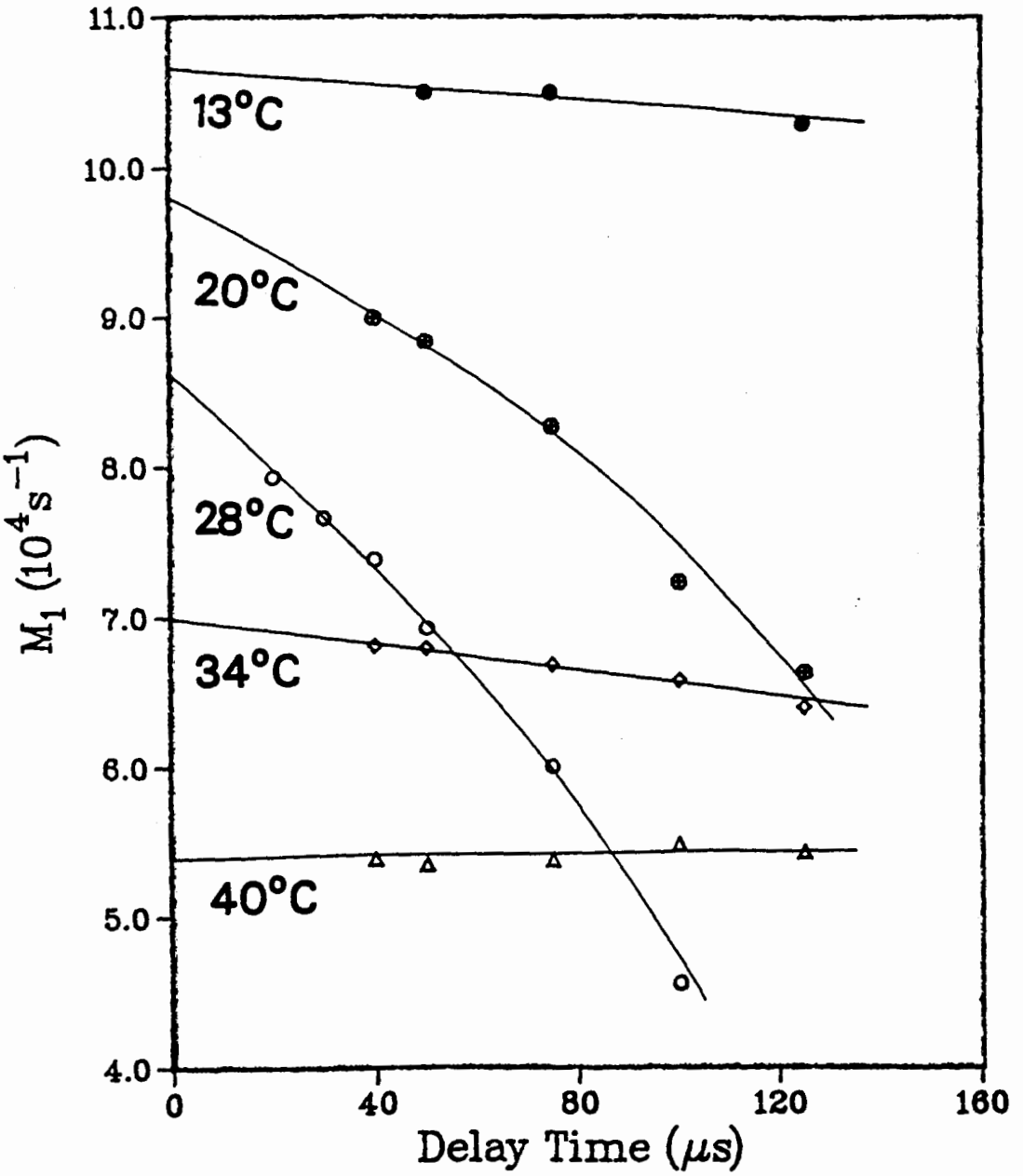

Figure 19: Variation of the first moment (M_1) with temperature for the ^2H NMR spectra of (•) PC-d_{31}, (⊕) PC-d_{31} + 5 mol% phytol and (o) PC-d_{31} + 20 mol% phytol.

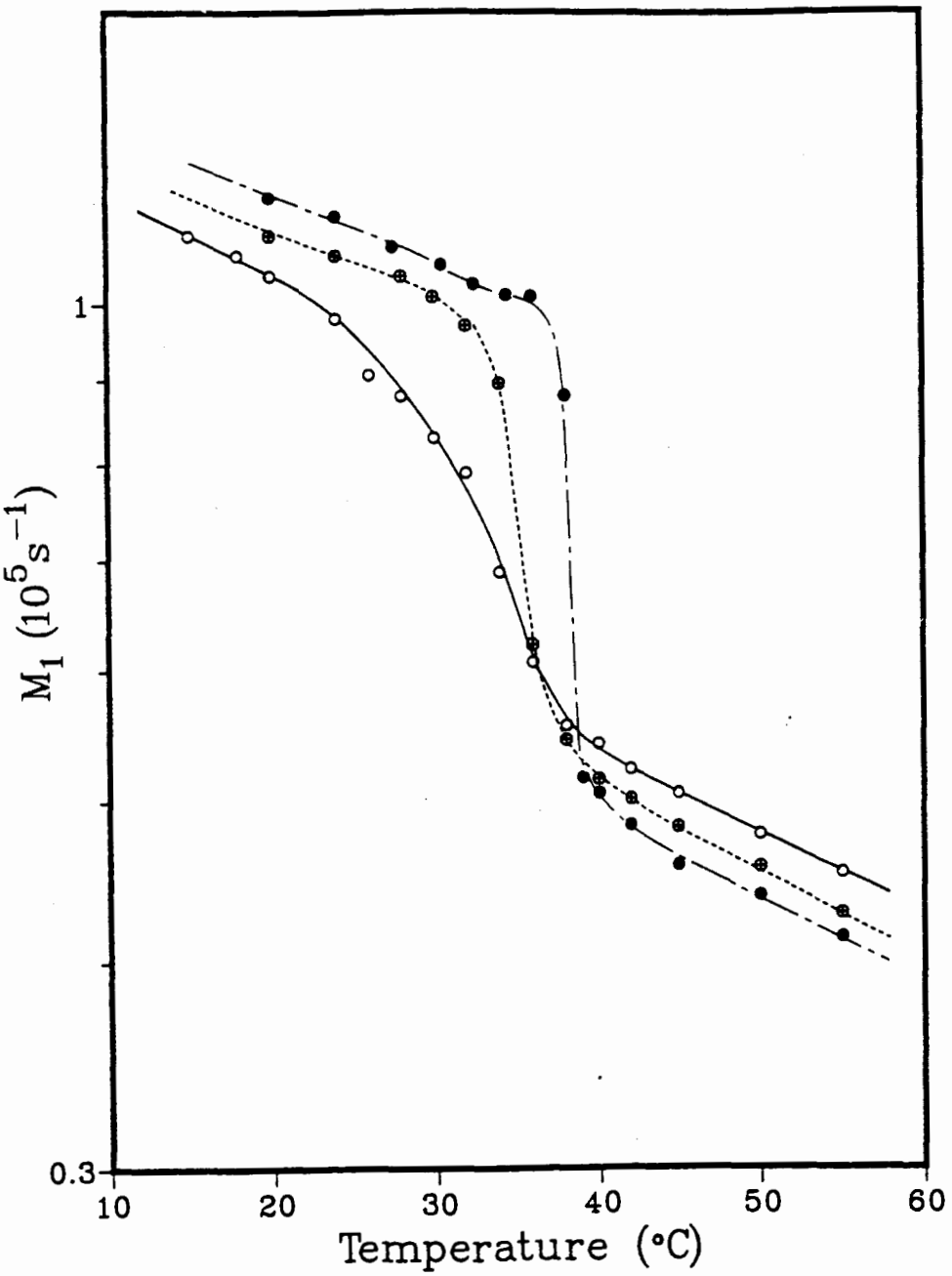

The ^2H NMR spectra of the liquid crystalline phase give information about the motionally averaged orientation of a C-^2H bond with respect to the normal to the bilayer plane. The orientational order parameter for the C-^2H along the entire sn-2 acyl chain can be deduced from a single spectrum of PC-d_{31}. Using a depaking program (Sternin *et al.*, 1983) "aligned" spectra with enhanced resolution were obtained from the powder pattern spectra. The depaked spectra for PC-d_{31}, 20 mol% phytol:PC-d_{31} and 20 mol% phytanic acid:PC-d_{31} dispersions at 50^{0}C are compared in Figure 20.

The depaked spectrum for PC-d_{31} (Figure 20a) contains five well-resolved pairs of peaks plus a broad, composite pair of outermost peaks possessing two shoulders on their inner side. The depaked spectrum of PC-d_{31} with incorporation of 20 mol% phytol (Figure 20b) is slightly different from PC-d_{31} alone. The inner peaks are better resolved than those for the latter. Also the broad outermost pair has a larger quadrupolar splitting, and the inner shoulders have grown up further. The depaked spectrum for 20 mol% phytanic acid:PC-d_{31} (Figure 20c) shows seven well-resolved doublets and the broad composite pair of outermost peaks are resolved into two pairs, indicating a longer T_{2e}. The peak assignments of the sn-2-[$^2H_{31}$]palmitoyl segments are based upon the assumption that quadrupolar splittings decrease monotonically towards the terminal methyl group except at the 2-position (Pauls *et al.*,

Figure 20: The depaked ^2H NMR spectra at 50°C of multilamellar dispersions of

(a) PC-d_{31},

(b) 20 mol% phytol:PC-d_{31},

(c) 20 mol% phytanic acid:PC-d_{31}.

Spectral parameters: pulse width = 6.5 μs (flip angle = 90°); τ, the interval between pulses in quadrupolar echo sequence, = 75 μs; t, the delay between echo sequences, = 1.5 s; sweep width = (a,c)±50 kHz, (b)±100 kHz; data size = 2K; line broadening = 50 Hz, number of acquisitions = (a)6000, (b)2000, (c) 7000.

Six iterations were performed in each depaking.

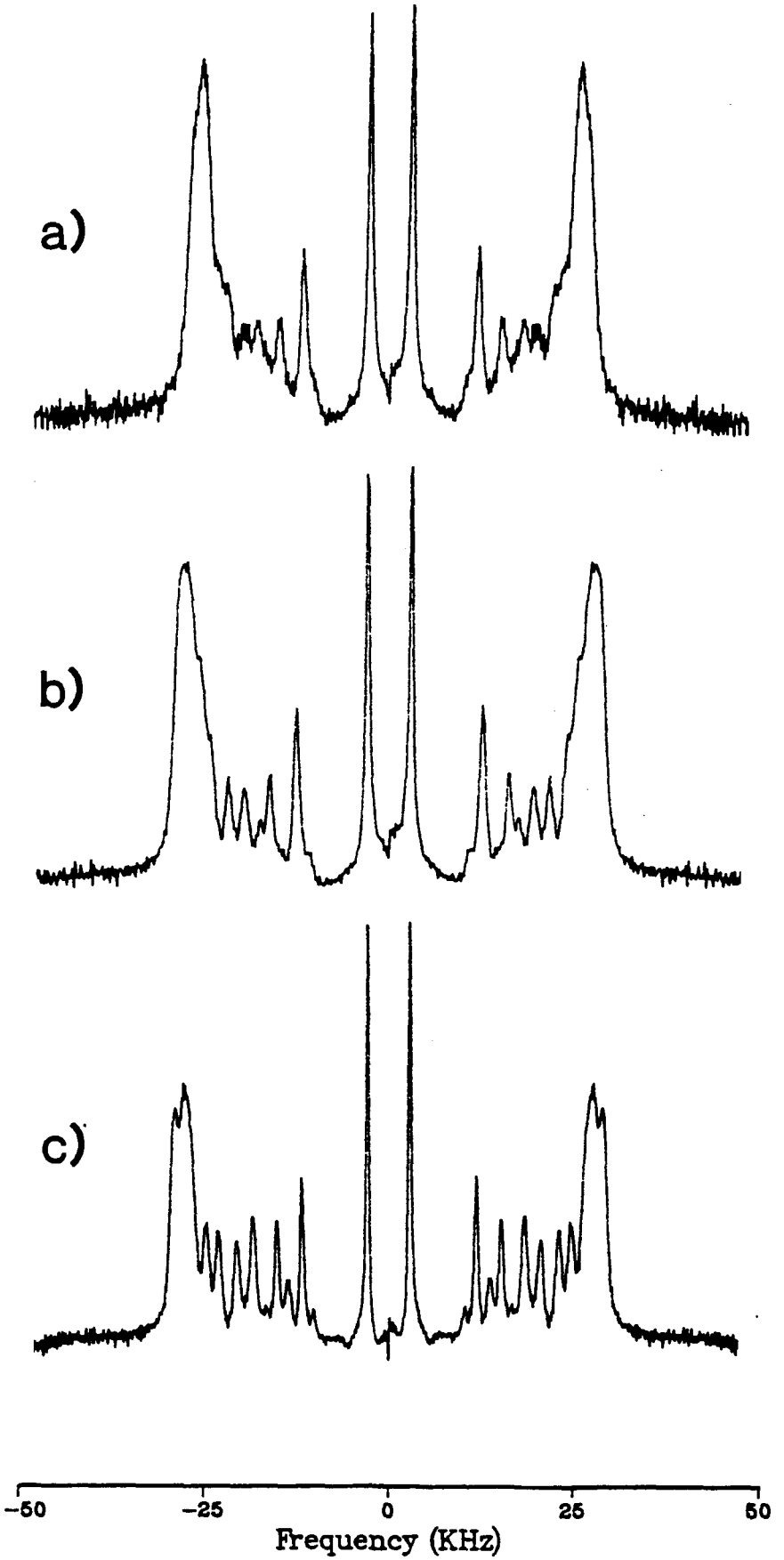
a)
b)
c)
−50
−25
0
25
50
Frequency (KHz)

1983; Thewalt et al., 1985). The respective assignments for the two broad composite pairs in Figure 20c need further study of selectively deuterated PC. The splitting of the broad composite pair indicates that the incorporated phytanic acid affects the various methylene segments in the plateau region differently. Spectra for multilamellar dispersions of PC-d_{31} containing 5 mol% of branched chain compounds at 50°C were depaked as well, and show similar features to the 20 mol% ones. The quadruple splittings, measured from the depaked spectra, are listed in Table IV.

Profiles of order parameter S_{CD} versus phospholipid acyl chain position calculated from the depaked spectra in Figure 20 are plotted in Figure 21. The vertical bar in the plateau region is used to denote the uncertainty in calculating these order parameters and is due to the width of the outermost composite peak in the depaked spectra. The shape of the profile is essentially unaffected by the incorporation of 20 mol% of branched chain compounds. The effect of branched chain compounds appears to be an overall higher degree of ordering along the lipid chain. The mean order parameters $\langle S_{CD} \rangle$, calculated from M_1 using equation (36) (Davis, 1979) are listed in Table V.

$$M_1 = \frac{4\pi}{3\sqrt{3}} \langle \Delta\nu_Q \rangle = \frac{\pi}{\sqrt{3}} \left(\frac{e^2 qQ}{h} \right) \langle S_{CD} \rangle \qquad (36)$$

Table IV: Quadrupolar Splittings for Segments of Aqueous Dispersions of PC-d_{31} and PC-d_{31} + Branched Chain Compounds at 50°C.

Acyl Chain Position	$\Delta\nu_Q$ (kHz)[a]				
	PC-d_{31}	Phytanic acid in PC-d_{31}		Phytol in PC-d_{31}	
		5 mol%	20 mol%	5 mol%	20 mol%
C-2	11.80	11.94	11.86	11.70	12.56
	18.00	18.40	18.52	17.84	19.16
C-3 to 9	25.52	27.40	28.90	25.48	27.80
		26.20	27.64		
C-10	23.44	23.70	24.62	23.24	25.64
C-11	22.10	22.38	23.20	22.16	24.00
C-12	19.64	20.14	20.66	19.80	21.76
C-13	18.00	18.40	18.52	17.84	19.60
C-14	14.84	15.22	15.22	14.88	16.16
C-15	11.80	11.94	11.86	11.70	12.56
C-16	2.76	2.80	2.80	2.76	2.90

[a] Quadruple powder pattern splitting is a half of the splitting measured from the depaked spectra.

Figure 21: Plot of order parameter (S_{CD}) at 50°C versus carbon position along the phospholipid sn-2 chain: (●) PC-d_{31}, (□) PC-d_{31} + 20 mol% phytanic acid, (o) PC-d_{31} + 20 mol% phytol.

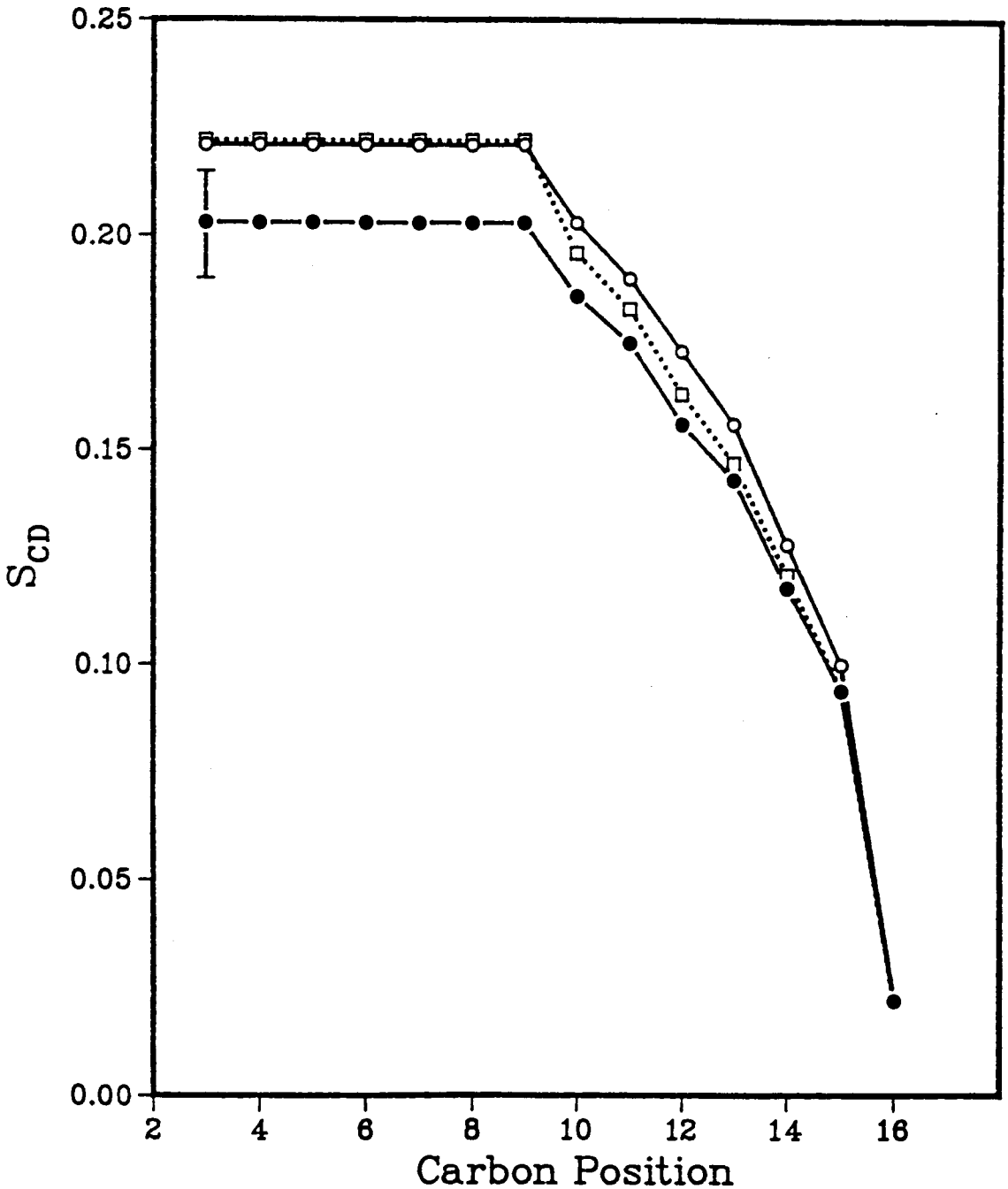

Table V: First Moment M_1 and Mean Order Parameter $\langle S_{CD} \rangle$ for PC-d_{31} Incorporated with Branched Chain Compounds at 50°C.

Sample	M_1[a] ($10^4 s^{-1}$)	$\langle S_{CD} \rangle$[a]	M_1[b] ($10^4 s^{-1}$)	$\langle S_{CD} \rangle$[b]
PC-d_{31}	4.22	0.138	4.38	0.144
5 mol% Phytanic Acid:PC-d_{31}	4.51	0.148	4.53	0.149
20 mol% Phytanic Acid:PC-d_{31}	4.62	0.152	4.78	0.157
5 mol% Phytol :PC-d_{31}	4.48	0.147	4.56	0.150
20 mol% Phytol :PC-d_{31}	4.73	0.155	4.80	0.157

[a] From the powder pattern relevant to Figure 20.
[b] From the values for extrapolation to $\tau = 0$.

The increased mean order parameters, i.e., $\frac{\langle S_{CD} \rangle - \langle S_{CD} \rangle (PC)}{\langle S_{CD} \rangle (PC)}$, of the incorporation of phytol and phytanic acid are compared with those of the incorporation of decanol, palmitic acid, α-tocopherol and cholesterol in Figure 22.

Figure 22: Comparison of the increased order parameter of PC-d_{31} for the various incorporated compounds: (o) phytol, (□) phytanic acid, (⧓) decanol (Thewalt et al., 1985), (Δ) α-tocopherol (Wassall et al., 1986), (•) palmitic acid (Pauls et al., 1983), (▪) cholesterol (Thewalt and Cushley, 1987).

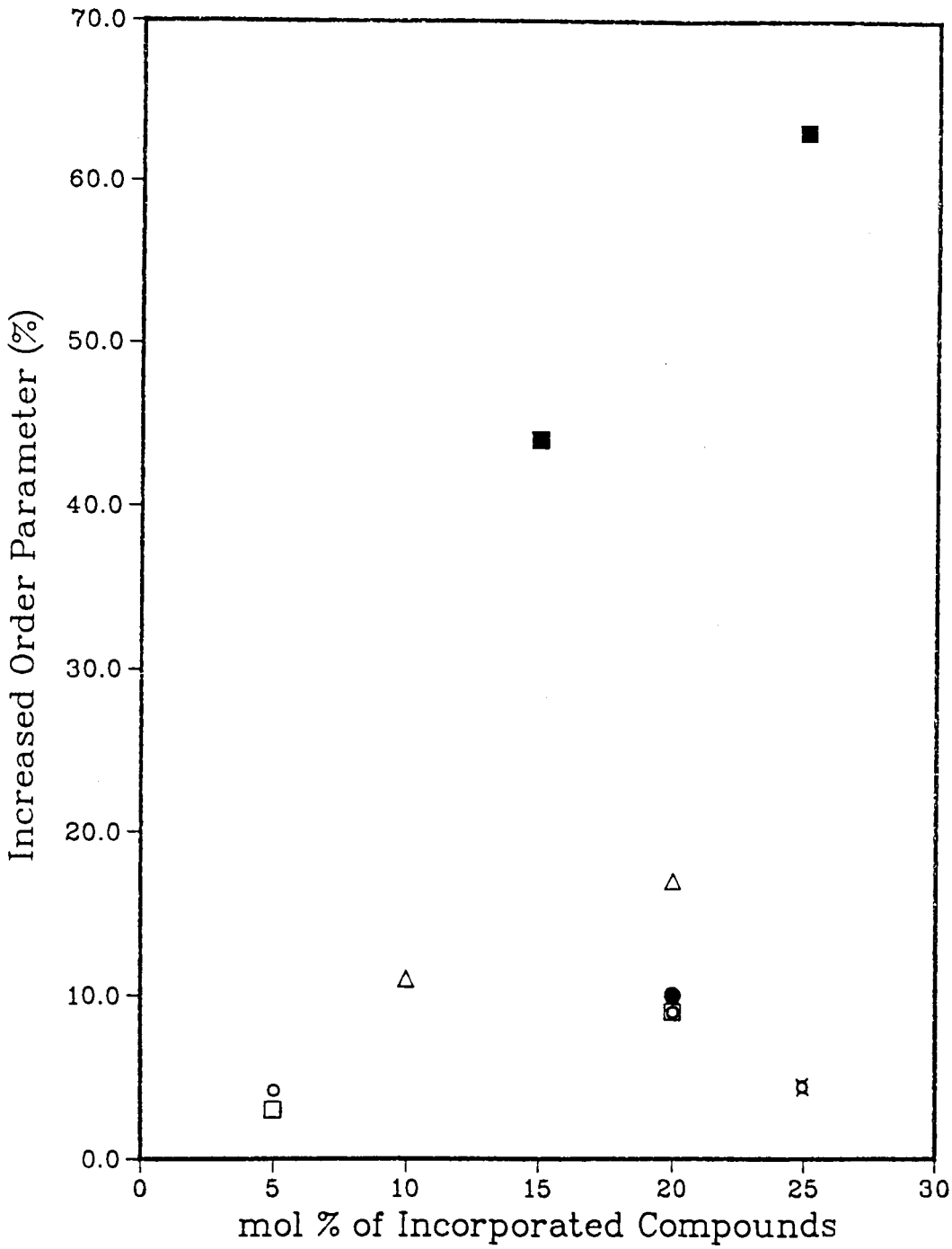

The spin-lattice relaxation time, T_1, was measured in the liquid crystalline phase for aqueous dispersions of PC-d_{31} and PC-d_{31} containing 20 mol% phytanic acid or phytol. Examination of the data of T_1 in Table VI reveals that T_1 increases with increasing temperature and with incorporation of either phytanic acid or phytol. At 45°C each of the branched chain compounds increases T_1 of the terminal methyl group by ≈11%. In the plateau region, phytol and phytanic acid increase T_1 by 19% and 5%, respectively.

T_{2e}, the time constant for the decay of quadrupolar echo, was measured as a function of temperature. Figure 23 presents semi-log plots of quadrupolar echo *versus* 2τ at various temperatures for 5 mol% phytol:PC-d_{31}. Figures 24 and 25 are the plots of T_{2e} *versus* temperature for PC-d_{31} incorporated with phytanic acid and phytol, respectively. T_{2e} passes through a minimum value as temperature increases. The minimum T_{2e} values (corresponding temperature in parenthesis) are 115 μs (36°C), 116 μs (33°C), and 70 μs (24°C) for PC-d_{31}, 5 mol% phytanic acid:PC-d_{31} and 20 mol% phytanic acid:PC-d_{31}, respectively. The corresponding T_{2e} minima for phytol-containing dispersions are: 116 μs at 31±1°C for 5 mol% phytol and 62 μs at 22±2°C for 20 mol% phytol.

Table VI: Spin-lattice Relaxation Times for Multilamellar Dispersions of PC-d_{31} and PC-d_{31} Containing Branched Chain Compounds.

Sample	Temp (°C)	T_1* (ms)	
		plateau region C^2H_2[a]	C^2H_3[b]
PC-d_{31}	45	28.1±0.2	309±5
	50	30.3±0.2	343±11
	55	35.6±0.2	367±12
20 mol% Phytol :PC-d_{31}	45	33.5±0.4	342±10
20 mol% Phytanic acid:PC-d_{31}	45	29.6±0.2	346±8
DPPC	45	26.4(C-4)[c] 32.5(C-8)[c]	275[d]

* T_1 values and the standard deviation were obtained by using a weighted least squares fit routine, samples of fitting can be found in Figure 43.

[a] T_1 was measured from the inversion recovery of the outmost composite peak of the powder pattern. The relaxation delay values were 2, 5, 10, 20, 30, 40, 50, 60 and 1500 ms. The pulse repetition delay time was 1 s.

[b] The relaxation delay were 60, 100, 150, 200, 250 and 1500 ms. The pulse repetition delay time was 2 s.

[c] from selectively deuterated DPPC, at 34.4 MHz (Brown and Davis, 1981)

[d] at 34.4 MHz (Davis, 1979)

Figure 23: Semi-log plot of the quadrupolar echo versus 2τ for 5 mol% phytol:PC-d_{31} at different temperatures.

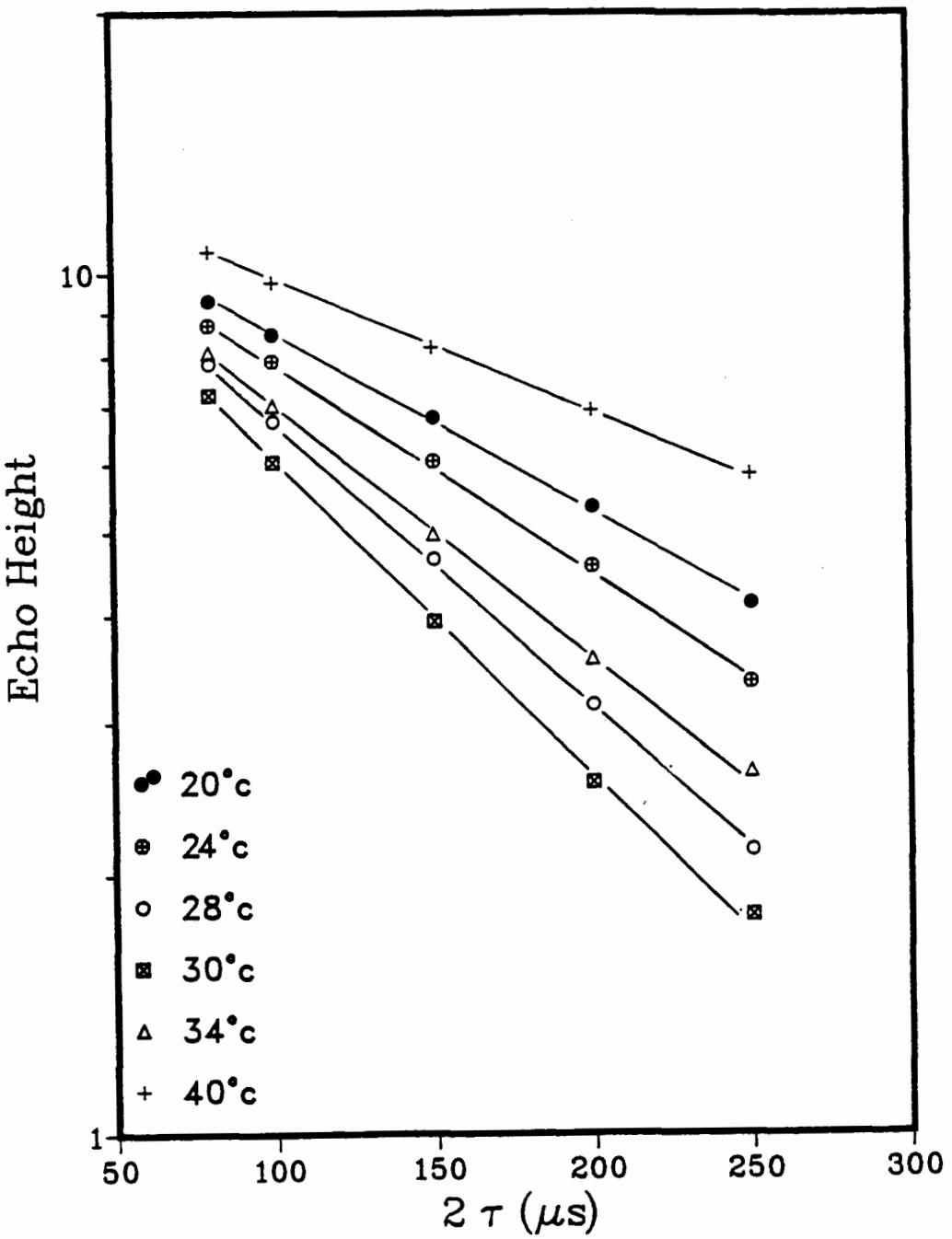

Figure 24: Plot of T_{2e} versus temperature for (•) PC-d_{31} (●) 5 mol% phytanic acid:PC-d_{31} and (o) 20 mol% phytanic acid:PC-d_{31}. In most cases, τ values of 40-125 μs were employed. For 20 mol% phytanic acid:PC-d_{31} τ values of 20-70 μs were employed for temperatures $T \leq T_s$.

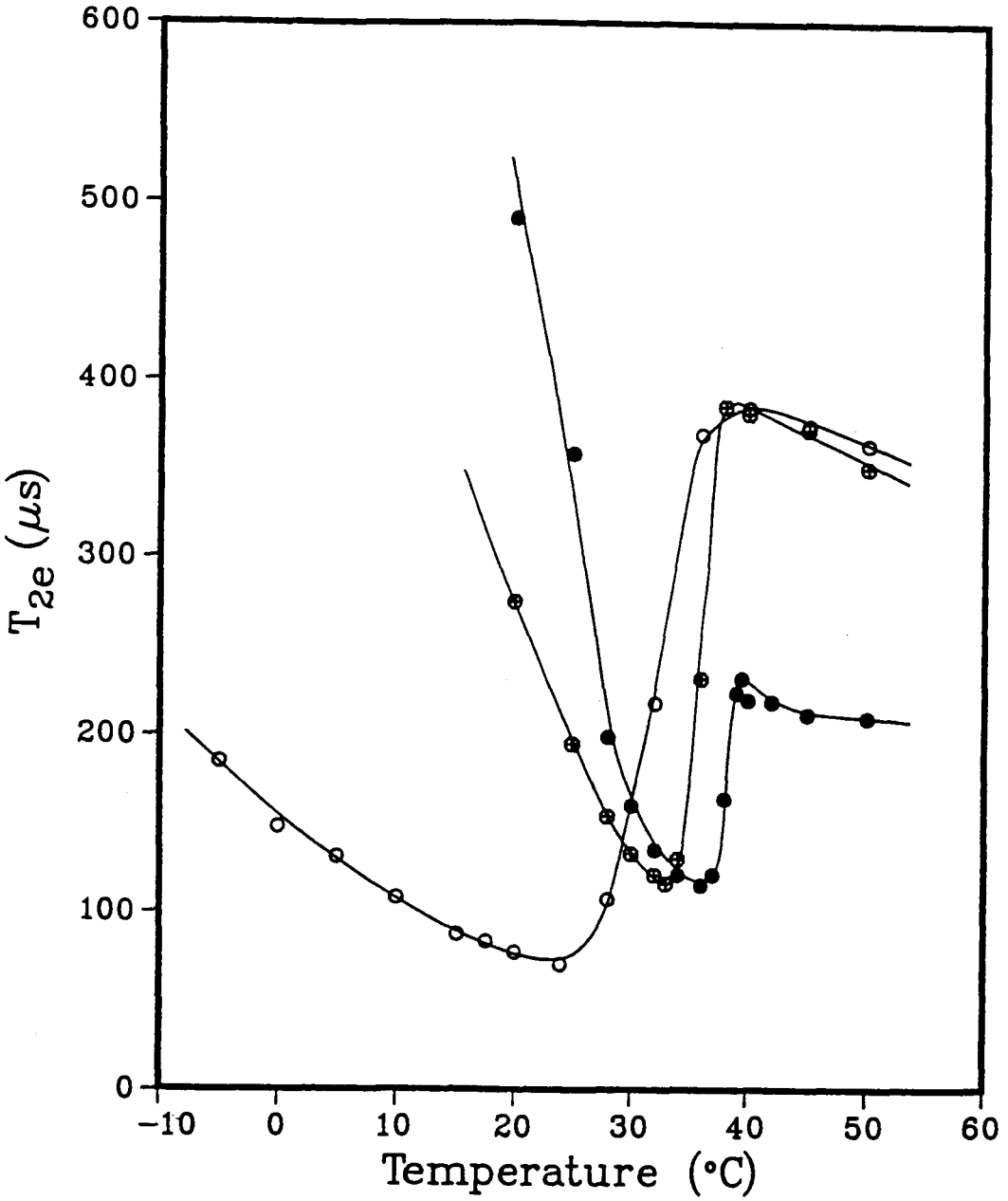

Figure 25: Plot of T_{2e} versus temperature for (•) PC-d_{31} (●) 5 mol% phytol:PC-d_{31} and (o) 20 mol% phytol: PC-d_{31}. In most cases, τ values of 40-125 μs were employed. For 20 mol% phytol:PC-d_{31} τ values of 20-70 μs were employed for temperatures $T \leq T_s$.

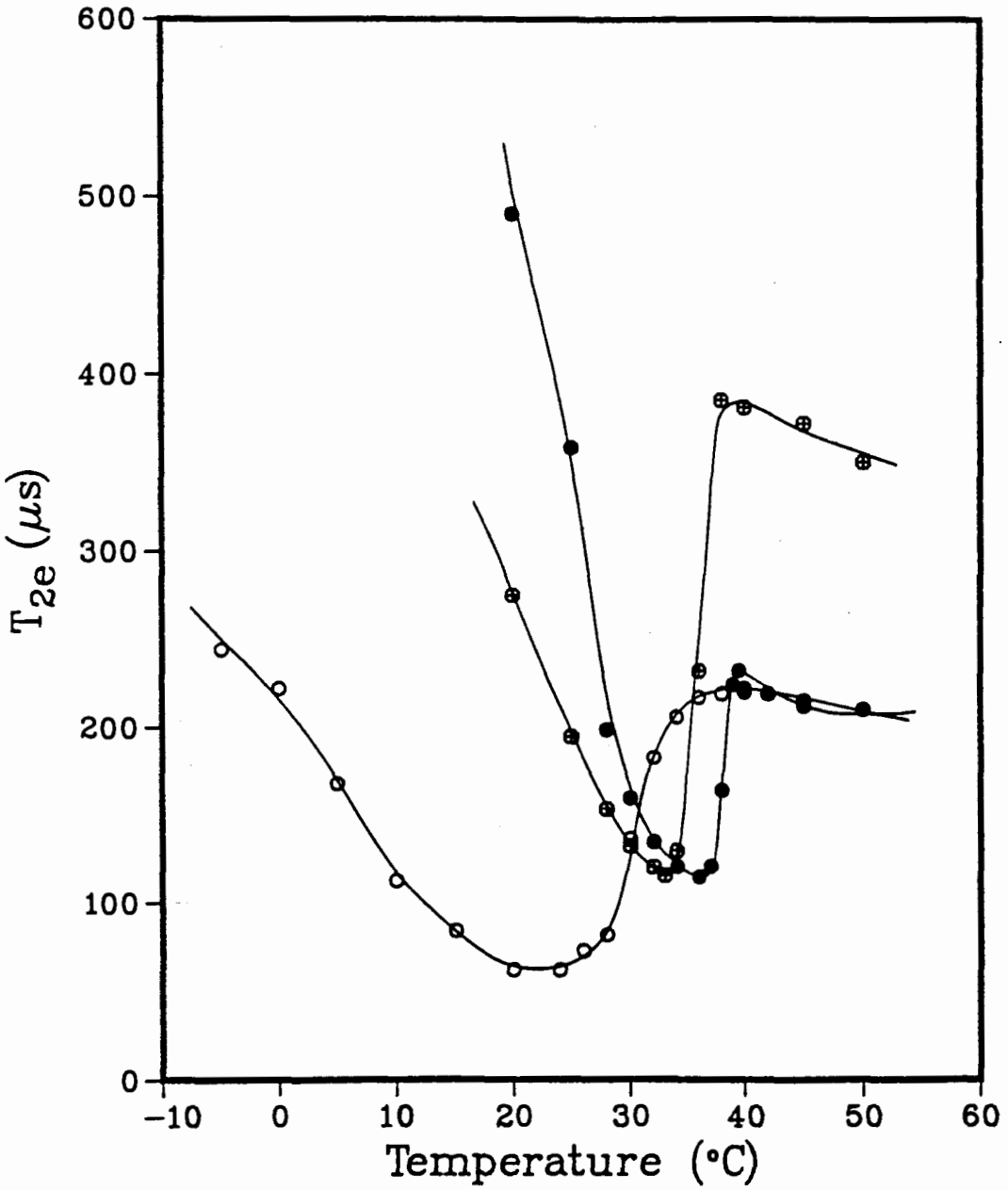

B. Discussion

For paraffinic C-^{2}H bonds the static quadrupolar coupling constant e^2qQ/h equals 168 kHz (Burnett and Muller,1971; Davis and Jeffrey, 1977). The quadrupolar splitting $\Delta\nu_Q$ for such static C-^{2}H bonds is 126 kHz. Even in a solid the rapid rotation of C^2H_3 group about the symmetry axis exists, this motion reduces the coupling constant to an effective value of $\langle e^2qQ/h \rangle$ = 56 kHz (Meier *et al.*, 1983). The quadrupolar splitting for C-^{2}H bonds in methyl group is 42 kHz. Thus, a powder pattern for solid PC-d_{31} is predicted to have a broad component, $\Delta\nu_Q$ = 126 kHz, due to the C^2H_2 segments plus a narrow component with $\Delta\nu_Q$ = 42 kHz, due to the C^2H_3 group. The ratio of broad to narrow signal is expected to be ≈9:1, the ratio of $(C^2H_2)_{14}/C^2H_3$. The broad component in Figure 13, however, is clearly too small. A possible explanation involves distortion of the spectrum at large ±ω from the center of the powder pattern due to the duration of the π/2 pulse (Bloom *et al.*, 1980). The intensity of a quadrupolar echo is given by $F(\omega) = [\mathrm{Sin}(\theta k)/k]^3$ where θ = flip angle and $k = [1 + (\omega^2/4\omega_p^2)]^{1/2}$, where ω = frequency from the center of the powder pattern and $\omega_p = \theta/t_p$ with t_p = π/2 pulse width. For t_p = 6.5 μs, the intensity of the ±63 kHz edges gives $F(\omega)$ = 0.33, i.e., the intensity is only about 1/3 of the intensity which would be obtained using a narrow ($t_p \leq 2$ μs) pulse width.

At -5°C the C^2H_3 splitting for PC-d_{31} (17 kHz) is much less than the predicted value (42 kHz) for a static C^2H_3 group, indicating that the C^2H_3 group undergoes significant motion while a great amount of the methylenes are static. On the other hand, the typical gel-phase spectrum and a second, smaller methyl splitting (≈8 kHz) caused by incorporation of 20 mol% phytanic acid indicates the onset of a new motion at -5°C not seen with pure PC-d_{31} until ≈30°C. With incorporation of 20 mol% phytol, this new motion is suggested by the appearance of a pair of shoulders on the inner side of methyl peaks at 0°C. In all probability this motion involves C^2H_2 segments near the terminal C^2H_3 end of the phospholipid acyl chain caused by onset of gauche-anti isomerization of the last few C^2H_2 segments (Huang et al., 1980; Meier et al., 1983; Westman et al., 1982) in addition to the hindered rotation about the molecular long axis. At higher temperatures more rapid rotation about the acyl chain long axis, further gauche-anti isomerization and fluctuations of the axis itself will contribute to the spectral lineshape.

The significantly reduced intensity of the sloping region in Figure 13h,i,n,o is a consequence of spectral distortion caused by shorter T_{2e} values in the presence of the branched chain compounds (see Figure 24 and 25). Figure 15 illustrates the lineshape changes due to such a distortion: as the spacing between 90° pulses in the quadrupolar echo sequence, τ, increases, the intensity of the sloping region decrease

dramatically. The intensities of the broad component measured from the spectra in Figure 15 are 64%, 47%, 23% and 10% for τ values of 20, 40, 75 and 125 μs, respectively. Figure 15 also implies that T_{2e} for C^2H_2 is much shorter than that for C^2H_3. Since T_{2e} was determined as the time constant of echo decay, the difference of T_{2e} values for C^2H_2 and C^2H_3 were not measurable for PC-d_{31}. A theoretical basis for the distortion effect of short T_{2e} can be found in Spiess and Sillescu (1981).

The motions of deuterated acyl chains in the liquid crystalline phase are described in terms of the spin-lattice relaxation time T_1. It has been suggested that both fast (gauche-anti isomerization) and slow (collective director fluctuation) motions may contribute to T_1 of DPPC due to the $1/\omega^{1/2}$ dependence of T_1 (Brown et al., 1983). We only consider the simplest case and assume that the rate of the fast motion can be expressed with a single correlation time τ_c. The linear plot of ln T_1 versus 1000/T(^{0}K) provides the activation energy, E_a. For C^2H_2 and C^2H_3 values of E_a are 5±1 and 3.7±0.3 kcal/mol, respectively. The E_a value for C^2H_3 is consistent with the average E_a value of 3.5 kcal/mol for DPPC (Brown et al., 1979). The E_a value for C^2H_2 is however in agreement with the value of 5.0-5.2 kcal/mol for positions 3 and 4 of potassium palmitate above 85^{0}C (Davis et al., 1978). Apparently, incorporation of the branched chain compounds increases T_1, i.e., reduces the correlation time of the fast motion. This effect may be attributed to the suppression of the phase

transition temperature.

Since the phase transition temperature is reduced by the incorporation of branched chain compounds, it is reasonable to compare T_1 values at the same reduced temperature. Reduced temperature is defined as $\theta=(T-T_m)/T_m$ (Seelig and Browning, 1978). With comparison of T_1 for PC-d_{31} in the presence of 20 mol% branched chain compounds at 45°C with T_1 for PC-d_{31} alone at 50°C (see table VI), we conclude that phytol increases the rate of the fast motion of C-$^2H_2$ in plateau region and has no effect in center region of bilayer; phytanic acid doesn't have any effect on the fast motion of the acyl chain of PC.

The motions of the deuterated acyl chains in PC-d_{31} are also described by the behavior of the quadrupolar echo relaxation time, *i.e.*, T_{2e},. Pauls *et al.* (1985) have described that for fast reorientation of the deuteron spins T_{2e} is proportional to $1/\tau_c$, (τ_c is the correlation time for the deuteron motions), whereas, for slow motions T_{2e} is proportional to τ_c. Thus, the value of T_{2e} must pass through a minimum value at some intermediate motion, as shown in Figure 24 and 25. PC-d_{31} is shown to have a narrow valley with a rapid increase in T_{2e} through the phase transition, which then levels off in the liquid crystalline phase. The minima for PC-d_{31} incorporated with phytol (62 μs at 22°C) and phytanic acid (70 μs at 24°C) are broad and much below the PC-d_{31} minimum (115 μs at 36°C). The corresponding temperatures of the T_{2e} minima are in good agreement with the temperatures at which the M_1 values

deviate from the gel phase slope and start to drop down (Figure 17 and 19). Above the phase transition T_{2e} for PC-d_{31} becomes approximately 2-fold longer upon addition of 5, 20 mol% phytanic acid, or 5 mol% phytol. A similar observation has been found for incorporation of n-alkanol anesthetics into PC-d_{31} (Thewalt *et al.*, 1985). This T_{2e} effect is responsible for the increased resolution in the depaked spectrum at 50°C (Figure 20c). Incorporation of 20 mol% phytol, however, does not increase PC-d_{31}'s T_{2e} above the phase transition (Figure 25). This implies that in contrast to the effect of phytanic acid and small amount of phytol (5 mol%), a substantial amount of phytol does not affect the acyl chain slow motions.

The effects of branched chain compounds on the phase transition of PC-d_{31} are most clearly enunciated from the variation of first moments M_1 with temperature (Figure 17 and 19). At temperatures between 10-30°C a slight decrease in M_1 is shown for PC-d_{31}. At the phase transition onset temperature, T_s (approximately 39°C), there is a rapid drop of M_1 from approximately $1X10^5$ s^{-1} to $5X10^4$ s^{-1}. Above the completion temperature (*i.e.*, T_l), M_1 also slightly decreases with increasing temperature. Below the phase transition, incorporation of phytanic acid (Figure 17) progressively lowers M_1 and decreases T_s for gel to liquid crystalline melting; whereas above T_l it increases M_1. Phytanic acid addition abolishes the pretransition while the completion

temperature remains essentially the same. The effect of progressive addition of phytol (Figure 19) is remarkably similar to phytanic acid. Meier *et al.* (1983) have been able to show that below the pretransition of DMPC the population of gauche conformation of chain terminal group increases as temperature increases. That M_1 of PC-d_{31} decreases below pretransition temperature can be attributed to the increase of gauche conformation. The low M_1 value in the gel phase for dispersions containing branched chain compounds implies that the branched chain compounds induce an increase of gauche conformations. The most notable effect of phytol and phytanic acid on PC-d_{31} is to lower the onset temperature at which liquid crystalline phase begins to emerge.

The branched-chain compounds phytol and phytanic acid have quite different effects on the phospholipid gel to liquid crystalline phase transition than do their straight-chain analogues: hexadecanol and palmitic acid. In contrast to the transition temperature lowering effects of the branched chain compounds, hexadecanol and palmitic acid elevate the transition temperature of DPPC. DSC results (Eliasz *et al.*, 1976) have shown that a 25 mol% hexadecanol concentration raises the transition onset temperature of DPPC by 3.5^{0}C, and broadens the half-height width of the transition to 9.2^{0}C from 1.5^{0}C. Similarly, ESR results (Pringle and Miller, 1979) have indicated that a 20 mol% hexadecanol concentration raises the DPPC transition temperature T_m by 2^{0}C. In contrast, 20 mol%

phytol lowers the T_s of PC-d_{31} by 10°C (measured from the M_1 plot, Figure 19) and lowers T_m by 4°C (measured from DSC, Table I).

A 20 mol% palmitic acid concentration causes a 3°C elevation of T_s, and increases the half-height width of the DSC peak from 1.5°C to 6.3°C (Eliasz *et al.*, 1976). A ^2H NMR study (Pauls *et al.*, 1983) have shown that 20 mol% palmitic acid incorporation raises T_s of [$^2H_{62}$]DPPC by 2°C and increases the transition range from 2 to 10°C. In contrast, a 20 mol% concentration of phytanic acid lowers the T_s by 10°C (measured from M_1 curve, Figure 17) and lowers T_m by 5°C (measured from DSC, Table I). Compounds which raise the phase transition temperature of phospholipids are able to intercalate between the all-anti, closely packed phospholipid acyl chains and stabilize the gel phase. Evidently, the branched-chain compounds phytol and phytanic acid cause significant gel phase disruption of the phospholipid. We propose that the isoprenoid compounds force nearest neighbor hydrocarbon chains of PC-d_{31} apart in the gel phase, thus lowering the transition temperature.

The slight effects of phytol and phytanic acid on PC-d_{31} organization at 50°C are shown in Figure 21. The order of the plateau region increases in the sequence PC-d_{31} (S_{CD}=0.20) < PC-d_{31}/20 mol% phytol (S_{CD}=0.22) ≈ PC-d_{31}/20 mol% phytanic acid (S_{CD}=0.22). Phytanic acid also slightly increases the order of the segments 10-14. On the other hand, phytol increases the

order including segment 15. α-Tocopherol, another branched chain compound, causes approximately twice the order increase in the plateau region and three to four times the order increase over segments 10-16 (Wassall *et al.*, 1986). From the mean order parameters, calculated from the M_1 values (Table V column 5), we find 20 mol% phytol or phytanic acid increase $\langle S_{CD} \rangle$ by 9%. α-Tocopherol (20 mol%) has been shown to increase $\langle S_{CD} \rangle$ by 17% (Wassall *et al.*, 1986). A 20 mol% concentration of palmitic acid has been shown to increase the order of [$^2H_{62}$]DPPC by ≈10% (Pauls *et al.*, 1983), while 5% increase of $\langle S_{CD} \rangle$ by 25 mol% decanol incorporation has been observed by Thewalt *et al.* (1985). Phytol has a greater effect upon phospholipid order than decanol does, which may be caused by the four methyl branches or by the longer acyl chain. However, phytanic acid has the same effect upon phospholipid order as palmitic acid, in spite of containing the four methyl branches. The effect upon the last two segments is consistent with phytanic acid incorporating with the carboxyl function located at the hydrophilic region of the bilayer, while phytol and Vitamin E sit relatively lower in the bilayer, their chains penetrating deeper into the bilayer.

A word may be added about the seeming inability of phytol and phytanic acid to affect the bilayer order more than palmitic acid, in spite of their containing bulky methyl branches, while α-tocopherol increases the bilayer order substantially (*vide supra*). α-Tocopherol contains a rigid

two-ring chromanol moiety situated in the plateau region of the bilayer. Incorporation of 25 mol% cholesterol increases the mean order parameter $\langle S_{CD} \rangle$ of PC-d_{31} approximately 63% (Thewalt and Cushley, 1987) and cholesterol has a rigid four-ring steroid moiety in the plateau region of the bilayer. We conclude that a rigid structural element in the plateau region is the main determinant in increasing order significantly in liquid crystalline phospholipid bilayer.

Our further observations of ^2H NMR study on a head group deuterated phospholipid (DPPC-d_4) show that the pretransition of DPPC-d_4 at 20 mol% incorporation of branched chain compounds can be detected by the first moment of ^2H NMR spectra measurement (see Chapter V). This implies that the elimination of the pretransition is only a consequence of the broadening of the endothermal peak, while the transition of the head group motion is still perceived.

V. The Effects of Branched Chain Compounds on Head Group Deuterated Phosphatidylcholine Membranes

1. Results

Multilamellar dispersions of 40 wt% DPPC-d_4 in DDW, ≈15 wt% DPPC-d_4 in DDW and in Tris buffer, ≈15 wt% phytol(or phytanic acid)/DPPC-d_4 (molar ratio 1:4) in DDW and in Tris buffer were prepared using the methods described in Chapter III. The liposome particles were examined by phase contrast microscopy. Dispersions of DPPC-d_4, 20 mol% phytol:DPPC-d_4 and 20 mol% phytanic acid:DPPC-d_4, all in DDW, showed spherical morphology; mean diameters were measured to be: 0.7±0.3, 0.7±0.2 and 1.5±0.8 μm, respectively. Different morphology was observed for dispersions of DPPC-d_4, 20 mol% phytol:DPPC-d_4 and 20 mol% phytanic acid:DPPC-d_4, all in Tris buffer. These particles appeared more transparent, *i.e.*, less dense than those in DDW. Their mean diameters were 1.0±0.7, 0.4±0.1 and 1.5±0.8 μm, respectively. Of these three dispersed samples (in buffer), the one containing phytanic acid showed extremely transparent particles. The microscope photographs for 20 mol% phytanic acid:DPPC-d_4 dispersed in DDW and in buffer are compared in Figure 26.

DPPC has been shown to display a calorimetric pretransition and a gel to liquid crystalline phase transition

Figure 26: Phase contrast microscope photographs for dispersions of 20 mol% phytanic acid:DPPC-d_4 (a) in DDW and (b) in Tris buffer (25 mM, pH 7.4). (magnification = 3,000X)

a)

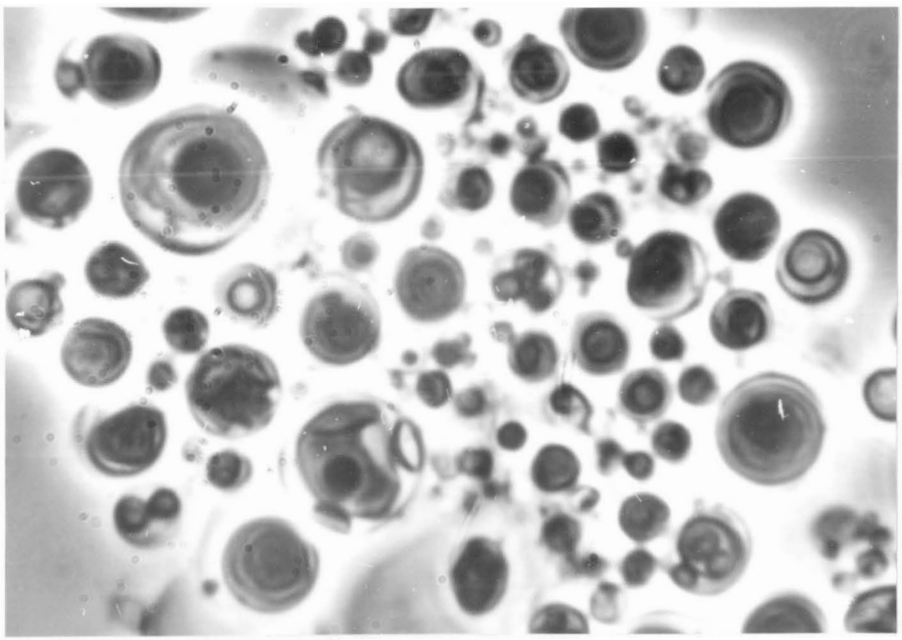

b)

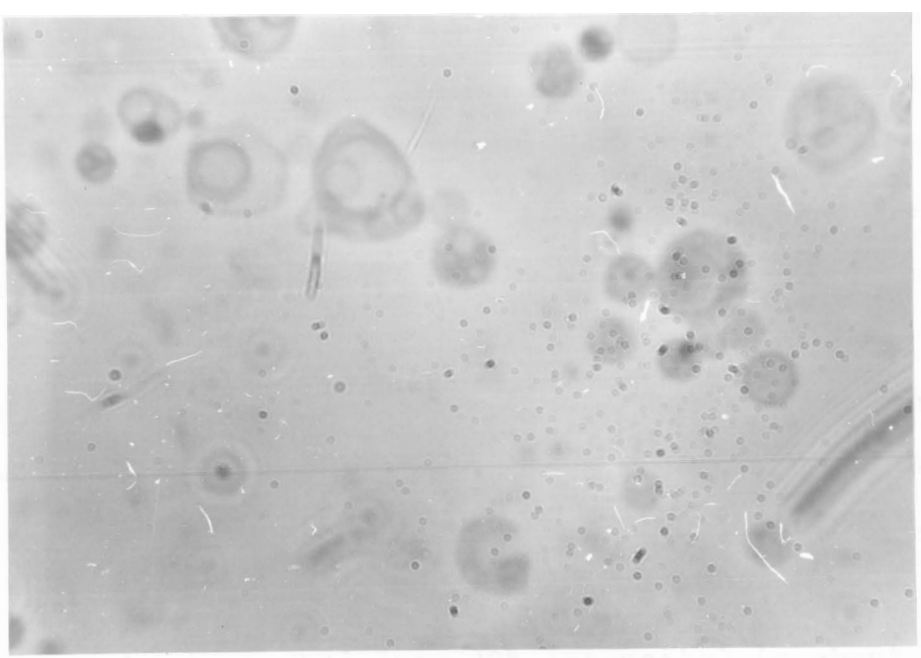

at approximately 35°C and 41°C, respectively (Mabrey and Sturtevant, 1976). The DSC measurement was performed on an aqueous dispersion of DPPC-d_4. Figure 27 is the DSC trace of DPPC-d_4, which shows a pre-transition onset at 34.7°C and a main gel to liquid crystalline phase transition peak at 42.1°C. The onset and completion temperature for the main transition are 41.5 and 43.7°C, respectively (half-height width 1.3°C). DSC measurements show that the phase behavior of DPPC-d_4 is identical to that of DPPC, in spite of the substitution of the four deuterons.

^2H NMR spectra of 40 wt% dispersions of DPPC-d_4 in DDW, and ≈15 wt% dispersions of DPPC-d_4, DPPC-d_4 containing 20 mol% phytanic acid and DPPC-d_4 containing 20 mol% phytol in DDW or Tris buffer were measured over the temperature range 15°C to 55°C. Figure 28 presents the ^2H NMR spectra of 40 wt% DPPC-d_4 dispersions in DDW at various temperature. At temperatures below the pretransition (gel phase), the ^2H NMR spectrum is a smooth curved broad band, whose width decreases from 9.7 kHz to 8.6 kHz (measured at 80% intensity) as the temperature increases from 20°C to 30°C. At the pretransition temperature (31°C) the band shows a square feature, *i.e.*, a plateau of 6 kHz of the width on the top region of the spectrum. With temperature further increasing the intensity at the edges of the plateau becomes higher than that at the center. At 33-35°C region a pair of broad peaks were observed. The splitting of these peaks (measured from 80% intensity) is about 7.2 kHz

Figure 27: Differential scanning calorimetry trace of multilamellar dispersions of 40 wt% DPPC-d_4. Scanning rate 5^0C/min over the range -30 to 60^0C.

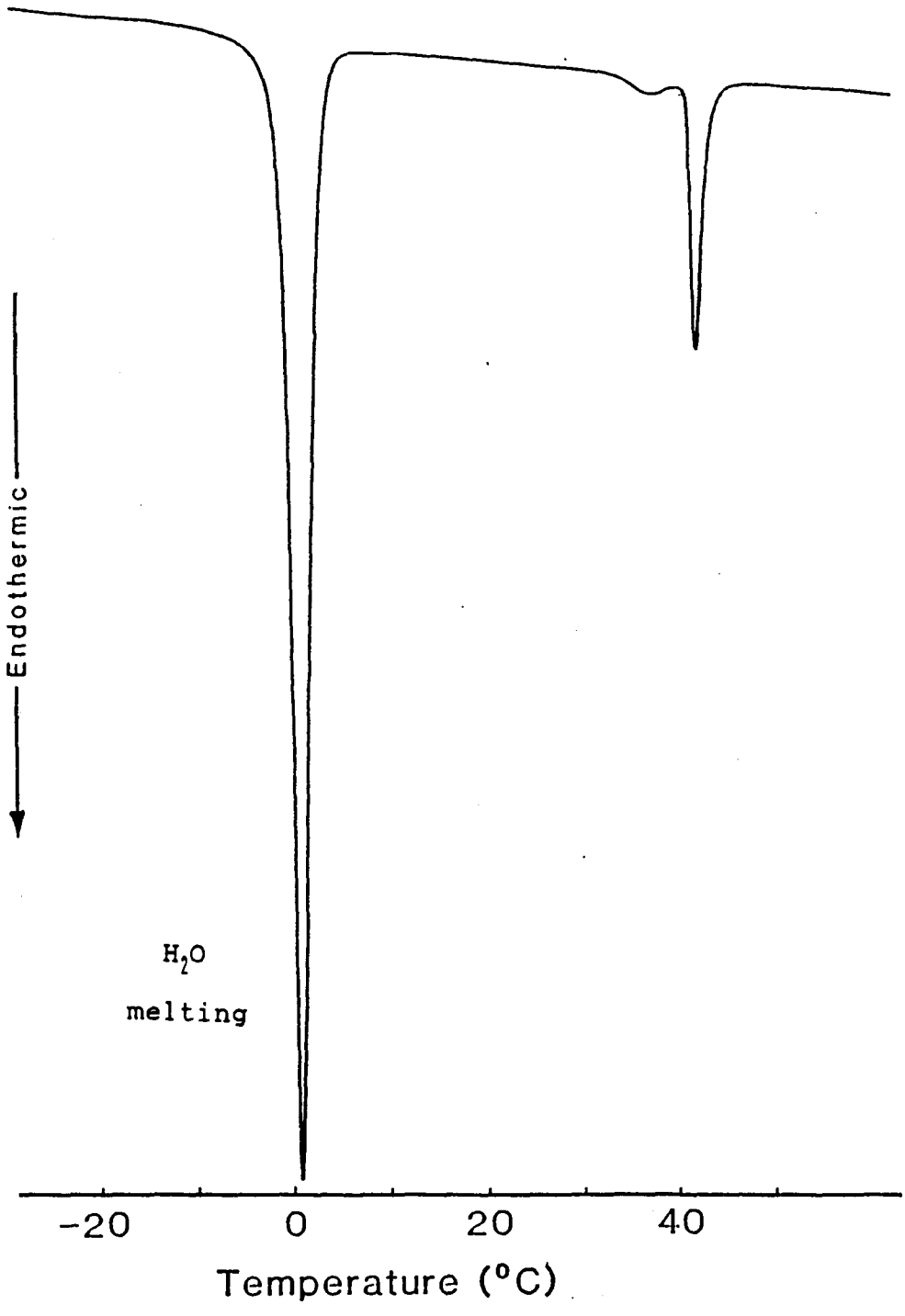

throughout the temperatures between pre- and main transition. Also, in this temperature range, the intensity at the center and the wings decreases with increasing temperature. The width for each peak was measured to be about 2.4 kHz at 40°C. The total width of low field to high field shoulder decreases from about 30 kHz to about 20 kHz, as temperature increases from 31 to 40°C. Above the main transition temperature, the spectrum is a typical powder pattern. As temperature increases further the inner splitting narrows, providing better resolution.

The ^2H NMR spectra of DPPC-d_4 dispersions containing 20 mol% of branched chain compound were measured as a function of temperature (Figure 29). At 14.5°C the spectra for DPPC-d_4 incorporated with phytol or phytanic acid show an broad featureless band (width = 6.1 kHz, see Figure 29a,f), which is narrower than DPPC-d_4 without incorporation (Figure 28, 25°C). As temperature increases, the broad band narrows, and a broad splitting develops (Figure 29c,h,i). This observation is very similar to DPPC-d_4 in the temperature between pre- and main transitions (Figure 28: 35, 40°C). At 34°C the spectrum for 20 mol% phytol:DPPC-d_4 (Figure 29j) shows an axially symmetric powder pattern indicating that the liquid crystalline phase has been reached, while the spectrum for 20 mol% phytanic acid:DPPC-d_4 (Figure 29e) shows a distorted powder pattern feature (*vide infra*). As temperature increases further, the inner splitting narrows and the outer splitting remains unchanged, which is the same as DPPC-d_4 without incorporation.

Figure 28: ^{2}H NMR spectra of 40 wt% multilamellar dispersions of DPPC-d_4 at different temperature. Spectral parameters: pulse width = 6.5 μs (flip angle = 90^0); τ, the interval between pulses in quadrupolar echo sequence, = 50 μs; t, the delay between echo sequences, = 400 ms; sweep width = ±50 kHz; data size = 4K in complex; line broadening = 25 Hz; number of acquisitions = 30,000(35^0C), 25,000(45^0C), 20,000(others).

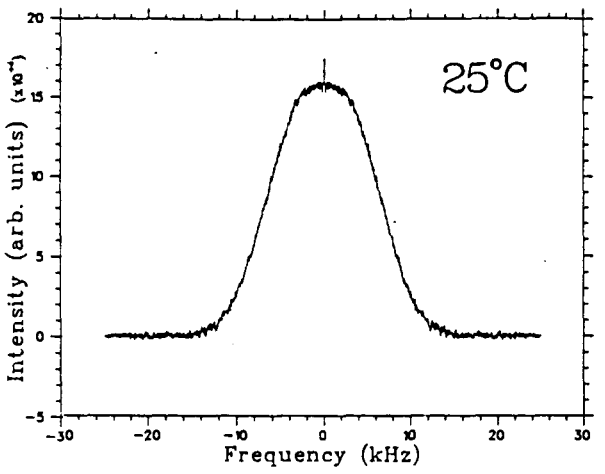
25°C
Intensity (arb. units) (x10⁻⁴)
Frequency (kHz)

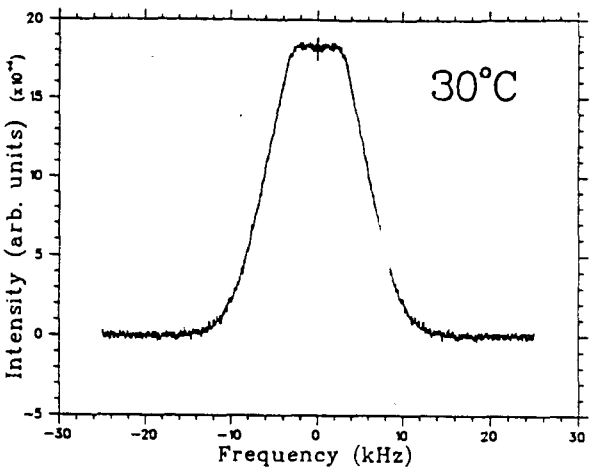
30°C
Intensity (arb. units) (x10⁻⁴)
Frequency (kHz)

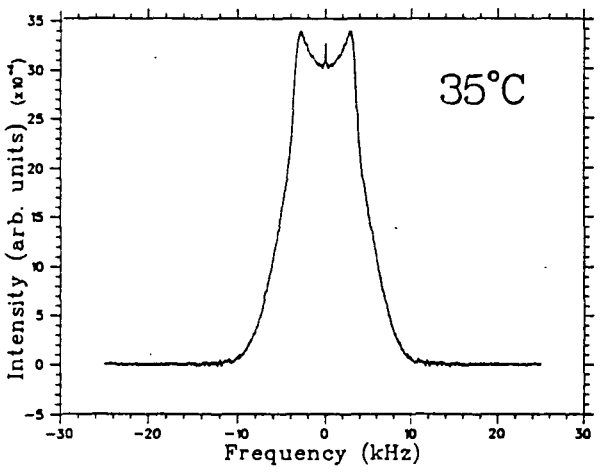
35°C
Intensity (arb. units) (x10⁻⁴)
Frequency (kHz)

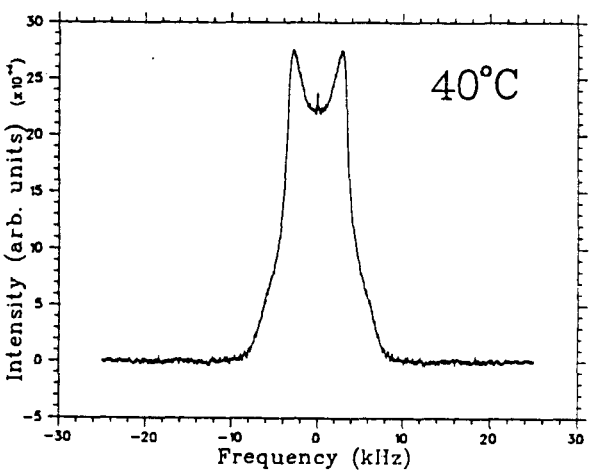
40°C
Intensity (arb. units) (x10⁻⁴)
Frequency (kHz)

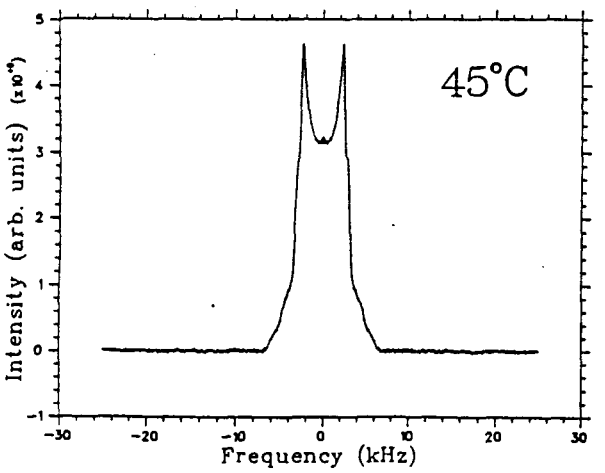
45°C
Intensity (arb. units) (x10⁻⁴)
Frequency (kHz)

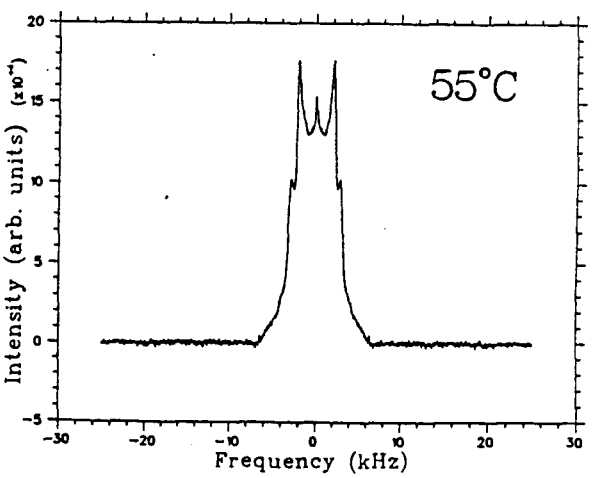
55°C
Intensity (arb. units) (x10⁻⁴)
Frequency (kHz)

Figure 29: ^{2}H NMR spectra of 15 wt% multilamellar dispersions of 20 mol% phytanic acid:DPPC-d_4 (a-e) and 20 mol% phytol:DPPC-d_4 (f-j) in Tris buffer at different temperature.

Spectral parameters: pulse width = 7.5 μs (flip angle = 90^0); τ, the interval between pulses in quadrupolar echo sequence, = 60 μs; t, the delay between echo sequences, = 200 ms; sweep width = ±50 kHz; data size = 4K in complex; line broadening = 50 Hz; number of acquisitions = 30,000.

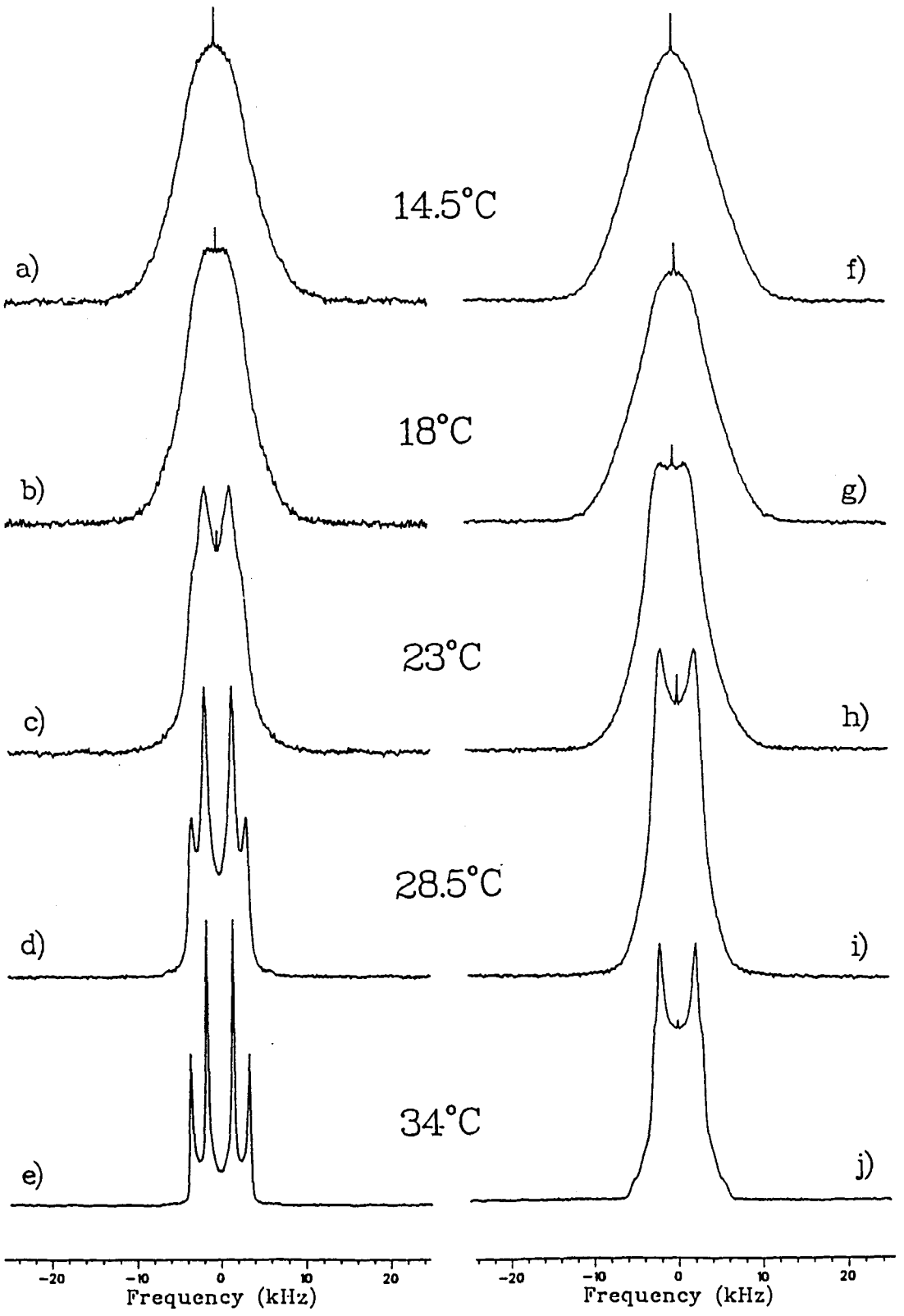
14.5°C
a)
f)
18°C
b)
g)
23°C
c)
h)
28.5°C
d)
i)
34°C
e)
j)
-20
-10
0
10
20
Frequency (kHz)
-20
-10
0
10
20
Frequency (kHz)

Representative ^2H NMR spectra of DPPC-d_4 with and without incorporated branched chain compounds at 45°C are shown in Figure 30. Spectrum a) in Figure 30 illustrates the characteristic powder spectrum for the choline deuteromethylene groups of DPPC-d_4. The outer doublet, $\Delta\nu_Q$ = 6.0 kHz, is assigned to the α-C^2H_2 segment while the inner doublet, $\Delta\nu_Q$ = 4.9 kHz, is assigned to the β-C^2H_2 (Gally et al., 1975). The spectrum of Tris buffer dispersion of DPPC-d_4 containing 20 mol% phytanic acid (Figure 30d) is an unique one. The intensity of the shoulders is essentially eliminated, the intensity of the region at 0 kHz is decreased markedly, and the peaks are narrowed revealing a doublet structure for the outer pair (Figure 30d, inset). DPPC-d_4 containing 20 mol% phytol (Figure 30e,f) shows decreased quadrupolar splittings due to incorporation of the branched chain compound, but the powder pattern is undistorted. The splittings are more clearly seen in Figure 31 where we present the depaked spectra of DPPC-d_4 with and without branched chain compounds added, at 45°C. Table VII lists the quadrupolar splitting of DPPC-d_4 multilamellar dispersions in the liquid crystalline phase in the presence and absence of incorporated branched chain compounds. Phytol decreases both the α- and β-C^2H_2 splittings while phytanic acid decreases the splitting of β-C^2H_2 but increases that of α-C^2H_2.

Figure 30: ^2H NMR spectra of 15 wt% multilamellar dispersions at 45^{0}C of

(a) DPPC-d_4 in DDW,

(b) DPPC-d_4 in Tris buffer, pH 7.4,

(c) 20 mol% phytanic acid:DPPC-d_4 in DDW,

(d) 20 mol% phytanic acid:DPPC-d_4 in Tris buffer,

(e) 20 mol% phytol:DPPC-d_4 in DDW,

(f) 20 mol% phytol:DPPC-d_4 in Tris buffer.

Spectral parameters: pulse width = 7.5 µs (flip angle = 90^0); τ = 100 µs; t, the delay between echo sequences, = 200 ms; sweep width = ±50 kHz; data size ◻ 4K in complex; line broadening = 25 Hz; number of acquisitions = 30,000 (a,c,d,f), 25,000 (b), 40,000 (e).

The inset in (c) and (d) is an expansion of the peak for the C_α-segment without line broadening. Figures g-i are the first quarter of the free induction decay patterns for b,d and f, respectively.

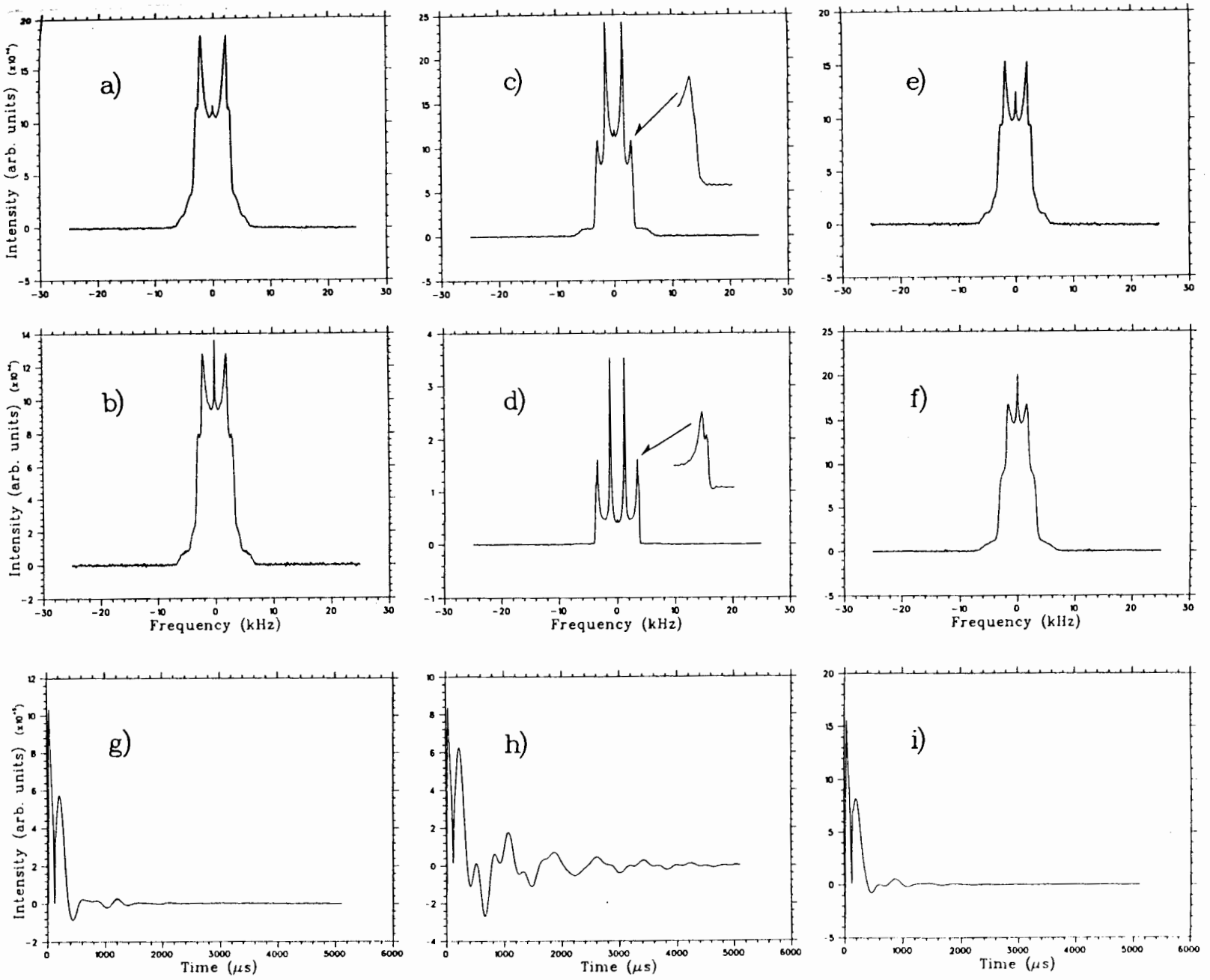
a)
b)
c)
d)
e)
f)
g)
h)
i)
Intensity (arb. units)
Frequency (kHz)
Time (μs)

Figure 31: Depaked ^2H NMR spectra of 15 wt% multilamellar dispersions at 45°C of

(a) DPPC-d_4 in DDW,

(b) DPPC-d_4 in Tris buffer, pH 7.4,

(c) 20 mol% phytanic acid:DPPC-d_4 in DDW,

(d) 20 mol% phytanic acid:DPPC-d_4 in Tris buffer,

(e) 20 mol% phytol:DPPC-d_4 in DDW,

(f) 20 mol% phytol:DPPC-d_4 in Tris buffer.

Spectral parameters are same as in Figure 30. Six iterations were performed in each depaking.

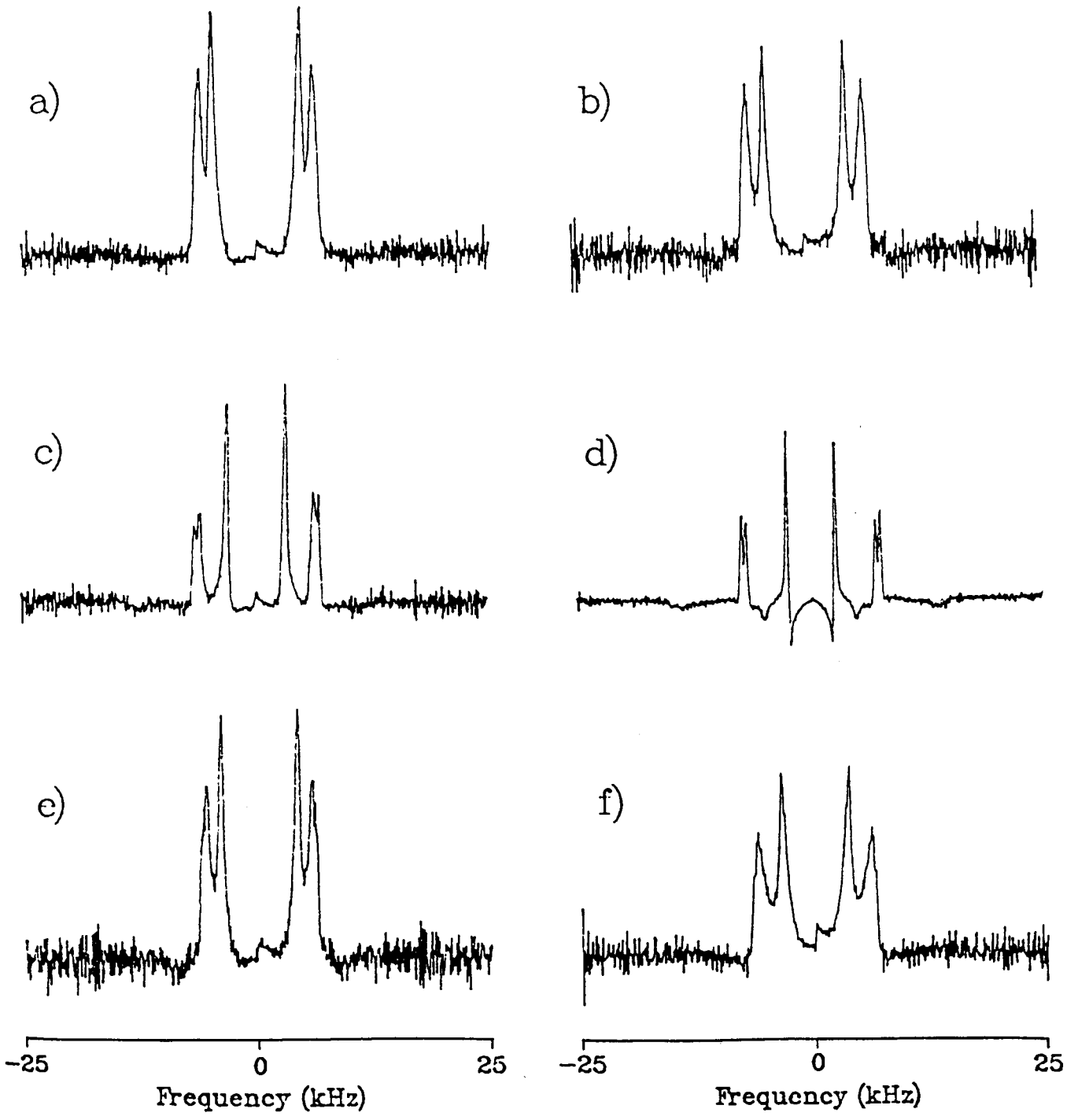
a)
b)
c)
d)
e)
f)
−25
0
25
Frequency (kHz)
−25
0
25
Frequency (kHz)

Table VII: Quadrupolar Splitting of DPPC-d_4 Multilamellar Dispersions Containing Branched Chain Compounds

Lipid	Temperature (°C)	Quadrupolar Splitting[a] (kHz) α-C^2H_2 DDW	α-C^2H_2 Buffer[b]	β-C^2H_2 DDW	β-C^2H_2 Buffer[b]
DPPC-d_4	45	6.0	6.3	4.9	4.6
	50	6.0	6.3	4.6	4.2
	55	6.1	6.4	4.4	3.9
20 mol% Phytol:DPPC-d_4	40	5.7	6.1	4.4	3.9
	45	5.7	6.1	4.1	3.6
	50	5.7	6.2	3.8	3.3
20 mol% Phytanic acid:DPPC-d_4	40	6.5,6.0	7.5,7.1	3.3	2.8
	45	6.6,6.1	7.5,7.0	3.1	2.6
	50	6.5,6.0	7.5,7.0	2.9	2.4

[a] Measured from depaked spectra, accuracy = ±0.1 kHz. Quadrupolar powder pattern splittings are reported, which are a half of the splittings from the depaked spectra.

[b] 25 mM Tris buffer in DDW, pH 7.4.

First (M_1) and second (M_2) moments of the temperature-dependent ^2H NMR spectra were calculated according to eq. 22. The results of the calculations are presented in Figure 32. Moment analysis of the spectra is quite straightforward in ^2H NMR. M_1 (M_2) gives the mean (mean square) quadrupolar splitting of deuterium, which is sensitive to the degree and type of orientational averaging occurring at the ^2H site. Unlike PC-d_{31}, the moments of ^2H NMR spectra of DPPC-d_4 do not show a τ dependency. The data of M_1 and M_2 in Figure 32 are the averages of four to five different spectra determined at different τ values (60-150 μs). The standard deviations are about 2% and 6% for M_1 and M_2, respectively. In Figure 32 there are discontinuities in both M_1 and M_2 curves of DPPC-d_4 at 31°C and 42°C, corresponding to the pretransition and main gel to liquid-crystalline phase transition. Below the pretransition both M_1 and M_2 decrease as temperature increases. For temperatures between the pre- and main transitions there is an abrupt decrease in both M_1 and M_2, and above the main transition both M_1 and M_2 decrease slightly.

^{31}P NMR studies were conducted in order to verify the unique character of the ^2H NMR spectrum of phytanic acid:DPPC-d_4 (Figure 30d). Figure 33 shows the ^{31}P NMR spectra for DPPC-d_4 and 20 mol% phytanic acid:DPPC-d_4 dispersions in Tris buffer. The spectra were taken in the following order: at 15°C (Figure 33a,d), 45°C (Figure 33b,e), 15°C (Figure 33c,f). The spectra for DPPC-d_4 show a powder pattern in both gel and liquid-

Figure 32: Variation of the first moment, M_1, and second moment, M_2, with temperature for the ^2H NMR spectra of (•,Δ) DPPC-d_4, (□) 20 mol% phytanic acid:DPPC-d_4, and (o) 20 mol% phytol:DPPC-d_4, all in Tris buffer, pH 7.4.

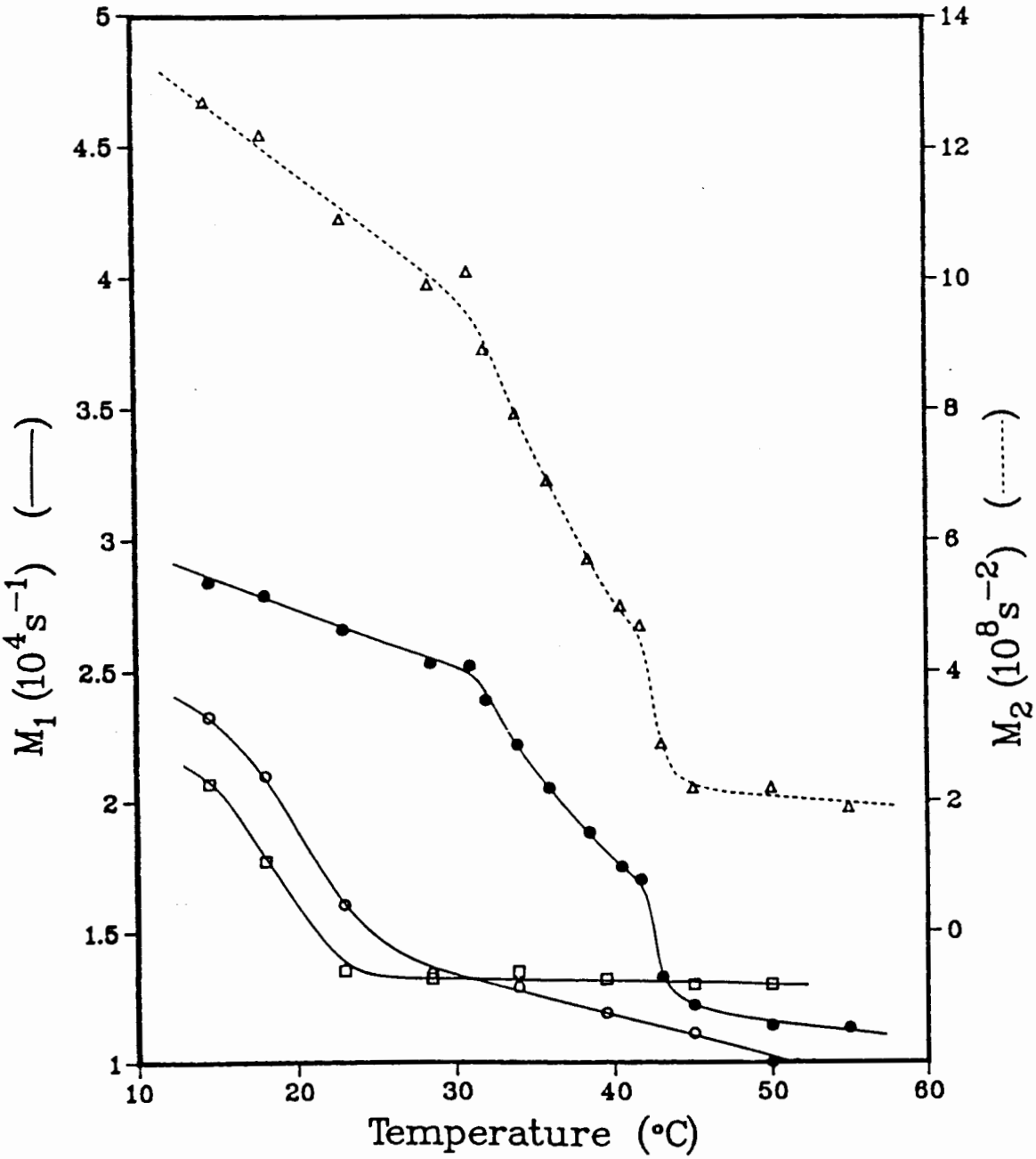

Figure 33: ^{31}P NMR spectra of 15 wt% multilamellar dispersions of: (a-c) DPPC-d_4 and (d-f) 20 mol% phytanic acid:DPPC-d_4, all in Tris buffer, pH 7.4. Spectrum (g) is the difference of (f) and (d).

Spectral parameters: one pulse experiment, no phase cycling; pulse width = 6.5 µs (flip angle = 60^0); delay between pulses = 3 s; delay before acquisition = 10 µs; sweep width = 50 kHz; data size = 4K in complex; line broadening = 25 Hz; number of acquisitions = 2,000 (e), 3,000 (others). The chemical shift is given in ppm relative to external H_3PO_4.

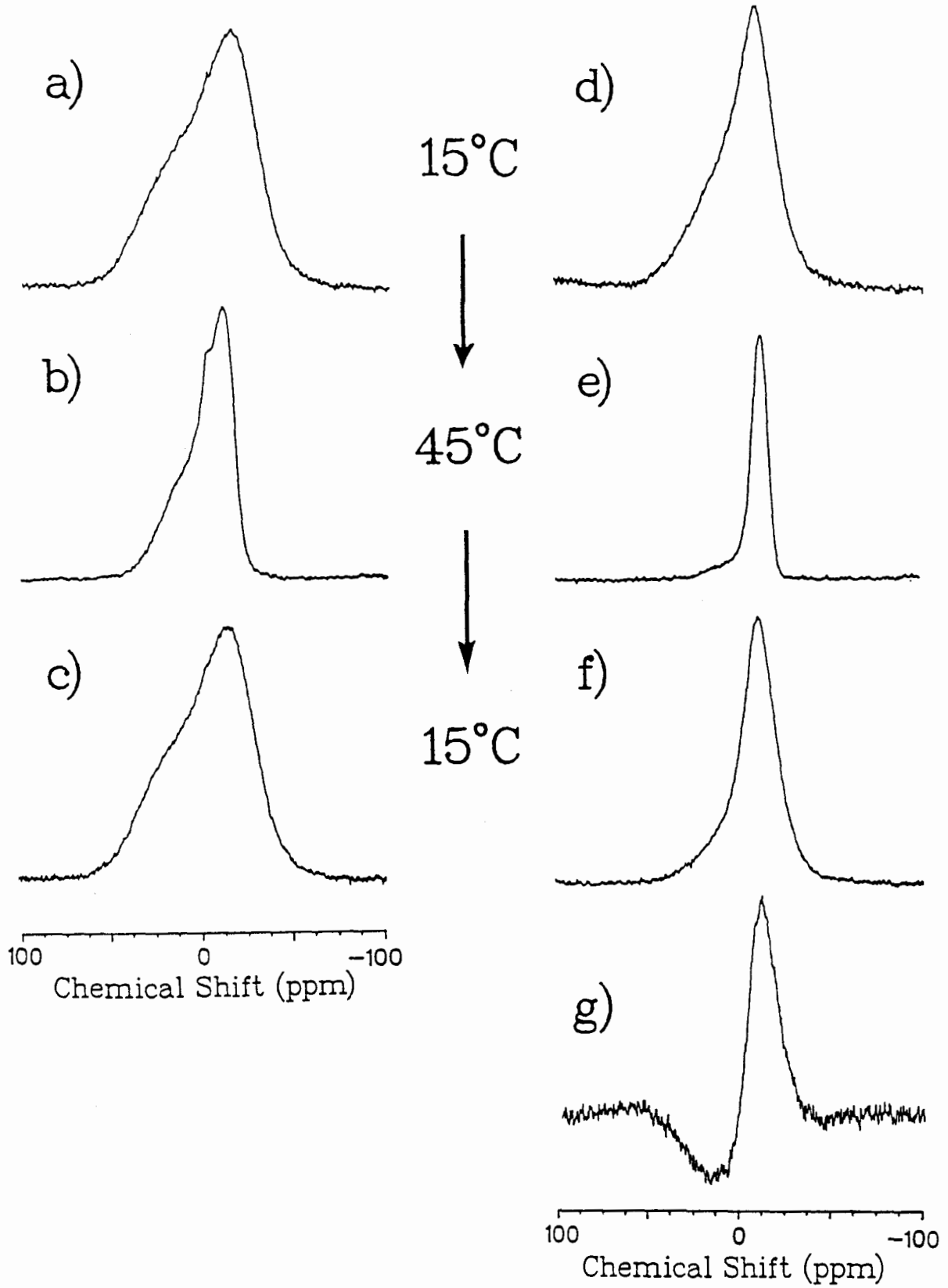
a)
15°C
d)
b)
45°C
e)
c)
15°C
f)
g)
100
0
−100
Chemical Shift (ppm)
100
0
−100
Chemical Shift (ppm)

crystalline phase (Figure 33a,b). The spectra of DPPC-d_4 containing phytanic acid show a powder pattern in the gel phase (Figure 33d) but a distorted powder pattern in the liquid crystalline phase (Figure 33e).

In order to clarify that the distortion of the NMR spectra is the characteristic for phytanic acid:PC dispersions in buffer prepared with the freeze-thaw method, dispersions of 20 mol% phytanic acid:PC-d_{31} and PC-d_{31} alone were prepared in four types for ^2H NMR spectroscopy. For example, 20 mol% phytanic acid:PC-d_{31} was dispersed in DDW and in Tris buffer (pH 7.4), with and without the freeze-thaw method, respectively. Among these eight samples, only one, *i.e.*, 20 mol% phytanic acid:PC-d_{31} in buffer prepared by the freeze-thaw method was observed to possess the distorted ^2H NMR spectrum, as shown in Figure 34.

Spin-lattice relaxation times, T_1, and spin-spin relaxation times, T_{2e}, were determined for DPPC-d_4 with or without incorporated branched chain compound (≈15 wt% dispersions in Tris buffer) over the temperature range 14-55^{0}C. The temperature dependence of T_1 for three dispersion samples is plotted in Figure 35. There are two abrupt T_1 changes for DPPC-d_4 at the pre-(31^{0}C) and main(42^{0}C) phase transition temperatures, while for DPPC-d_4 incorporated with phytol or phytanic acid only one inflexion can be observed at the temperature around 25^{0}C.

Figure 34: ^{2}H NMR spectra for multilamellar dispersions prepared with freeze-thaw method measured at $45^{0}C$: (a,b) PC-d_{31}, (c,d) 20 mol% phytanic acid:PC-d_{31}, where (a,c) are dispersions in DDW and (b,d) in Tris buffer, pH 7.4.

Spectral parameters: pulse width = 7.5 μs (flip angle = 90^{0}); τ, the interval between pulses in quadrupolar echo sequence, = 75 μs; t, the delay between echo sequences, = 1 s; sweep width = ±50 kHz; data size = 4K in complex; line broadening = 25 Hz; number of acquisitions = 8,000.

* Spectra were obtained without zeroing the out of phase channel.

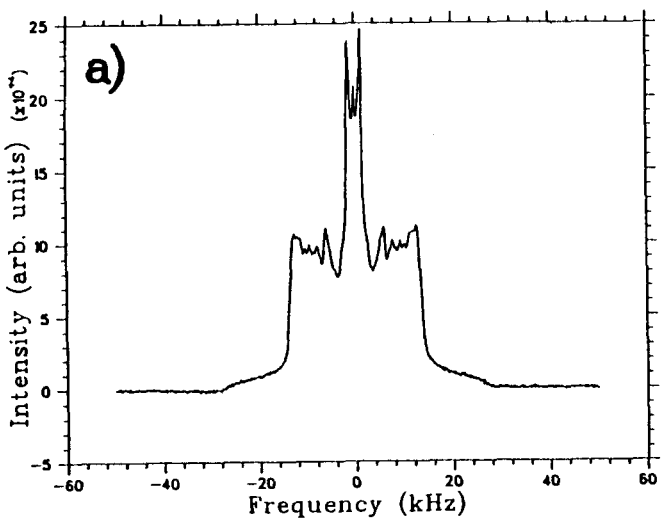
a)
Intensity (arb. units) (x10⁻⁴)
Frequency (kHz)

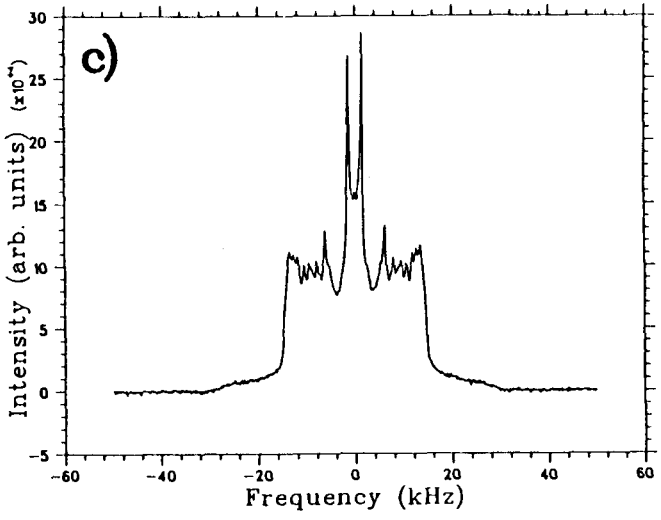
c)
Intensity (arb. units) (x10⁻⁴)
Frequency (kHz)

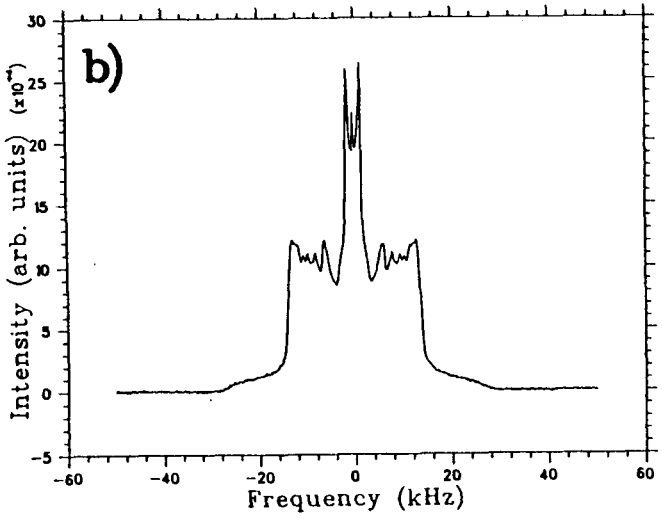
b)
Intensity (arb. units) (x10⁻⁴)
Frequency (kHz)

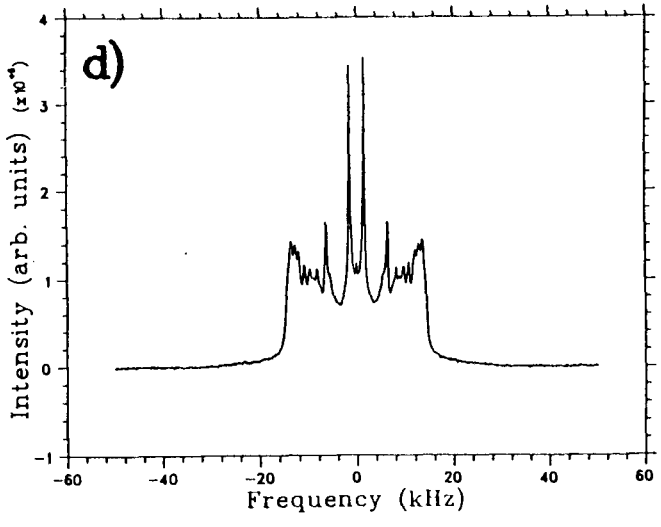
d)
Intensity (arb. units) (x10⁻⁴)
Frequency (kHz)

Figure 35: Temperature dependence of deuterium spin-lattice relaxation time, T_1, of multilamellar dispersions of: (•) DPPC-d_4, (o) 20 mol% phytol:DPPC-d_4 and (Δ) 20 mol% phytanic acid, all in Tris buffer, pH 7.4. T_1's were measured by the inversion recovery method, five to eight different relaxation delay values (τ_1) were used, delay between pulse sequences were 250 ms. Echo heights were used to calculate T_1's. Thus T_1's are average values for α- and β-C^2H_2.

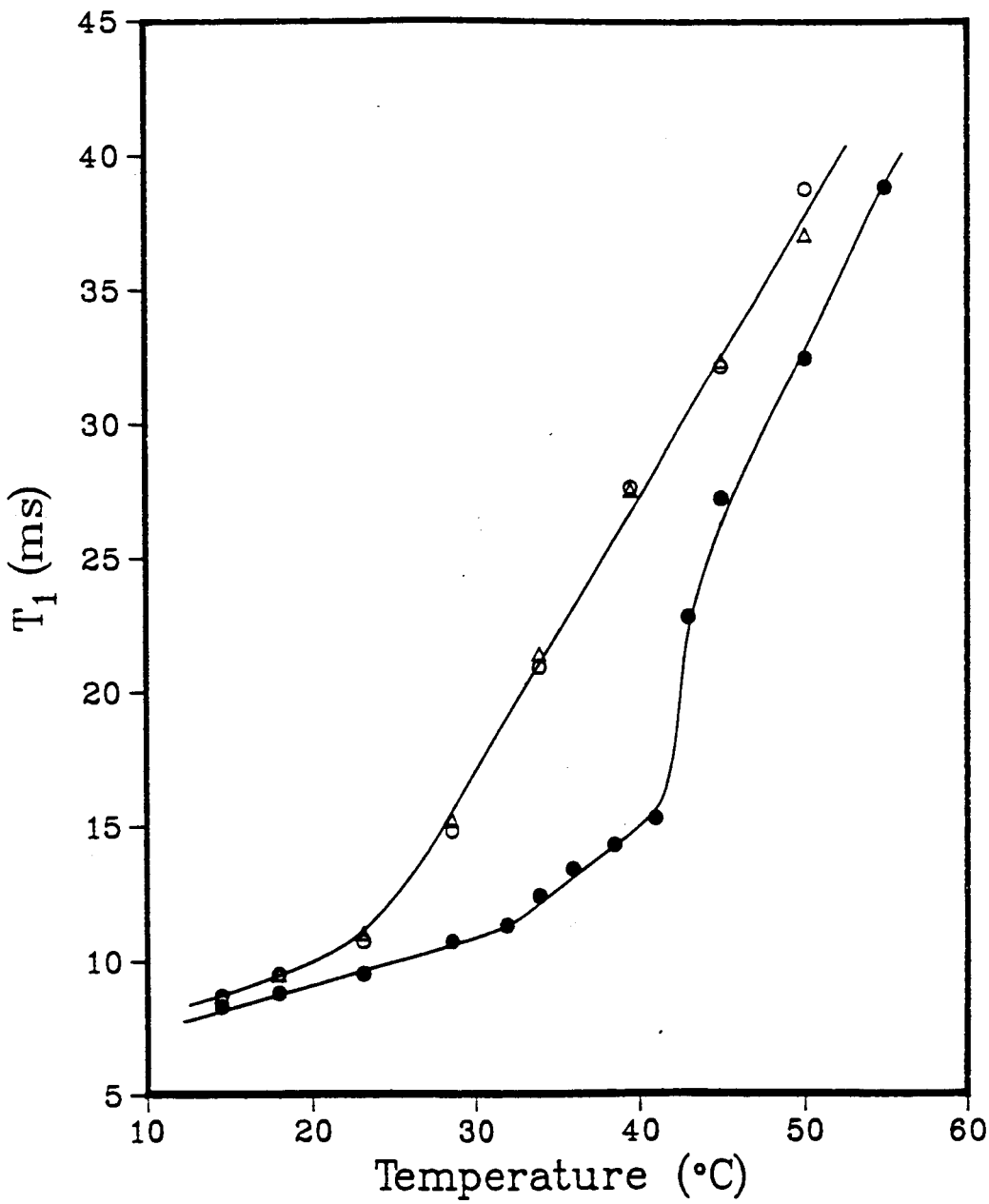
45
40
35
30
25
20
15
10
5
T_1 (ms)
10
20
30
40
50
60
Temperature (°C)

Figure 36: Plots of $\log(A_\infty - A)$ versus τ_1 for 15 wt% dispersions of 20 mol% phytol:DPPC-d_4 in Tris buffer at 14.5°C (a), 23°C (b), 34°C (c) and 45°C (d).

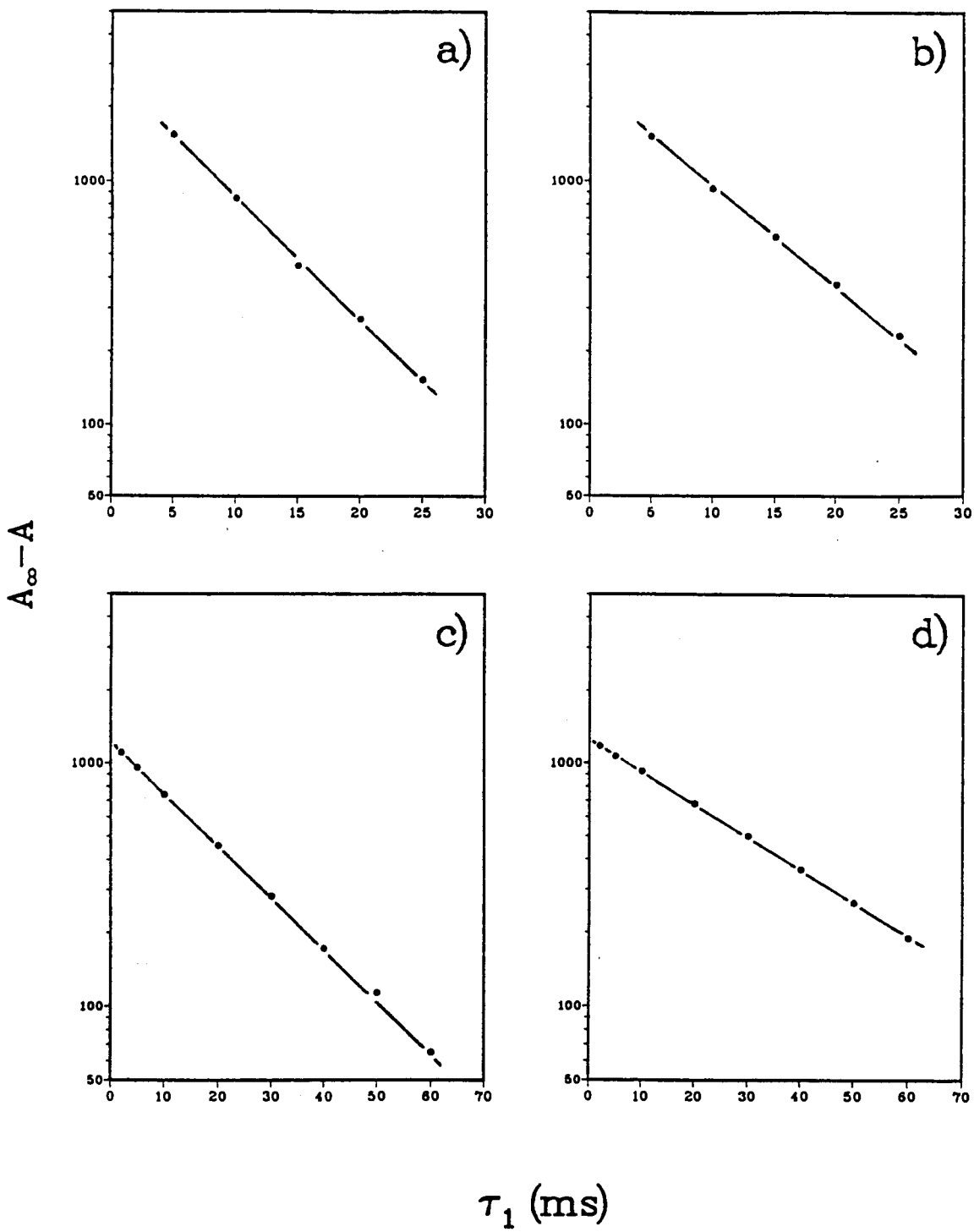

The linear plots of $\log(A_\infty - A)$ versus τ_1, the relaxation delay of the inversion recovery pulse sequence, for 20 mol% phytol:DPPC-d_4 at different temperatures are given in Figure 36.

Semilog plots of quadrupolar echo versus 2τ, where τ is the delay between quadrupolar pulses, are shown in Figure 37. We found that T_{2e} was very much dependent on the method of sample preparation. For 40 wt% DPPC-d_4 in DDW the quadrupolar echo follows a single exponential decay over a wide range of τ values (50-300 μs) at temperatures below or above the main phase transition, and slightly deviates from an exponential decay at temperatures around the transition. For the other samples the echo decays do not follow a single exponential at the large τ values. In those cases, T_{2e} was obtained from the initial slope of the semilog plot of echo intensity versus 2τ. For 20 mol% phytanic acid:DPPC-d_4 in Tris buffer T_{2e} was not able to be measured in the liquid crystalline phase since the echo intensity remains constant at short τ values.

Figure 38 shows the temperature dependence of T_{2e} for 40 wt% dispersions of DPPC-d_4 in DDW, and 15 wt% dispersions of DPPC-d_4, 20 mol% phytol:DPPC-d_4 and 20 mol% phytanic acid:DPPC-d_4, all in Tris buffer. The curves for DPPC-d_4 dispersions show a narrow valley with T_{2e} rapidly increasing through the main transition temperature. The T_{2e} minima occur at temperatures between the pre- and main transitions. The minimum for DPPC-d_4 containing phytol (23°C) is broad and lower

Figure 37: Semilog plots of quadrupolar echo intensity versus 2τ at 45^0C of: (Δ) DPPC-d_4 in DDW, (o) DPPC-d_4, (□) 20 mol% phytol:DPPC-d_4 and (•) 20 mol% phytanic acid:DPPC-d_4, all in Tris buffer, pH 7.4. DPPC-d_4 in DDW is 40 wt% multilamellar dispersions; all others are ≈15 wt%.

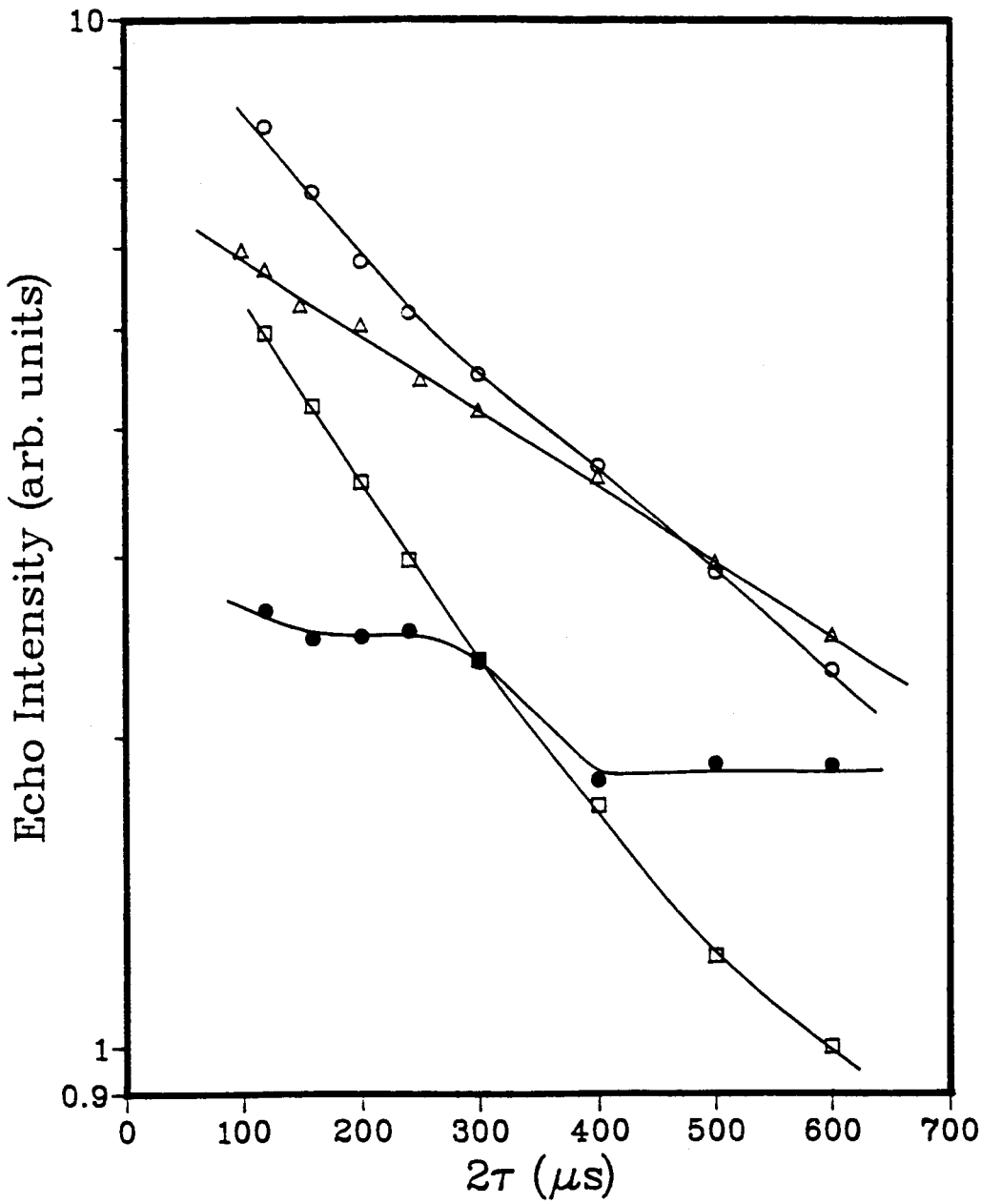

Figure 38: Plot of T_{2e}, the time constant for the decay of the quadrupolar echo, versus temperature of: (Δ) DPPC-d_4 in DDW, (o) DPPC-d_4, (□) 20 mol% phytol: DPPC-d_4, and (•) 20 mol% phytanic acid:DPPC-d_4, all in Tris buffer, pH 7.4. DPPC-d_4 in DDW is 40 wt% multilamellar dispersions; all others are ≈15 wt%.

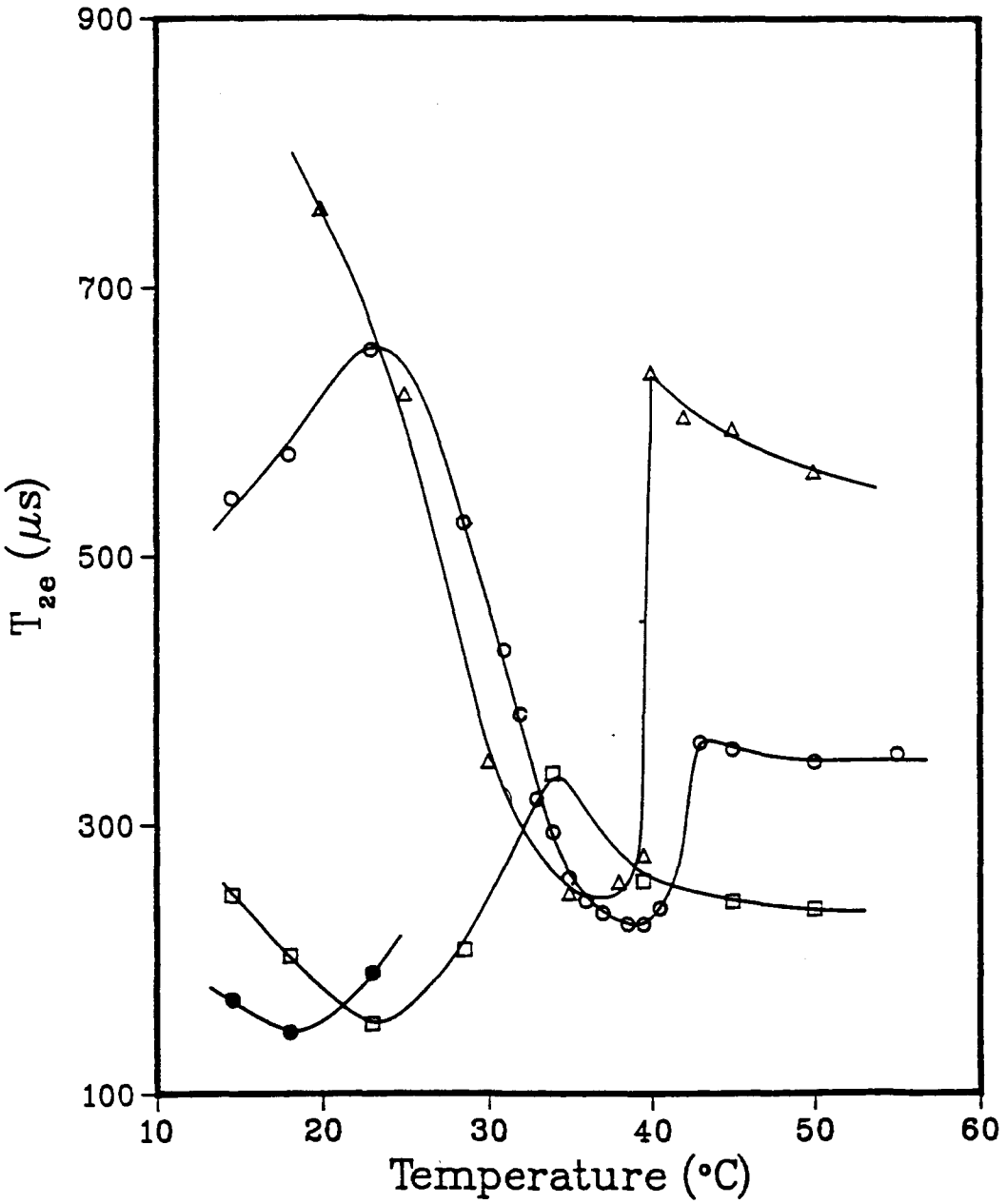

than the DPPC-d_4 minimum (35 or 38°C), while the minimum in the presence of phytanic acid is even lower (18°C). These results are similar to those we obtained from acyl chain deuterated PC containing the two branched chain compounds (see Chapter IV).

2. Discussion

The Phase behavior of DPPC in excess water has been extensively studied by calorimetry (McElhaney, 1982), ^{13}C NMR (Wittebort *et al.*, 1981), ^{2}H NMR (Davis, 1979), X-ray diffraction (Janiak *et al.*, 1976, Ruocco and Shipley, 1982), Raman (Yellin *et al.*, 1977; Gaber, 1978) and FT-IR (Cameron and Mantsch, 1978; Cameron *et al.*, 1980). The main gel to liquid crystalline phase transition of DPPC has been proposed to be due to the melt of the fatty acyl chains (Phillips *et al.*,1969) while the pretransition to be due to the packing of the hydrocarbon chains changing from quasi-orthorhombic to hexagonal (Ruocco and Shipley, 1982), which is associated with the appearance of "ripples" on the bilayer surface (Doniach, 1979). Based on a ^{2}H NMR study of DMPC with a chain terminal deuteromethyl group, the pretransition was shown to coincide with the onset of a fast rotational motion about the molecular long axis (Westerman *et al.*, 1982). This rotational motion was also reported to be hindered in that the molecules flip about a two-fold symmetry axis.

Controversial results about the effect of pretransition on the head group region were reported. Gally *et al.* (1975) reported that no discontinuity was observed at pretransition temperature either in the phosphorus chemical-shift anisotropy or in the quadrupole splitting of the C_β or C_γ segment of aqueous dispersions of DPPC. Sixl and Watts (1982), however, showed an abrupt decrease of ^2H quadrupolar splitting of the C_γ segment of aqueous dispersions of DMPC. Also, Akutsu (1986) showed significant changes in the phosphorus chemical-shift anisotropy and large enhancement of the fluctuation of the rotational axis of the polar group at the pretransition temperature.

Our moment analysis of DPPC-d_4 (Figure 32) clearly shows that the ^2H NMR spectral moments change discontinuously at both the pre- (31^0C) and main (42^0C) transition temperatures. Since the pretransition discontinuity in the M_1 (M_2) *versus* temperature curves for DPPC-d_4 occurs about 4^0C lower than one measured by DSC, the moment analysis is detecting the onset of head group motion(s) at a temperature lower than found for the thermotropic phase transition. The discrepancy of 4^0C might be accounted for by kinetic reasons, i.e., the difference between the slow pretransition rate and the fast DSC scanning rate (Lentz *et al.*, 1978). Some have attempted to obtain the true equilibrium pretransition temperature by measuring the transition temperature as a function of scanning rate and extrapolating to zero scan rate (Lewis *et al.*, 1987). The M_1

method seems to be closer to the equilibrium transition temperature than does DSC.

As shown in Figure 17, in dispersions of PC-d_{31} there was a decrease in the acyl chain M_1 due to the pretransition and we noted changes in the quadrupolar splitting of the chain terminal methyl deuterons beginning at $\approx 30^0$C. However, in the case of the chain perdeuterated compound the DSC pretransition also occurred at $\approx 30^0$C. Thus, the motional property of both choline methylenes on the surface of the bilayer and the acyl chain terminal methyl on the center of the bilayer are related to the pretransition. Furthermore, the change in the bilayer center happens at a slightly higher temperature than that on the bilayer surface.

The effect of phytanic acid and phytol on the head group region of the DPPC bilayer is quite significant as shown by the M_1 versus temperature curve (Figure 32). At 14.5^{0}C the M_1 values for DPPC-d_4, 20 mol% phytol:DPPC-d_4 and 20 mol% phytanic acid:DPPC-d_4 are $2.84X10^4$, $2.33X10^4$ and $2.07X10^4$ (s^{-1}), respectively. The low M_1 value of DPPC-d_4 containing phytanic acid and phytol at temperatures below the main phase transition(42^{0}C) is due to the fact that the branched chain compounds lower the phase transition temperature, producing a different orientation of the head group. The PC-d_{31} results (Chapter IV) show that incorporation of 20 mol% of either phytanic acid or phytol causes the gel to liquid crystalline phase transition onset temperature to drop from 38^{0}C to 28^{0}C,

with no significant change in the completion temperature of the phase transition (see Figure 17, 19). As shown in Figure 32, the rapid M_1 decrease for DPPC-d_4 containing branched chain compounds occurs at temperatures around 15-20^{0}C with no further rapid decrease above 25^{0}C. This finding suggests that, in the presence of phytol and phytanic acid, the M_1 curve reflects pretransition changes and is insensitive to main transition effects. However, the pretransition was not detected by DSC and ^{2}H NMR on acyl chain deuterated PC containing 20 mol% branched chain compound. The decrease in M_1 of DPPC-d_4 due to the pretransition is about 55% of the total M_1 decrease while the decrease in acyl chain M_1 due to the pretransition is only 5% of the total. This small M_1 depression is abolished in the presence of branched chain compounds. The significant M_1 decrease of DPPC-d_4 in the presence of the branched chain compounds at 15-20^{0}C implies that the transition associated with the head group motion does not contribute to the enthalpy change, although it corresponds to the pretransition of DPPC in the absence of the branched compounds. At 50 ^{0}C the M_1 value in the presence of phytol ($1.00X10^4$ s^{-1}) is smaller than for DPPC-d_4 alone ($1.14X10^4$ s^{-1}) while with phytanic acid it is larger ($1.30X10^4$ s^{-1}). This effect is simply due to the fact that phytol narrows $\Delta\nu_Q$ of C_α- and C_β- segments from 6.3 and 4.2 kHz to 6.2 and 3.3 kHz, respectively, whereas phytanic acid narrows the splittings of β-C^2H_2 to 2.4 kHz but increases the splitting of α-C^2H_2

significantly (to 7.5 kHz), resulting in a larger M_1.

As we have suggested (Chapter IV), the branched chain compounds incorporated into phospholipid bilayers force nearest neighbor hydrocarbon chains apart, thus loosening the packing of the choline in the hydrophilic region of the membranes. The ^{31}P chemical shift anisotropies for PC-d_{31}, 20 mol% phytol:PC-d_{31} and 20 mol% phytanic acid:PC-d_{31} multilamellar dispersions at 45^{0}C are 45, 42 and 40 ppm, respectively. The decrease of chemical shift anisotropy induced by phytol and phytanic acid may be due to this looser packing. The decrease of $\Delta\nu_Q$ of both α- and β-C^2H_2 of DPPC-d_4 induced by phytol can be attributed to the same cause. This is similar to the effect of cholesterol on the head group region of a DPPC model membrane (Brown and Seelig, 1978).

Phytanic acid has a totally different effect on the choline group; the decrease in $\Delta\nu_Q$ of β-C^2H_2 and increase in $\Delta\nu_Q$ of α-C^2H_2 implies a conformational change of the head group. As shown in Table VII, these changes are enhanced by the buffer solution. The pH value for DDW dispersions of 20 mol% phytanic acid:PC-d_4 was 5.2, thus, in buffer (pH 7.4), more phytanic acid was ionized, indicating a conformational change in the head group. The negatively charged carboxyl group near the membrane surface attracts the positively charged end of the zwitterionic choline group. This observation is consistent with those of Sixl and Watts (1983) as well as Scherer and Seelig (1987), who found that negatively charged lipids mixed

with phosphatidylcholine increased $\Delta\nu_Q$ of α-C^2H_2 and decreased $\Delta\nu_Q$ of β-C^2H_2. Table VII also shows that in the liquid crystalline phase all six samples have the same temperature dependence, i.e.,the quadrupolar splittings for β-C^2H_2 decrease while those for α-C^2H_2 remain unchanged as temperature increases. This suggests that in all six samples the average orientation of the α-C^2H_2 segment is quite stable while the orientation of β-C^2H_2 changes due to rotation of the C(α)-C(β) bond. This rotation is less pronounced in the presence of phytanic acid.

Cushley et al. (1979) have reported that phytanic acid dramatically increases the permeation rate of Pr^{3+} through the egg yolk PC bilayer while phytol only slightly increases permeability. The effects of phytanic acid and phytol on the dynamic structure of the hydrophobic region of the phospholipid bilayer were observed to be similar to each other (see Chapter IV), but their effects on the head group organization are different (*vide supra*). Therefore, we suggest that the permeation rate is related to the organization of the hydrophilic region of the phospholipid membrane. This argument is supported by the recent work of Gutknecht (1988) who has found that long chain fatty acids increase proton conductance of the phospholipid bilayer membranes and that the increase by phytanic acid is 2-fold more than that by straight chain fatty acids.

Seelig *et al.* (1987) have shown that the phosphatidyl-

choline head group is sensitive to the surface charge of the membrane and that $\Delta\nu_Q$ for α-C^2H_2 follows a linear relationship with charge density, σ, in the range of $\leq$ 0.3 e/lipid. Using Figure 6 in Seelig's report (Seelig et al., 1987) the surface charge density of 20 mol% phytanic acid:DPPC-d_4 dispersions in Tris buffer can be estimated to be $\sigma \approx$ 0.09-0.12 e/lipid. On the basis of this σ value we calculate that the pK value of the phytanic acid carboxyl group is 7.2 -7.5, which is in good agreement with the value of 7.0 for stearic acid (Tscharner and Radda, 1981) and with 7.5 for oleic acid (Small et al., 1984) in PC vesicles. Tsui et al. (1986) have proposed that the rationale for the shift of pK values for the carboxyl group of fatty acids from 4.8 (in aqueous phase) to the physiological pH (7.4) range in membranes is partially due to the low dielectric constant of the PC surface.

Recently, Roux et al. (1989) have proposed a continuum model for the interaction between charged particles near the membrane surface and the head group. The treatment of Roux et al. makes several simplifying assumptions, the most serious one being that the head group is a "quasirigid body hinged at the glycerol backbone". Nevertheless, the model qualitatively relates reorientation to surface charge density. Using their method and assuming that the rotation angle of the head group about the hinge point can be considered as the change of the orientational angle of the C_α-$^2H_2$ bonds with respect to the bilayer normal, we estimate that the carboxylate from the

branched chain acid is between 0.1 Å to 0.9 Å below the planar surface charge.

Another effect of phytanic acid on the ^2H NMR spectrum of DPPC-d_4 is shown by the doublet splitting of the α-C^2H_2 group (Figure 30d, inset). The different quadrupolar splittings for the α-deuterons in the presence of phytanic acid is more clearly shown in the depaked spectra (Figure 31c,d). The nonequivalence of the α-deuterons is an orientation effect. The C^2H_2 segment rapidly interconverts between conformations where the individual C-^2H bonds of the segment are oriented differently with respect to the magnetic field. This may be the same situation as pertains to the C-2 position of the sn-2 acyl chain, whose ^2H NMR shows a doublet splitting (Pauls *et al.*, 1983). The lack of a doublet splitting for DPPC-d_4 and 20 mol% phytol:DPPC-d_4 implies that phytanic acid may enhance such an orientational difference and/or may enhance resolution by narrowing the spectral lines. The latter is supported by the long T_{2e} recorded for the sample containing phytanic acid. T_{2e} values for DDW dispersions of DPPC-d_4, 20 mol% phytol:DPPC-d_4 and 20 mol% phytanic acid:DPPC-d_4 at 45°C are 540±10, 510±40 and 1000±200 μs, respectively. The particle sizes for these three samples are 0.7±0.3, 0.7±0.2 and 1.5±0.8 μm, respectively, as determined by phase contrast microscopy. The long T_{2e} in the presence of phytanic acid results from the large sized particles (*vide infra*). That 20 mol% phytanic acid:DPPC-d_4 dispersions in Tris buffer give excellent

resolution (Figure 30d) is the consequence of phospholipid orientation ("alignment") in the magnetic field (*vide infra*).

In order to examine the effect of phytanic acid and phytol on the motions of the choline head group, spin-lattice relaxation times (T_1) and quadrupolar echo relaxation times (T_{2e}) were determined. For all three samples (≈15 wt% DPPC-d_4, 20 mol%phytol:DPPC-d_4 and 20 mol% phytanic acid:DPPC-d_4 in Tris buffer prepared with freeze-thaw method), T_1 increases as the temperature increases (Figure 35), which is indicative of motion in the fast correlation time limit, usually associated with fast conformational changes about the single bonds. Figure 35 shows that phytol and phytanic acid have an identical effect on the average T_1 of α- and β- C-^{2}H bond, *i.e.*, they slightly decrease the correlation time for the C^2H_2 motion. The increase of T_1 or the decrease of τ_c by the branched chain compounds is the consequence of depression of the phase transition temperature, because the T_1 differences at the same reduced temperature are negligible. For DPPC-d_4, the activation energies were calculated from the linear plot of log T_1 *versus* the reciprocal of temperature to be 3.1±0.2, 5.6±0.4 and 7.4±0.2 kcal/mole for gel phase, intermediate phase and liquid-crystalline phase, respectively. The activation energy for the C_α-segment above the phase transition temperature has been reported as 5±2 kcal/mol (Gally *et al.*, 1975), which is comparable with our data. For 20 mol% phytol:DPPC-d_4 and 20 mol% phytanic acid:DPPC-d_4, the

Table VIII: Spin-Lattice Relaxation Times, T_1, of Head Group Deuterated Phosphatidylcholine (DPPC-d_4) Containing Branched Chain Compounds

Lipid	Temperature (°C)	T_1[a] (ms)		
		α-C^2H_2	β-C^2H_2	Average
DPPC-d_4	45	25.0[b]	27.1[b] (27.8[c])	27.2[b] (27.4[c])
	50	29.9	33.5 (33.2)	32.8 (32.4[c])
20 mol% Phytol:DPPC-d_4	45	28.4	30.4	32.1
20 mol% Phytanic acid:DPPC-d_4	45	26.8	32.2	32.3

[a] Intensities of echo (for "average") and powder pattern peaks (for α-C^2H_2 and β-C^2H_2) were used to fit a semi-log linear regration, correlation constant $r \geq 0.999$. τ = 150 µs; τ_1 values: 5, 10, 20, 30, 40, 50, 60 and 150 ms; t = 200 ms.

[b] τ = 100 µs.

[c] τ = 60 µs, data show reproducible in the measurements.

activation energies in the liquid crystalline phase are 6±1 and 5.7±0.2 kcal/mole, respectively. These values are lower than that for DPPC-d_4 in the liquid crystalline phase. We suggest that the looser packing in the presence of the branched chain compounds may cause the lower energy barrier to the head group conformational change. Examination of the T_1 values for the C_α- and C_β- segments (Table VIII), shows that the phytanic acid slightly reduces the rate of the C_α-segment motion and increases the rate of the C_β-segment motion, compared to phytol. This result is consistent with a conformational change of the choline group in the presence of phytanic acid.

Figure 38 shows that the T_{2e} minimum of DPPC-d_4 shifts from 38°C to 23°C (in the presence of phytol) and to 18°C (in the presence of phytanic acid), which is similar to what we have observed for the acyl chains (see Figures 24, 25). T_{2e} is more sensitive to slow motions such as the lateral diffusion of phospholipid molecules in the bilayer, or the rotational diffusion of the whole particle. Above the phase transition temperature the T_{2e} values depend on the method of sample preparation. The T_{2e} values for DPPC dispersions in DDW without freeze-thawing are about twice as long as those for dispersions in Tris buffer with freeze-thawing. The difference may result from the different morphology of the liposomes (see Results). The short T_{2e} value for DPPC liposomes containing phytol is consistent with the small liposome particles

observed by phase contrast microscopy. The unusual T_{2e} behavior of Tris buffer dispersions of DPPC-d_4 containing phytanic acid in the liquid crystalline phase may be explained by the deformation of the liposome particles caused by the magnetic field ordering (*vide infra*). The diffusion of phospholipids in such oriented bilayers does not change the orientation of the C-^{2}H bond with respect to the magnetic field, resulting in extremely long correlation times, τ_c. In the slow motion region τ_c is proportional to T_{2e} (Pauls *et al.*, 1985), thus a long τ_c results in an extremely long T_{2e}. This would explain the plateauing of the echo intensities for short τ values (Figure 37).

The most interesting observation is that phytanic acid causes a distortion of the ^{2}H spectrum of DPPC-d_4 (Figure 30d). There are two possible reasons for this distortion: one being the orientational dependency of spin-spin relaxation and the other being orientation of the phospholipids in the magnetic field. We exclude the former possibility, *i.e.* the orientational dependency of T_{2e} as the cause of the distortion of the powder pattern lineshape, because the ^{2}H NMR spectra are similar in spite of using various τ values (60-150 μs) in the quadrupolar echo pulse sequence, and also the first moments (M_1) of these spectra are close to within 5%. Thus, Figure 30d is evidence for sample orientation in the magnetic field. This is supported by the FID (Figure 30h) which is seen to be much longer than the FIDs for DPPC-d_4 or DPPC-d_4:phytol,

and is indicative of intensity loss in the wings.

The ^{31}P NMR spectra confirm that the distortion effect is due to magnetic orientation. In the ^{31}P NMR spectrum of DPPC-d_4 incorporated with 20 mol% phytanic acid in Tris buffer at 45°C (Figure 33e) the intensity of the 90° edge ($\sigma_\perp$) is enhanced, while the intensities for other angles are diminished (compare with Figure 33b). When the sample is cooled to the gel phase in the magnetic field, the orientation effect persists (Figure 33f) and this is quantified by the difference spectrum (Figure 33g).

The driving force for magnetic orientation is the negative diamagnetic anisotropy of the phospholipid acyl chains. When such chains become parallel to each other in the bilayer they enhance the tendency to orient with their long axis perpendicular to the magnetic field. To our knowledge only two examples for this kind of orientation have been reported. Seelig *et al.* (1985) have reported the magnetic field orientation of the phospholipids in 15 wt% dispersions of a mixture of POPE and POPG (83/17 w/w) in 0.1 M NaCl:10 mM PIPES:1 mM EDTA, pH 7.0. Recently, Speyer *et al.* (1987) have reported a high degree of orientation in the magnetic field of 50 wt% dispersions of mixtures of N-palmitoylsphingomyelin and DMPC (60:40 mole:mole).

The magnetic orientation has been proposed to be due to either a deformation of spherical liposome particles or an alignment of elliptically-shaped liposome particles (Speyer et

al., 1987). Our results are consistent with the former mechanism. When our 15 wt% dispersions were prepared with a five-fold freeze-thaw procedure, bilayers in the center of the liposome particles were ruptured, leading to a decreased number of bilayers in the multilamellar structure and to an increased interlamellar space. It has been also shown in the literature that repetitive freeze-thaw cycles can induce a homogenous distribution of solute inside and out of the egg PC bilayers, and increase trapped volumes dramatically (Mayer *et al.*, 1985). The deformation under Brownian flow, of the large, less dense particles containing phytanic acid, was clearly observed using the phase contrast microscope. Since the DDW dispersions of 20 mol% phytanic acid:DPPC-d_4 did not orient in the magnetic field, it is apparent that increased negative charge in the surface of the bilayers caused by ionization of phytanic acid in Tris buffer, facilitates the deformation, presumably by decreasing the number of bilayers in the liposome particles. This is analogous to the observation that the negatively charged phospholipids such as phosphoglycerol forms large single bilayer vesicles spontaneously when dispersed in water. As shown in Figure 26 the particles of DDW dispersions are denser than the buffer dispersion, and the particles of buffer dispersion resemble "hollow" particles, which tend to deform easily in the magnetic field. In fact, the deformation of these "hollow" particles under flow was observed under the microscope.

In order to clarify the condition for the magnetic orientation, we measured the ^2H NMR spectrum at 45°C for dispersions of 20 mol% phytanic acid:DPPC-d_4 in Tris buffer without the freeze-thaw procedure and no spectral distortion was detected. Furthermore, we measured ^2H NMR spectra (Figure 34) for PC-d_{31} and 20 mol% phytanic acid:PC-d_{31} dispersed in DDW and in Tris buffer with the freeze-thaw procedure. The spectrum for 20 mol% phytanic acid:PC-d_{31} dispersions in buffer (Figure 34d) shows a distortion effect, i.e., the intensity of the powder pattern shoulder is reduced. This suggests that the magnetic orientation occurs for whole phospholipid molecules.

VI. The Effect of Phytanic Acid and Phytol on the Lateral Diffusion of Phosphatidylcholine in Bilayers

In the liquid crystalline phase, 20 mol% of phytanic acid increases T_{2e} of PC-d_{31} by two-fold while 20 mol% of phytol has no effect on T_{2e} of PC-d_{31} (Chapter IV, Figures 24,25). In Chapter V we have demonstrated that T_{2e} values depend on the method of sample preparation and the resulting morphology of the liposomes. However, under the phase contrast microscope, the dispersions (50 wt% in DDW) of PC-d_{31}, 20 mol% phytanic acid:PC-d_{31} and 20 mol% phytol:PC-d_{31} show a similar morphology (Figure 39). The diameters of liposome particles for these three samples were measured to be 1.1±0.6, 0.8±0.5 and 0.8±0.7 μm, respectively. Bloom and Sternin (1987) have recently shown that a large fraction of the ^2H NMR T_{2e} relaxation in model membranes is due to extremely slow motion such as lateral diffusion of the phospholipid molecules along the curved membrane surface. That the PC-d_{31} dispersions containing phytanic acid and phytol possess almost the same particle sizes but unequal T_{2e} values implies that these two isoprenoid compounds might have different effects on the lateral diffusion of PC in bilayers. In this Chapter we present evidence that phytanic acid and phytol influence the lateral diffusion of phospholipids in the bilayer differently.

Figure 39: Phase contrast microscope photographs for DDW dispersions of (a) PC-d_{31}, (b) 20 mol% phytol:PC-d_{31} and (c) 20 mol% phytanic acid:PC-d_{31}. (magnification = 3,000 times)

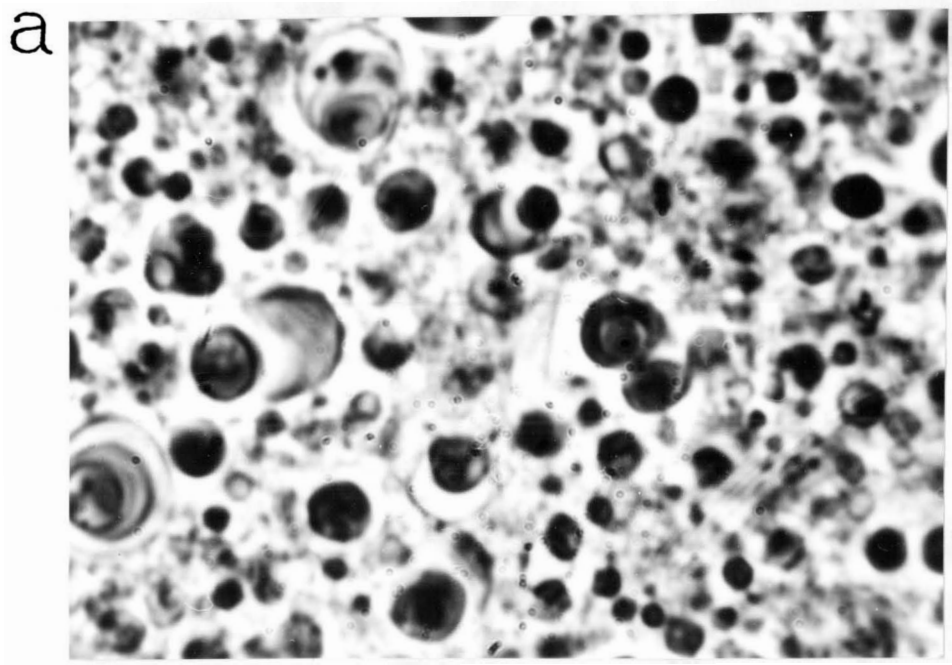

b

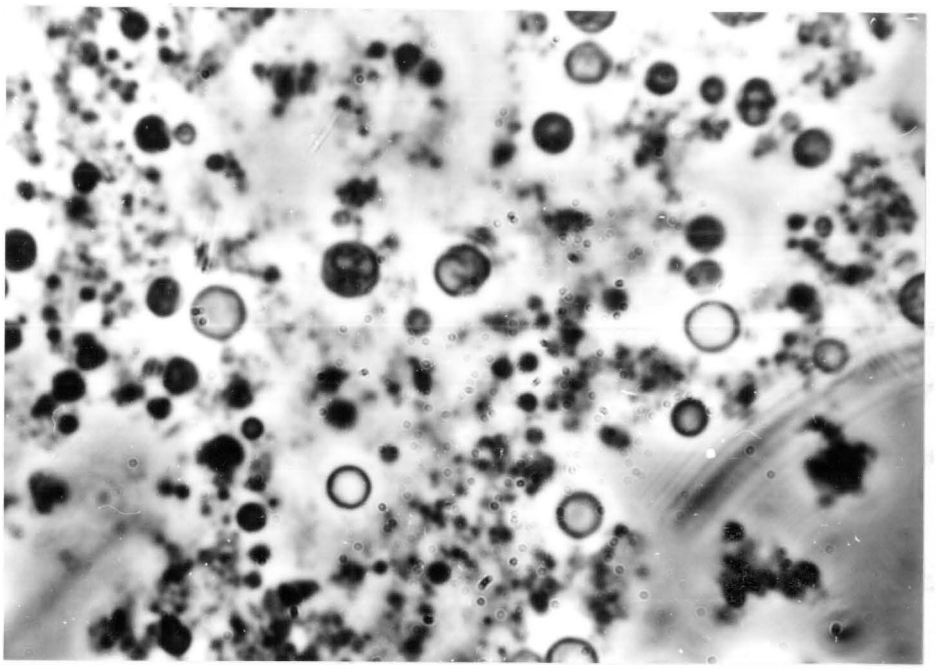

c

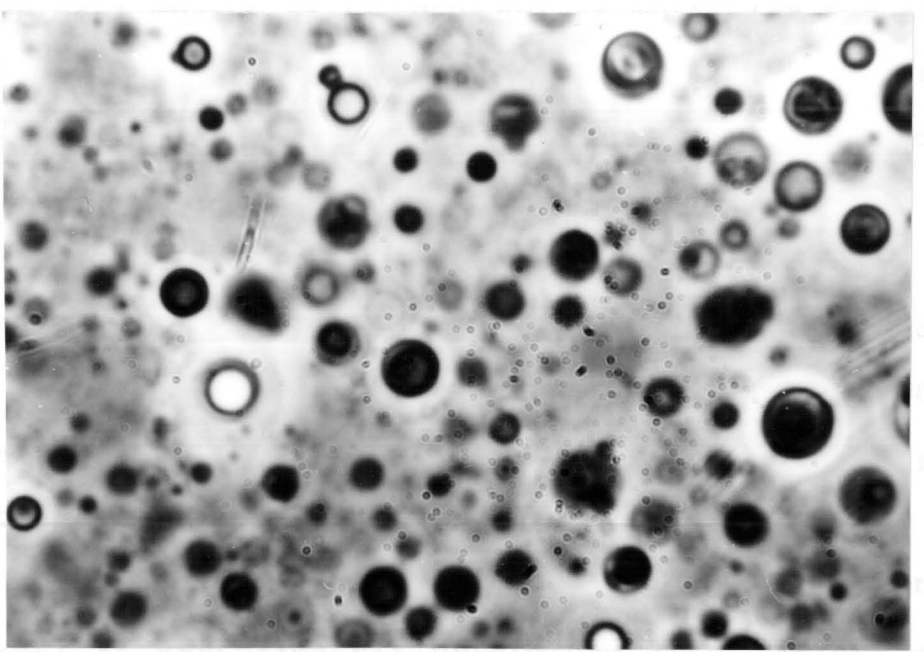

1. Results

A. ^2H NMR study using quadrupolar Carr-Purcell-Meiboom-Gill (CPMG) pulse sequence

In a ^2H NMR study on multilamellar membrane system spin-spin relaxation time (T_{2e}) is measured from the decay of the quadrupolar echo, which has been interpreted in terms of the changes in the apparent second moment of the powder pattern spectra due to rotation (Pauls et al. 1985). No quantitative relationship between T_{2e} and correlation time has been deduced so far, if the motions responsible for T_{2e} are extremely slow. In order to compare the effects of phytanic acid and of phytol on the slow motion of phosphocholine molecules the spin-spin relaxation times (T_2), were measured on DDW dispersions of PC-d_{31}, 20 mol% phytol:PC-d_{31} and phytanic acid:PC-d_{31}, respectively, using a quadrupolar CPMG pulse sequence, 90^0_y-[τ-90^0_x-τ]$_n$-t (Bloom and Sternin, 1987).

The typical data of a series of echoes from a quadrupolar CPMG experiment are plotted in Figure 40a. Each 90_x pulse generates an echo, the intensity of echo progressively decays due to relaxation. As shown in Figure 40b, the decay of echo intensity in the whole time range deviates from exponential. However, we approximately determined $T_2^{q\text{-}CPMG}$ values assuming echo decays exponentially in a certain time domain:

$$A(2n\tau) = A(0) \exp[-2n\tau/T_2^{q\text{-}CPMG}] \quad (37)$$

where $A(2n\tau)$ is the intensity for nth echo. Table IX lists $T_2^{q\text{-}CPMG}$ values for three samples studied (T_{2e} values are also listed for comparison). For the same sample, $T_2^{q\text{-}CPMG}$ is much longer than T_{2e}. $T_2^{q\text{-}CPMG}$ determined from the time range of 2-4 ms is much longer than that from the initial time range of 0-1 ms. Nevertheless, $T_2^{q\text{-}CPMG}$ or T_{2e} for these three samples shows similar order, *i.e.*, phytanic acid: PC-d_{31} > PC-d_{31} ≈ phytol:PC-d_{31}.

Table IX Spin-spin Relaxation Times T_{2e} and $T_2^{q\text{-}CPMG}$ (τ=50 μs) of 50 wt% PC-d_{31} Dispersions Containing Phytol and Phytanic Acid at 50°C

Sample	T_{2e} (μs)	$T_2^{q\text{-}CPMG}$ (ms)	
		$0<2n\tau<1$ ms	$2<2n\tau<4$ ms
PC-d_{31}	210	0.81	4.31
20mol% Phytanic acid:PC-d_{31}	360	1.83	6.70
20mol% Phytol: PC-d_{31}	210	0.74	4.40

Figure 40:

(a) Echoes recorded from a q-CPMG experiment for 50 wt% dispersions of 20 mol% phytanic acid:PC-d_{31} in DDW at 50^{0}C.
Spectral parameter: 90^0 pulse width = 6.5 μs; τ, the interval between pulses, = 75 μs; t, the delay between echo sequences, = 3 s; dwell time = 5 μs; data size = 2K; number of acquisitions = 2,000.

(b) Semilog plot of echo intensity *vs.* time for data in Fig.(a).

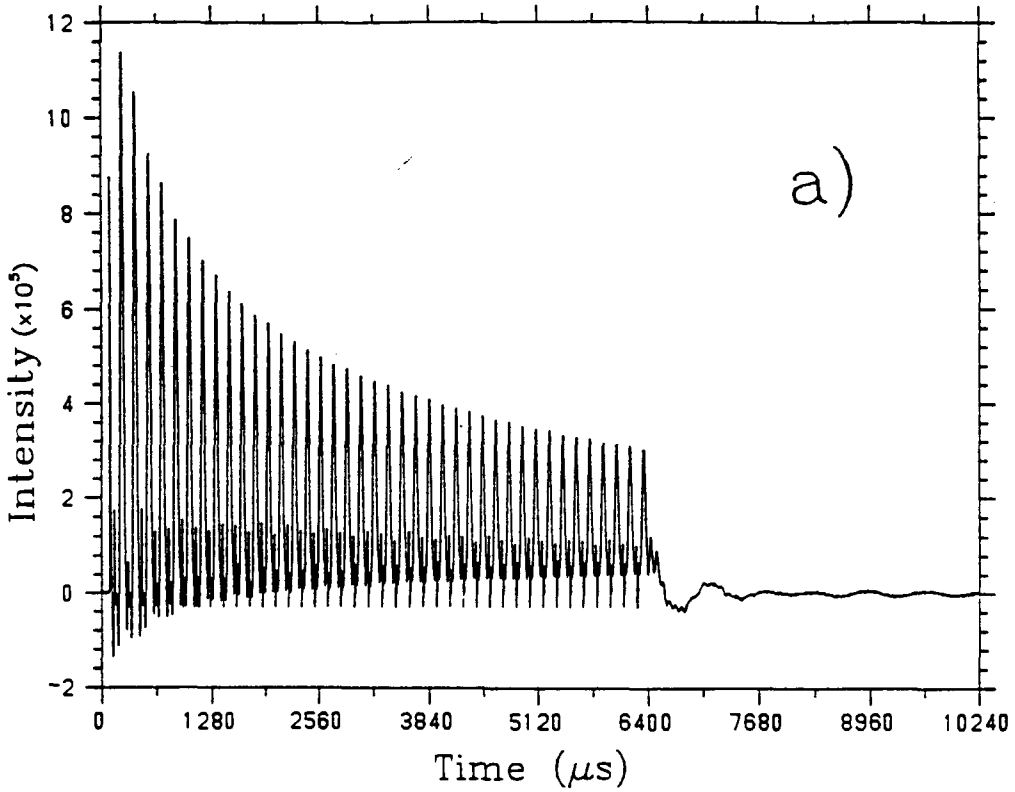
a)
Intensity (x10^5)
12
10
8
6
4
2
0
-2
0
1280
2560
3840
5120
6400
7680
8960
10240
Time (μs)

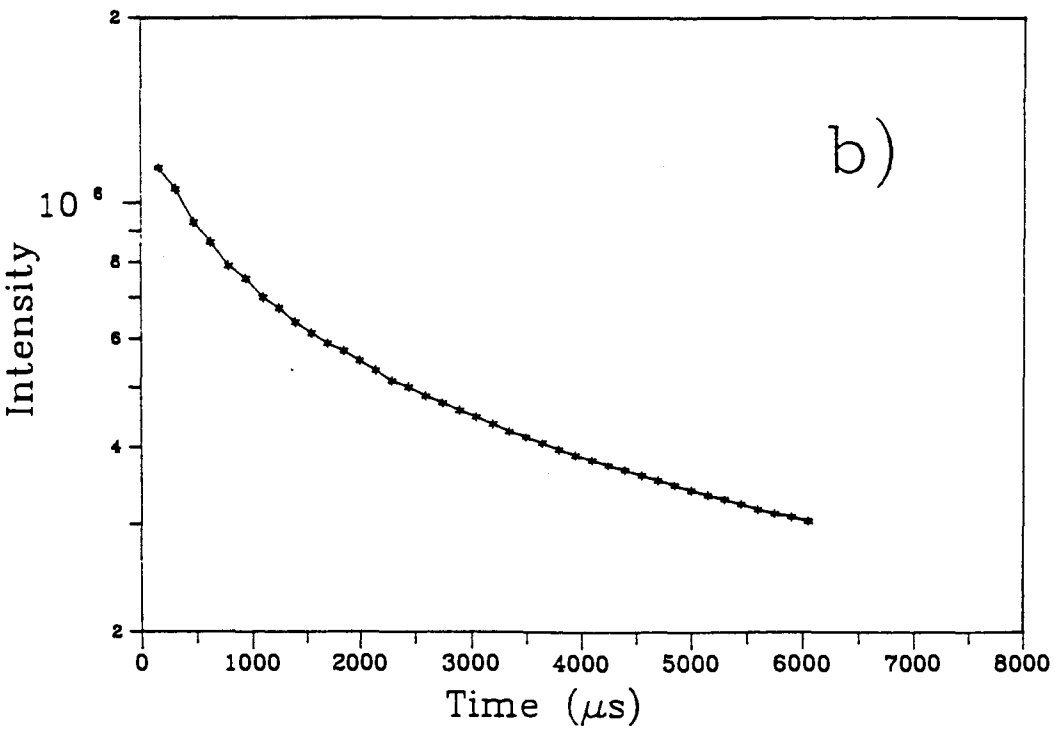
b)
Intensity
10^6
8
6
4
2
0
1000
2000
3000
4000
5000
6000
7000
8000
Time (μs)

According to Bloom and Sternin (1987), the extremely slow motion, such as diffusion of phospholipid along the curved bilayer of the membranes, can be distinguished from the other motions contributing to the spin-spin relaxation process. The equation is:

$$\langle 1/T_2^{q\text{-CPMG}} \rangle \approx (2M_{2r}D_T/R^2_{eff})\tau^2 + \langle 1/T_2 \rangle \qquad (38)$$

where τ is the interval in the q-CPMG pulse train, $T_2^{q\text{-CPMG}}$ is measured from the initial region of decay, M_{2r} is the residual second moment of the ^2H NMR spectrum, R_{eff} is the effective radius for diffusion relaxation, and T_2 is the spin-spin relaxation time due to motions with correlation time $<< \Delta M_2^{-1/2}$.

For three samples (50 wt% dispersions of PC-d_{31}, 20 mol% phytanic acid:PC-d_{31} and 20 mol% phytol:PC-d_{31}), we performed the quadrupolar CPMG experiment at 50°C using various τ values (50, 75, 100, and 125 μs). By fitting the first few echo intensities to a single exponential decay, the $T_2^{q\text{-CPMG}}$ values were determined. Table X lists those values and the number of echoes being used in the fitting. From τ^2 dependence of $1/T_2^{q\text{-CPMG}}$, the linear least square fitting plots (Figure 41) were obtained according to equation 38. The resulting intercept $\langle 1/T_2 \rangle$ and slope $(2M_{2r}D_T/R^2_{eff})$ are also listed in columns 5 and 6 of Table X. M_{2r} values were measured to be $2.9\text{X}10^9$ and $3.2\text{X}10^9$ s^{-2} for PC-d_{31} and PC-d_{31} incorporated with phytol or phytanic acid, respectively.

Figure 41: Least-square fitting of $1/T_2^{q\text{-CPMG}}$ *vs.* τ^2 for
(a) PC-d_{31},
(b) 20 mol% phytanic acid:PC-d_{31} and
(c) 20 mol% phytol:PC-d_{31}.
The error bars of the data represent the standard deviations.

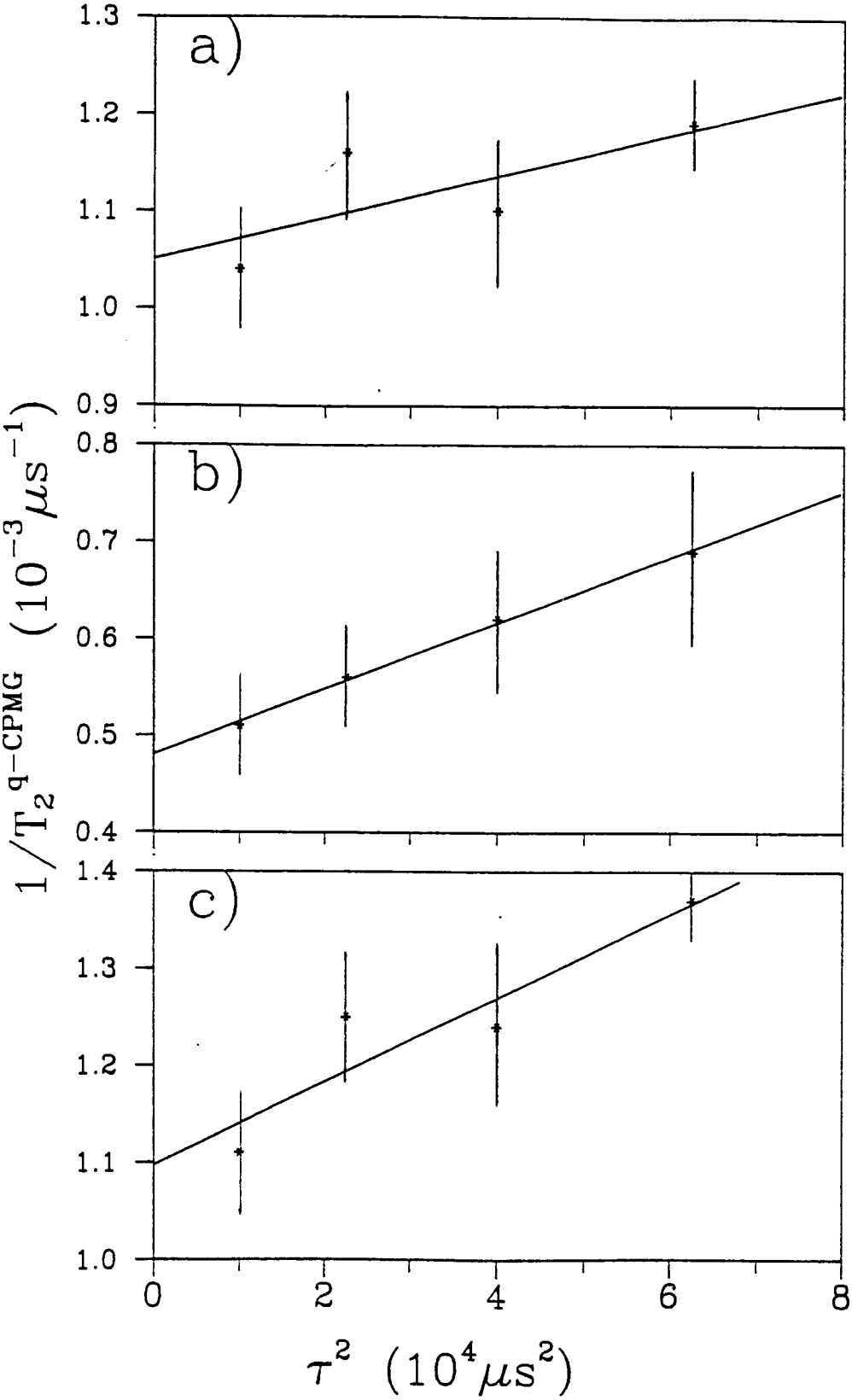
a)
b)
c)
1.3
1.2
1.1
1.0
0.9
0.8
0.7
0.6
0.5
0.4
1.4
1.3
1.2
1.1
1.0
0
2
4
6
8
$1/T_2^{q-CPMG}$ $(10^{-3}\mu s^{-1})$
τ^2 $(10^4\mu s^2)$

Using the average particle size as the effective radius of diffusion, we calculated the lateral diffusion coefficient D_T to be $1.2X10^{-9}$, $0.9X10^{-9}$ and $1.1X10^{-9}$ cm^2s^{-1} for PC-d_{31}, 20 mol% phytanic acid:PC-d_{31} and 20 mol% phytol:PC-d_{31}, respectively. Also the spin-spin relaxation time (T_2), due to the motion with correlation time $\tau_c << \Delta M_2^{-1/2}$ was obtained from the intercept to be 1.0, 2.1 and 0.9 ms for PC-d_{31}, 20 mol% phytanic acid:PC-d_{31} and 20 mol% phytol:PC-d_{31}, respectively.

Table X Spin-spin Relaxation Times $T_2^{q\text{-CPMG}}$ as Function of τ for 50 wt% PC-d_{31} Dispersions Containing Phytol and Phytanic Acid at 50°C

Sample	τ (μs)	Point of fitting	$1/T_2^{q\text{-CPMG}}$ ($10^{-3}\mu s^{-1}$)	$1/T_2$ ($10^{-3}\mu s^{-1}$)	Slope ($10^{-9}\mu s^{-3}$)
PC-d_{31}	50	8	1.04	1.05±0.04	2.2±1.2
	75	5	1.16		
	100	3	1.10		
	125	3	1.19		
20mol% Phytanic acid:PC-d_{31}	50	8	0.51	0.48±0.01	3.5±0.2
	75	5	0.56		
	100	4	0.62		
	125	3	0.69		
20mol% Phytol :PC-d_{31}	50	8	1.11	1.09±0.04	4.4±0.7
	75	5	1.25		
	100	4	1.24		
	125	3	1.37		

B. ^2H NMR study using selective inversion recovery (DANTE) pulse sequence

The diffusion of phosphatidylcholine molecules along the bilayer surface can be also demonstrated by a selective inversion recovery experiment. Brown and Davis (1981) have reported such an experiment on 4,4-DPPC-d_2/H_2O dispersions, using a soft 180^0 pulse to selectively invert the frequencies near the middle of the spectrum. They found that the recovery of these inversions was non-exponential, the initial slope was due to the transfer of magnetization across the spectrum. We have modified a phase-rotating DANTE pulse sequence, 90^0_y-t_D-90^0_{-y}-, to selectively invert the magnetization in certain frequency domains. This pulse sequence followed by a delay time τ_1 and a quadrupolar echo pulse sequence forms the selective inversion recovery pulse sequence employed in this study. Figure 42 demonstrates such a selective inversion recovery experiment of 5,5-DPPC-d_2/H_2O dispersions. For short delay (τ_1= 0.5 ms), the principal peaks of the powder pattern are inverted (Figure 42a). With τ_1 increasing, the peak intensity becomes positive and increases, and the spectrum shows a normal powder pattern at longest delay (τ_1= 160 ms, Figure 42b).

Figure 42: ^2H NMR spectra for different values of delay time (a, τ_1= 0.5 ms; b, τ_1= 160 ms), recorded at 38.8 MHz using a selective inversion recovery pulse sequence, 90^0_y-t_D-90^0_{-y}-τ_1-90^0_y-τ-90^0_x-t, for 50 wt% dispersions of 5,5-DPPC-d_2/H_2O at 45°C.

Spectral parameters: 90^0 pulse = 6.5 μs, t_D = 35 μs, τ = 50 μs, t = 250 ms; sweep width = ±100 kHz; data size = 4K in complex; line broadening = 50 Hz; number of acquisitions = 8,000.

* 5,5-DPPC-d_2 is a kind gift from Dr. R.S. Chana.

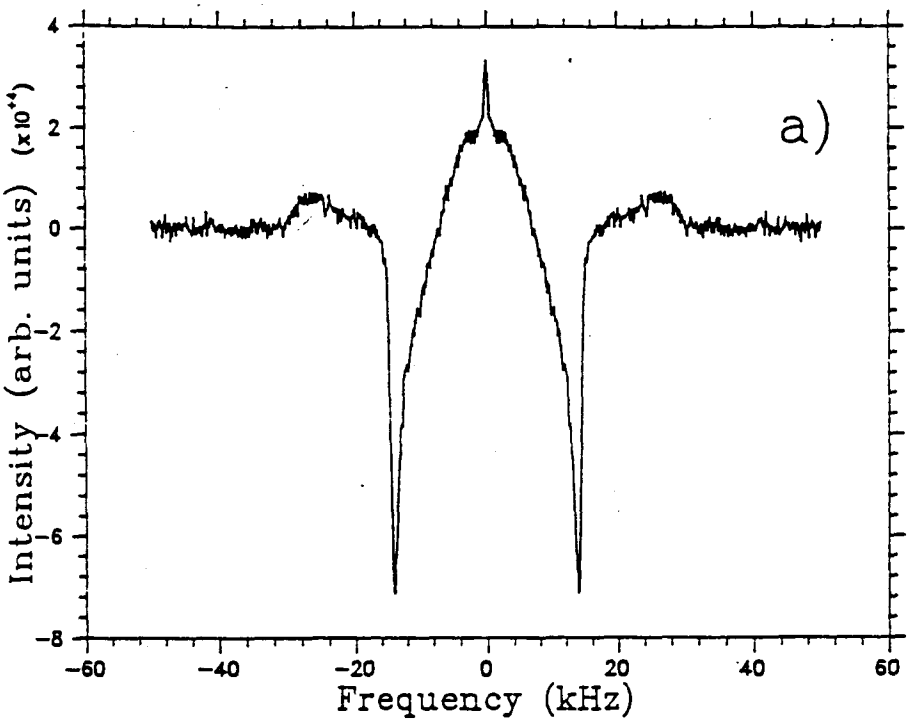
a)
Intensity (arb. units) (x10⁻⁴)
Frequency (kHz)
4
2
0
-2
-4
-6
-8
-60
-40
-20
0
20
40
60

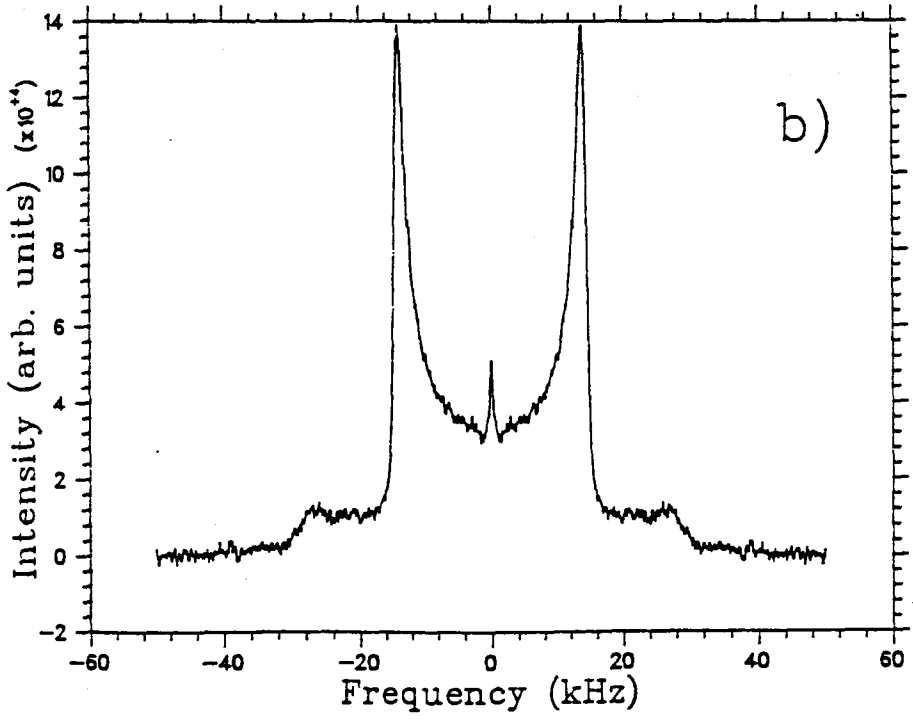
b)
Intensity (arb. units) (x10⁻⁴)
Frequency (kHz)
14
12
10
8
6
4
2
0
-2
-60
-40
-20
0
20
40
60

The spectra for dispersions of PC-d_{31}, 20 mol% phytanic acid:PC-d_{31} and 20 mol% phytol:PC-d_{31} were taken using the selective inversion recovery with various delay times at 45°C. The time interval, t_D, was adjusted to invert the principle peaks of the powder pattern for the methlene segments of the plateau region (C3-C9). The semilog plots for the peak intensity recovery ($A-A_0$) *vs.* delay time τ_1 are compared with those for spin-lattice relaxation measurement, which are depicted in Figure 43. The initial decay for selective inversion recovery is non-exponential, while the decay in the long time range (τ_1 > 10 ms) is parallel to that for T_1 experiments. The least square fits for the selective inversion recovery data in τ_1 > 10 ms range give the rate constants: 27.9, 30.3 and 31.5 ms for PC-d_{31}, 20 mol% phytanic acid:PC-d_{31} and 20 mol% phytol:PC-d_{31}, respectively. These values are very close to those of T_1 measured from the normal inversion recovery experiments (Table VI). In order to compare the diffusion rates for these three samples, the relative intensity $(A-A_0)/2A_0$ is plotted *versus* τ_1 (Figure 44). Qualitatively, Figure 44 illustrates that the rate for phospholipid molecules diffusing from a 90° (or 32°) orientation to the other orientation angle with respect to the magnetic field is in the order: phytol:PC-d_{31} > PC-d_{31} > phytanic acid:PC-d_{31}.

Figure 43: Semilog plots of (A_0-A) *versus* τ_1 for inversion recovery experiment (-••-) and selective inversion recovery experiment (-o-) at 45°C.
(a) 50 wt% dispersions of PC-d_{31} in DDW,
(b) 50 wt% dispersions of 20 mol% phytanic acid:PC-d_{31} in DDW,
(c) 50 wt% dispersions of 20 mol% phytol:PC-d_{31} in DDW.

A is the spectral intensity of the composed peaks of the powder pattern, which were assigned to the deuteron attached to carbon position C3-9 of the acyl chain. The time interval, t_D, in selective inversion recovery pulse sequence was adjusted properly in order to obtain the maximum inversion of these peaks.

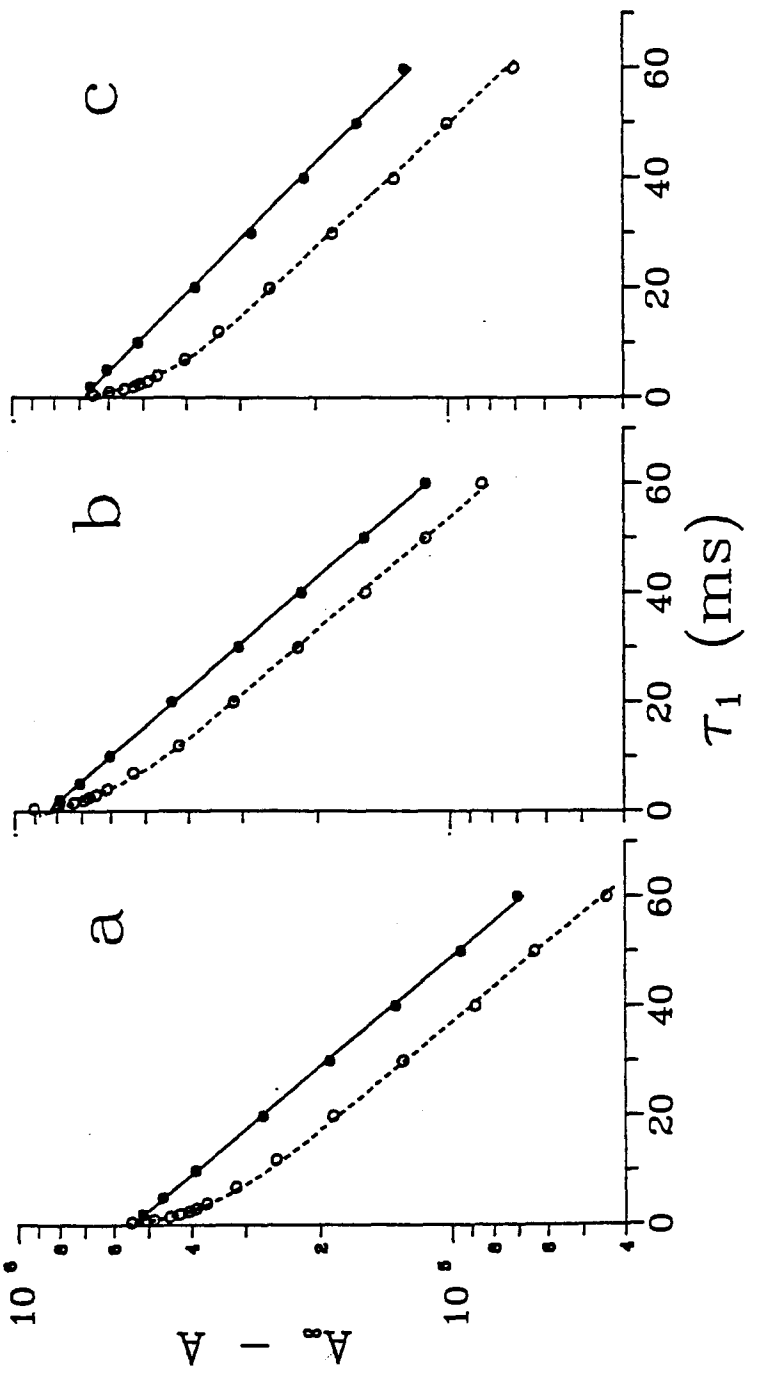
a
b
c
$A_\infty - A$
10^6
10^5
6
5
4
2
0
20
40
60
τ_1 (ms)

Figure 44: Semilog plot of $[(A_\infty - A)/2A_\infty]$ versus τ_1 in short τ_1 range for PC-d_{31} (o), 20 mol% phytanic acid:PC-d_{31} (+) and 20 mol% phytol:PC-d_{31} (x).

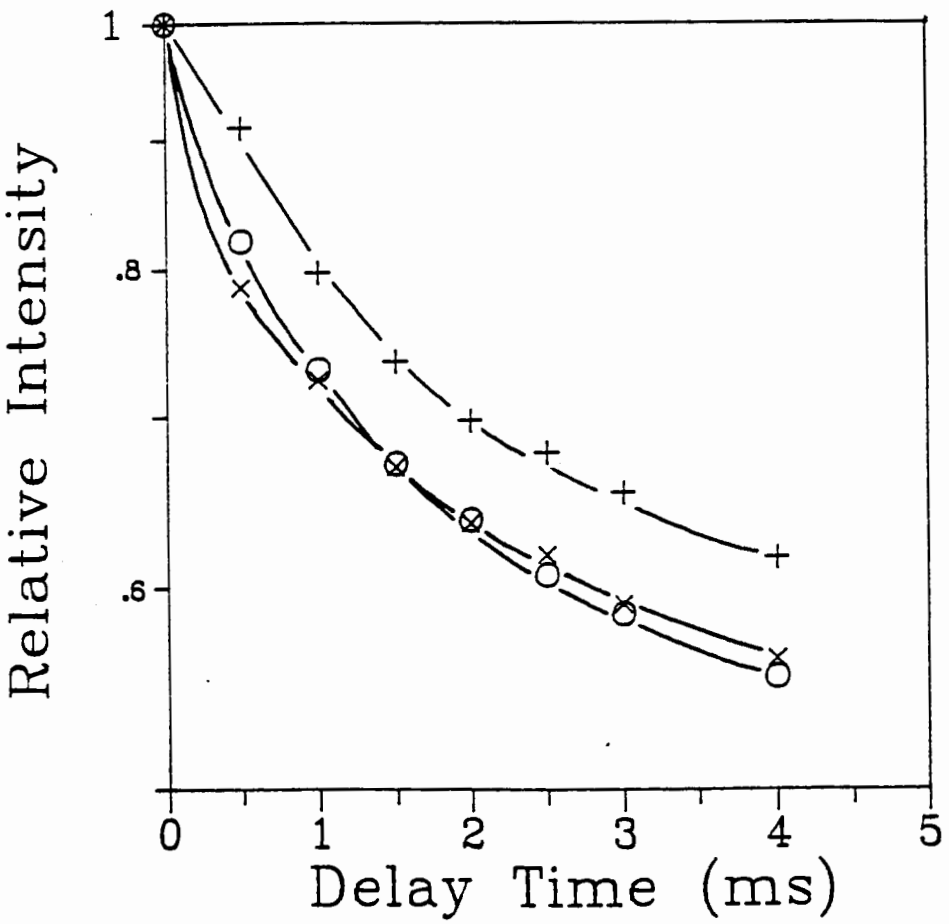

C. ^{31}P NMR study on DPPC vesicles containing phytanic acid and phytol

We simulated the ^{31}P NMR spectra for the vesicles of DPPC, 20 mol% phytol:DPPC and 20 mol% phytanic acid:DPPC using a computing program obtained from Dr. E. E. Burnell, University of British Columbia. The computing program is based on the theory of Freed *et al.* (1971), which was originally used to calculate the ESR lineshape under the rotationally dependent perturbation in the spin-Hamiltonian. In Burnell's model (Burnell *et al.*, 1980), they assumed that the ^{31}P nucleus possessed an axially symmetrical chemical-shift tensor, and that the reorientational motion of the ^{31}P nucleus was governed by the isotropic diffusion equation (see eq. 28). The program needs three parameters to simulate the spectra: the chemical shift anisotropy, Lorentzian line broadening and the effective correlation time of the isotropic motion. In our simulation, we assumed that the ^{31}P chemical shift anisotropies for DPPC in vesicles were the same as those found in multilamellar liposomes of PC-d_{31}. The chemical shift anisotropies were measured to be 45, 42 and 40 ppm for PC-d_{31}, 20 mol% phytol:PC-d_{31} and 20 mol% phytanic acid:PC-d_{31}, respectively. We employed Lorentzian line broadenings of 65 Hz (for 20 mol% branched chain compounds:DPPC) and 215 Hz (for DPPC), which were consistent with the 50 and 200 Hz used in the experimental spectra plus a 15 Hz natural line width. The best simulation

was obtained by varying the effective correlation time τ_e. Figure 45 presents both the simulated and experimental spectra. From the τ_e values of the simulated spectra, we calculated the diffusion coefficient, D_T, using equation 28. The D_T values were determined as $6.1X10^{-8}$, $1.6X10^{-8}$ and $4.7X10^{-9}$ cm^2s^{-1} for DPPC in vesicles by itself, with 20 mol% phytol incorporation and with 20 mol% phytanic acid incorporation, respectively (Table XI).

Table XI Data for Lateral Diffusion Measurement

Vesicles	r (nm)	$(\sigma_{\parallel}-\sigma_{\perp})^a$ (Hz)	τ_e (s)	η^b (poise)	D_T (cm^2s^{-1})
DPPC	65.5	4600	$1.0X10^{-4}$	0.119	$6.1X10^{-8}$
20 mol% phytanic acid:DPPC	26.1	4100	$1.1X10^{-4}$	0.119	$4.7X10^{-9}$
20 mol% phytol	31.1	4250	$0.8X10^{-4}$	0.119	$1.6X10^{-8}$

[a] These values were measured from multilamellar liposomes samples.
[b] 75% glycerol in water at 45°C (Chana, 1989).

$$1/\tau_e = (1/\tau_t) + (1/\tau_{diff})$$
$$= (3kT/4\pi\eta r^3) + (6D_T/r^2) \qquad (28)$$

Figure 45: Simulated (---) and experimental (——) 102 MHz ^{31}P NMR spectra for vesicles of
(a) 20 mol% phytanic acid:DPPC, 45°C, 75% glycerol,
(b) 20 mol% phytol:DPPC, 45°C, 75% glycerol,
(c) DPPC, 45°C, 75% glycerol.

Spectral parameters: one pulse experiment, no phase cycling; pulse width = 6.5 μs (flip angle = 73°); delay between pulses = 2 s; delay before acquisition = 10 μs; sweep width = 25 kHz; data size = 4K in complex; number of acquisitions = 20,000; line broadening = 50 Hz (a,b), 200 Hz (c).

Simulation parameters:
(a) $(\sigma_{\parallel}-\sigma_{\perp})$ = 4100 Hz (40.1 ppm), τ_e = 1.1 X 10^{-4} s, line broadening 65 Hz,
(b) $(\sigma_{\parallel}-\sigma_{\perp})$ = 4250 Hz (41.6 ppm), τ_e = 0.8 X 10^{-4} s, line broadening 65 Hz,
(c) $(\sigma_{\parallel}-\sigma_{\perp})$ = 4600 Hz (45.0 ppm), τ_e = 1.0 X 10^{-4} s, line broadening 215 Hz.

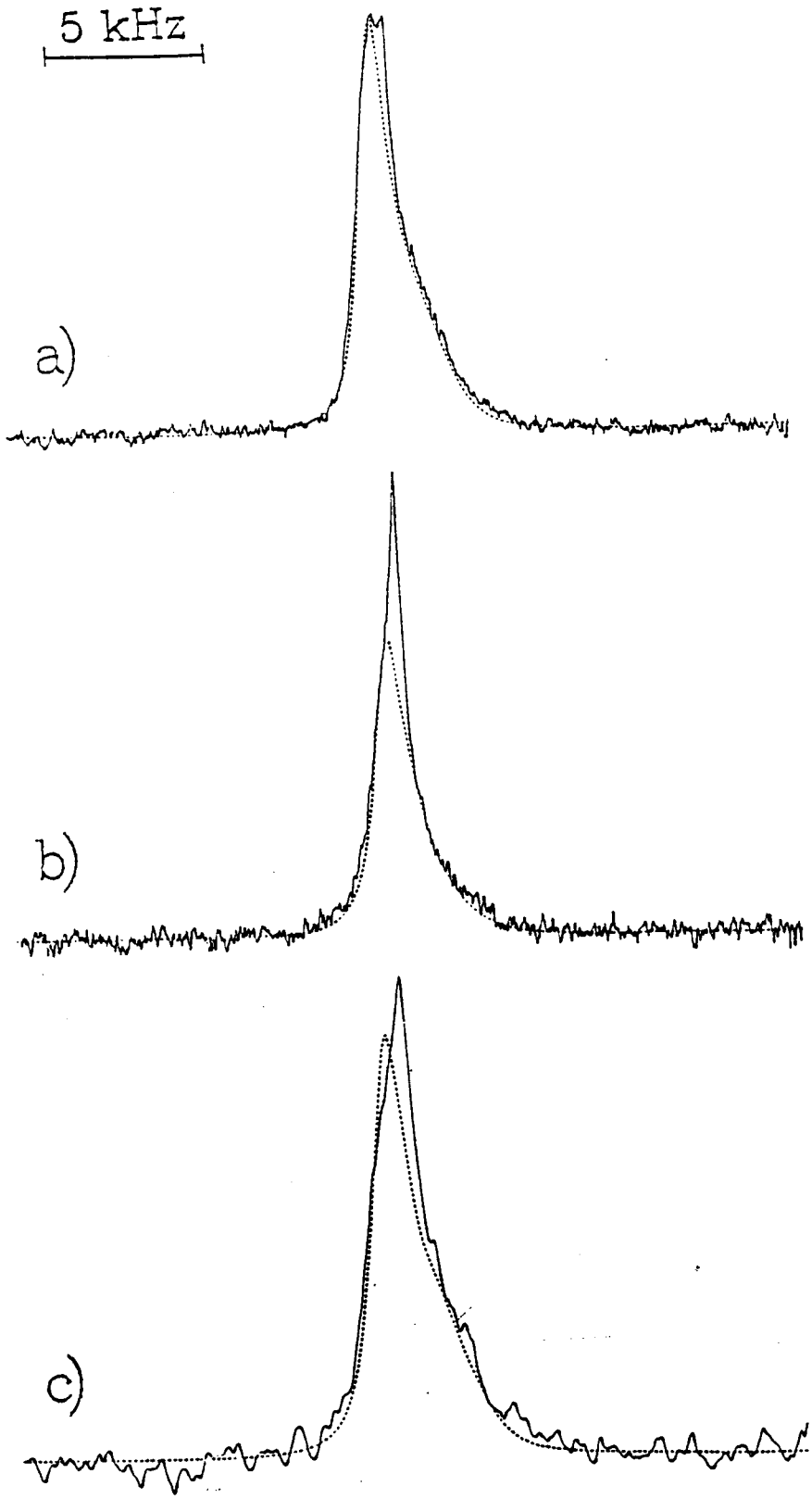
5 kHz
a)
b)
c)

2. Discussion

We have used three methods, *i.e.*, 1) ^{2}H NMR: quadrupolar CPMG pulse sequence, 2) ^{2}H NMR: selective inversion recovery pulse sequence and 3) ^{31}P NMR: lineshape fitting, to study the effects of phytol and phytanic acid on the diffusion properties of PC in the bilayer membranes above the gel to liquid crystalline phase transition temperature.

Using ^{2}H NMR quadrupolar CPMG method, the diffusion coefficient of phospholipid in the membrane, D_T, was measured from multilamellar liposome samples. The obtained D_T value of PC-d_{31} liposomes ($1.2X10^{-9}$ cm^2s^{-1}) is lower than the literature value ($D_T \approx 2\text{-}5\ X10^{-8}$ cm^2s^{-1} for DPPC, Cullis, 1976; Kuo and Wade, 1979) by one order of magnitude. Such a great deviation implies that the method of Bloom and Sternin (1987), which was used in our experiments, may not be appropriate to our cases. Nevertheless, if we assume that the above deviation is a systematic one, the comparison of D_T (or T_2) values for PC-d_{31}, 20 mol% phytol:PC-d_{31} and 20 mol% phytanic acid:PC-d_{31} may still be meaningful. The diffusion coefficient values for the three samples are similar to each other, which are $1.2X10^{-9}$, $0.9X10^{-9}$ and $1.1X10^{-9}$ cm^2s^{-1} for PC-d_{31}, 20 mol% phytanic acid:PC-d_{31} and 20 mol% phytol:PC-d_{31}, respectively. However, 20 mol% phytanic acid:PC-d_{31} has a longer T_2 value (2.1 ms) than PC-d_{31} (1.0 ms) and 20 mol% phytol:PC-d_{31} (0.9 ms). This finding implies that

phytanic acid increases the slow motion ($1/\omega_0 < \tau_c << \Delta M_2^{-1/2}$) of the phospholipid, whereas phytol does not affect the phospholipid motion in this frequency region.

We used a selective inversion recovery pulse sequence (^2H NMR) to investigate the diffusion property of the phospholipid in multilamellar bilayers. The sequence is a modified DANTE followed by a quadrupolar echo sequence, which is similar to Sternin's (1988). The ordinary DANTE pulse sequence is a pulse train of many short pulses P_D and delays t_D: $(P_D-t_D)_n$ (Morris and Freeman, 1978). The DANTE pulse sequence has been used for selective solvent suppression in ^1H NMR (Haasnoot, 1983) and the phospholipid lateral diffusion studies in ^{31}P NMR (Larsen *et al.*, 1987). Our modification is to use two 90^0 pulses with time separation of t_D and phase change π as the rotating-phase DANTE sequence (Blondet *et al.*, 1987) for a spin 1 system. The time t_D was adjusted to invert the principle peaks of the powder pattern. The principle peaks of the powder pattern represent the phospholipids in the domains whose bilayer normal is 90^0 or 32^0 with respect to the external magnetic field. The rapid initial non-exponential decay for selective inversion recovery (Figure 43) follows the transfer of magnetization across the spectrum, *i.e.*, the phospholipid molecules oriented at 90^0 or 32^0 diffuse to other orientation domains and *vice versa*. Unfortunately, no quantitative equation has been deduced to date for relating the selective inversion recovery to the lateral diffusion. The qualitative

comparison was, however, made according to the relative intensity plot (Figure 44), i.e., the rate for PC molecules to diffuse across a fixed orientation angle with respect to the magnetic field is in the order: phytol:PC-d_{31} > PC-d_{31} > phytanic acid:PC-d_{31}. The average particle sizes for three samples are: PC-d_{31} (1.1±0.6 μm) > phytanic acid:PC-d_{31} (0.8±0.5 μm) ≈ phytol:PC-d_{31} (0.8±0.7 μm). Thus, we conclude that phytanic acid slows down the diffusion of PC, whereas the effect of phytol is not clear from these experiments.

Diffusion coefficients, D_T, calculated from the simulated ^{31}P NMR spectra are $6.1X10^{-8}$, $1.6X10^{-8}$ and $4.7X10^{-9}$ cm^2s^{-1}, for DPPC, 20 mol% phytol:DPPC and 20 mol% phytanic acid:DPPC, respectively. The lineshape of ^{31}P NMR spectra is quite sensitive to the τ_e value around 10^{-4} s, the uncertainty of τ_e for simulation is about ± $0.2X10^{-4}$s. The uncertainty of D_T is estimated as ±(0.1-1)$X10^{-8}$ cm^2s^{-1}. The D_T value for DPPC (6.1 $X10^{-8}$ cm^2s^{-1}) is close to the reported one (2-5 $X10^{-8}$ cm^2s^{-1}, Cullis, 1976; Kuo and Wade, 1979). Apparently, phytol slightly slows down the diffusion of PC (D_T = $1.6X10^{-8}$ cm^2s^{-1}), while phytanic acid diminishes the D_T of DPPC by one order of magnitude.

From the last two methods, we conclude that the lateral diffusion rate of phosphatidylcholine in membranes is in the order: PC ≥ phytol:PC > phytanic acid:PC.

VII. Conclusion

The effects of the incorporation of phytol and phytanic acid have been studied on (1) phase behavior, (2) order parameter and quadrupolar splitting, (3) lateral diffusion of phosphatidylcholine, (4) relaxation times and (5) magnetic ordering of model membranes by means of ^{2}H NMR and ^{31}P NMR. ^{2}H NMR studies with an *sn*-2 chain perdeuterated PC (PC-d_{31}) and a choline methylene deuterated PC (DPPC-d_4) provide the structure and dynamical information for both hydrophobic and hydrophilic regions.

(1) **The phase behaviors** have been studied by moment analysis of ^{2}H NMR spectra and by DSC. Either branched chain compound broadens the gel to liquid crystalline phase transition of the phospholipid membranes and reduces the onset temperature of the transition. For PC-d_{31} the first moment M_1 of ^{2}H NMR spectra drops very rapidly from $1X10^{5}$ s^{-1} to $5X10^{4}$ s^{-1} at the main transition temperature over a range of approximately $1.5^{0}C$. The onset temperature for the main phase transition of PC-d_{31} is lowered from $38^{0}C$ to $34^{0}C$ and $28^{0}C$ by the incorporation of 5 mol% and 20 mol% of either branched chain compound, respectively. The M_1 transition range (T_l-T_s) increases with increasing the branched chain compound concentration: 34-$38^{0}C$ for 5 mol% incorporation and 28-$39^{0}C$ for 20 mol% incorporation, respectively. The moment analysis of

DPPC-d_4 spectra is very sensitive to the pretransition, the decrease in M_1 associated with the pretransition is much more significant (about 55% of the total) than that in PC-d_{31} (about 5%). Twenty mol% of either branched chain compound abolishes the pretransition of PC-d_{31}, however a transition at 15-20^{0}C has been observed in the M_1 curve of DPPC-d_4 in the presence of 20 mol% of either branched chain compound. The pretransition temperature of DPPC-d_4 determined from the M_1 curve (31^{0}C) is lower than that from DSC (35^{0}C), while the pretransition of PC-d_{31} detected from the M_1 curve is the same as that from DSC (30^{0}C). These observations suggest that both head group and acyl chain terminal group are involved in the pretransition, while the changes of the head group motion may not contribute to an enthalpy change which can be detected by DSC. The pretransition has also been suggested to take place as a compromise between the nonpolar hydrocarbon chains maintaining rigid structure and the polar head group achieving the laterally expanded state (Parsegian, 1983). Based upon our ^{2}H NMR results on PC-d_{31} and DPPC-d_4, we conclude that the pretransition occurs when the hydrocarbon terminal chain positions and the polar head group commence restricted motion.

The branched chain compounds broaden and lower the phase transition temperature of PC membranes; they also decrease the M_1 in the gel phase, indicating that the branched chain compounds cause significant disruption of the gel phase. The straight chain analogues of the branched chain compounds

(i.e., palmitic acid and hexadecanol) elevate the transition of DPPC (Eliasz et *al.*, 1976; Pringle and Miller, 1979). These controversial effects suggest that phytanic acid and phytol, with four methyl branching attached on the chain, force nearest neighbor hydrocarbon chains of PC apart in the gel phase, lowering the transition temperature.

(2) **Order parameters,** S_{CD}, for various chain positions have been calculated from depaked spectra. At 50°C there is no significant change in the profile of S_{CD} versus phospholipid acyl chain position, induced by either branched chain compound. Either branched chain compound (20 mol%) causes an approximate 9% increase in the mean order parameter $\langle S_{CD} \rangle$, mainly due to the increase in the plateau region (C3-C9). 20 mol% phytanic acid increases S_{CD} of C10-C14 positions by 2-5%. 20 mol% phytol increases S_{CD} of C10-C15 positions by 5-9%. The branched chain compounds have almost the same effect as palmitic acid (Pauls *et al.*, 1983), in spite of the four methyl groups on the chain.

From quadrupolar splitting of DPPC-d_4, we have learned that in the liquid crystalline phase, phytol induces more random movement of the head group while phytanic acid causes a conformational change of the choline group due to the increased negative charge at the surface of membrane.

(3) **The effect of branched chain compounds on the lateral diffusion of phospholipid in multilamellar bilayers** has been studied using a DANTE pulse sequence and a quadrupolar CPMG

pulse sequence. Phytanic acid significantly slows down the diffusion of phosphatidylcholine in the membranes. The observations are consistent with the lateral diffusion constant (D_T) values determined for DPPC unilamellar vesicles using ^{31}P NMR. The D_T values are $6.1X10^{-8}$, $1.6X10^{-8}$ and $4.7X10^{-9}$ cm^2s^{-1} for DPPC, 20 mol%phytol:DPPC and 20 mol% phytanic acid:DPPC, respectively.

(4) **Deuterium spin-lattice relaxation times** (T_1) **and spin-spin relaxation times** (T_{2e}, the decay of the quadrupolar echoes) for PC-d_{31} and DPPC-d_4 have been measured over a wide temperature range. The branched chain compounds increase the T_1 values, via depression of the phase transition temperature. Only 20 mol% phytol increases T_1 in the plateau region (C3-C9 on *sn*-2 chain) by 11% at the same reduced temperature, indicating that phytol increases the fast motion rate of the plateau segments. T_{2e} depends very much on the method of sample preparation and the morphology of the resulting liposomes. T_{2e} has a minimum at the temperature between pre- and main transition. Either branched chain compound lowers the T_{2e} minimum and the corresponding temperature in both PC-d_{31} and DPPC-d_4 membranes.

(5) **The orientation of the DPPC bilayer in the magnetic field** caused by the incorporation of 20 mol% phytanic acids is shown by both ^2H and ^{31}P NMR. The sample needs to be carried through several freeze-thaw cycles in the presence of Tris buffer in order that the phospholipid magnetic field ordering

occurs. Our results, along with those reported by others (Seelig *et al.*, 1985; Speyer *et al.*, 1987), prompt us to suggest a general method for routine preparation of oriented bilayers. Addition of sufficient lipids bearing a negative charge, together with repetitive freeze-thaw cycles, favors formation of "hollow" liposome particles, i.e., particles which tend to deform easily in a magnetic field. These oriented membranes may be valuable for further studies using ^{2}H NMR.

APPENDIX I

Calculation of the deuterated level of [$^{2}H_{31}$]palmitic acid was performed on the mass spectral analysis data.

Table AI Mass Spectral Data of [$^{2}H_{31}$]Palmitic Acid

Mass	Intensity			Number of deuterium atoms
	Experiment data	Corrected for M+2	Corrected for M+1	
283	2.2	2.2	2.2	27
284	7.3	7.3	7.3	28
285	26.3	26.3	25.3	29
286	65.4	65.3	62.6	30
287(M)	93.7	93.2	84.0	31
288(M+1)	14.4	13.2		
289(M+2)	1.7			

$$\text{Deuteration level} = \frac{2.2X27+7.3X28+25.3X29+62.6X30+84.0X31}{(2.2+7.3+25.3+62.6+84.0)X31}$$

$$= 97.4\ \%$$

LIST OF REFERENCES

Akutsu, H. (1986) *J. Magn. Reson.* **66**, 250-263.

Abragam, A. (1961) in *The Principles of Nuclear Magnetism*, pp 314-315, Clarndon press, Oxford, U.K., New York/London.

Albon, N. and Sturtevant, J.M. (1978) *Proc. Natl. Acad. Sci. USA* 75, 2258-2260.

Ames, B.N. (1966) in *Methods in Enzymology*, Vol. 8, Neufeld, E.F. and Ginsburg, V. (Eds), Academic Press, New York, pp 115-118.

Aoki, T. and Poulter, C.D. (1985) *J. Org. Chem.* **50**, 5634-5636.

Bangham, A.D. and Horne,R.W. (1964) *J. Mol. Biol.* **8**, 660-668.

Bayerl, T., Klose, G., Ruckpaul, K., Gast, K. and Möps, A. (1984) *Biochim. Biophys. Acta* **769**, 399-403.

Blicharski, J.S. (1986) *Can. J. Phys.*, **64**, 733-735.

Blondet, P., Albrand, J.P., Von Kienlin, M., Decorps, M. and Lavanchy, N. (1987) *J. Magn. Reson.* **71**, 341-346.

Bloom, M. (1987) Notes in NMR course in Department of Physics, University of British Columbia, Vancouver, Canada.

Bloom, M., Davis, J.H. and Valic, M.I. (1980) *Can. J. Phys.* **58**, 1510-1517.

Bloom, M. and Smith, I.C.P. (1985) in *Progress in Protein-Lipid Interactions*, Watts, A. and DePont, J.T.H.H.M. ed., Elsevier, New York. pp 61-88.

Bloom, M. and Sternin, E. (1987) *Biochemistry* **26**, 2101-2105.

Brown, M.F. (1979) *J. Magn. Reson.* **35**, 203-215.

Brown, M.F. and Davis, J.H. (1981) *Chem. Phys. Lett.* **79**, 431-435.

Brown, M.F., Ribeiro, A.A. and Williams, G.D. (1983) *Proc. Natl. Acad. Sci. USA* **80**, 4325-4329.

Brown, M.F. and Seelig, J. (1978) *Biochemistry* **17**, 381-384.

Brown, M.F., Seelig, J. and Haeberlen, U. (1979) *J. Chem. Phys.* 70, 5045-5053.

Burnell, E.E., Cullis, P.R. and Dekruijff, B. (1980) *Biochim. Biophys. Acta* 603, 63-69.

Burnett, D.F. and Muller, B.H. (1971) *J. Chem. Phys.* 55, 5829-5831.

Cameron, D.G., Casal, H.L. and Mantsch, H.H. (1980) *Biochemistry* 19, 3665-3672.

Cameron, D.G. and Mantsch, H.H. (1978) *Biochim. Biophys. Res. Commun.* 83, 886-892.

Campbell, R.F., Meirovitch, E. and Freed, J.H. (1979) *J. Phys. Chem.* 83, 525-533.

Chapman, D., Urbina, J. and Keough, K.M. (1974) *J. Biol. Chem.* 249, 2512-2521.

Chen, S.C. and Sturtevant, J.M. (1981) *Biochemistry* 20, 713-718.

Cullis, P.R. (1976) *FEBS Lett.* 70, 223-228.

Cushley, R.J. and Forrest, B.J. (1976) *Can. J. Chem.* 54, 2059-2067.

Cushley, R.J. and Forrest, B.J. (1977) *Can. J. Chem.* 55, 220-226.

Cushley, R.J., Forrest, B.J., Gillis, A. and Tribe, J. (1979) *Can. J. Chem.* 57, 458-465.

Cushley, R.J., Treleaven, W.D., Parmar, Y.I., Chana, R.S. and Fenske, D.B. (1987) *Biochim. Biophys. Res. Commun.* 146, 1139-1145

Davis, J.H. and Jeffrey, K.R. (1977) *Chem. Phys. Lipid* 20, 87-104.

Davis, J.H. (1979) *Biophys. J.* 27, 339-358.

Davis, J.H. (1983) *Biochem. Biophys. Acta* 737, 117-171.

Davis, J.H., Jeffrey, K.R., Bloom, M., Valic, M.I. and Higgs, T.P. (1976) *Chemical Physics Lett.* 42, 390-394.

Davis, J.H., Jeffrey, K.R. and Bloom, M. (1978) *J. Magn. Reson.* 29, 191-199.

DeBose, C.D., Burns, R.A., Jr., Donovan, J.M. and Roberts, M.F. (1985) *Biochemistry* 24, 1298-1306.

Diplock, A.T. and Lucy, J.A. (1973) *FEBS Lett.* 29, 205-210.

Diplock, A.T., Lucy, J.A., Verinder, M. and Zieleniewski, A. (1977) *FEBS Lett.* 82, 341-344.

Doniach, S. (1979) *J. Chem. Phys.* 70, 4587-4596.

Dufourc, E.J., Smith, I.C.P. and Jarrell, H.C. (1984) *Biochemistry* 23, 2300-2309.

Eibl, H. (1978) *Proc. Natl. Acad. Sci. USA* 75, 4074-4077.

Eibl, H. (1980) *Chem. Phys. Lipids* 26, 239-247.

Eibl, H. and Nicksch, A. (1978a) *Chem. Phys. Lipids* 22, 1-8.

Eliasz, A.W., Chapman, D. and Ewing, D.F. (1976) *Biochim. Biophys. Acta* 448, 220-230.

Erin, A.N., Spirin, M.M., Tabidze, L.V. and Kagan, V.E. (1984) *Biochim. Biophys. Acta* 774, 96-102.

Farrar, T.C. and Becker, E.D. (1971) in *Pulse and Fourier Transform NMR*, Academic press, pp 8.

Freed, J.H., Bruno,G.V. and Polnaszek, C,F. (1971) *J. Phys. Chem.* 75, 3385-3399.

Gaber, B.P., Yager P. and Peticolas W.L. (1978) *Biophys. J.* 21, 161-176.

Gaines, G.L. (1966) in *Insoluble Monolayers at Liquid-gas Interfaces*, Prigogine, I. ed., Wiley-Interscience, New York, p239.

Gally, H-U., Niederberger, W. and Seelig, J. (1975) *Biochemistry* 14, 3647-3652.

Grover, A.K. and Cushley, R.J. (1979) *J. Label. Comp. Radiopharm.* 16, 307-313.

Gutknecht, J. (1987) *Biochim. Biophys. Acta* 898, 97-108.

Gutknecht, J. (1988) *J. Membrane Biol.* 106, 83-93.

Haasnoot, C.A.G. (1983) *J. Magn. Reson.* 52, 153-158.

Harris, R.K. (1983) in *Nuclear Magnetic Resonance*

Spectroscopy, Pitman press, Great Britain.

Harrison, R. and Lunt, G.G. (1980) in *Biological Membranes: Their Structure and Function*, Blackie, Glasbow.

Hoult, D.I. and Richards, R.E. (1975) *Proc. Roy. Soc.* **344**, 311-340.

Hsiao, C.Y.Y., Ottaway, C.H. and Wetlaufer, D.B. (1974) *Lipids* **9**, 913-915.

Huang, T.H., Skarjune, R.P., Wittebort, R.J., Griffin, R.G. and Oldfield, E. (1980) *J. Am. Chem. Soc.* **102**, 7379-7381.

Jacobs, R.E. and Oldfield, E. (1981) *Prog. Nucl. Magn. Spectrosc.*, **14**, 113-136.

Jacobsen, J.P. and Schaumberg, K. (1976) *J. Magn. Reson.* **24**, 173-180

Janiak,M.J., Small, D.M. and Shipley, G.G. (1976) *Biochemistry* **15**, 4575-4580.

Jeffrey, K.R. (1981) *Bull. Magn. Reson.* **3**, 69-82.

Kahlke, W. (1964) *Klin. Wochenschr.* **42**, 1001-1005.

Kaneda, T. (1977) *Microbiol. Rev.* **41**, 391-418.

Klausner, R.D., Kleinfeld, A.M., Hoover, R.L. and Karnovsky, M.J. (1980) *J. Biol. Chem.* **255**, 1286-1295.

Kuo, A.-L. and Wade, C.G. (1979) *Biochemistry* **18**, 2300-2308.

Ladbrooke, B.D. and Chapman, D. (1969) *Chem. Phys. Lipids* **3**, 304-367.

Larsen, D.W., Boylan, J.G. and Cole, B.R. (1987) *J. Phys. Chem.* **91**, 5631-5634.

Lentz, B.R., Freire, E. and Biltonen, R.L. (1978) *Biochemistry* **17**, 4475-4480.

Lewis, R.N.A.H., Mark, N. and McElhaney, R.N. (1987) *Biochemistry* **26**, 6118-6126.

Lewis, R.N.A.H., Sykes, B.D. and McElhaney, R.N. (1987a) *Biochemistry* **26**, 4036-4044.

Mabrey, S. and Sturtevant, J.M. (1978) in *Methods in Membrane*

Biology, Vol. 9, Korn, E.D. (Ed.), Plenum Press, New York, pp 237-274.

MacBrinn, M.C. and O'Brien, J.S. (1968) *J. Lipid Res.* 9, 552-560.

Maggio, B. and Diplock, A.T. and Lucy, J.A. (1977) *Biochem. J.* 161, 111-121.

Mayer, L.D., Hope, M.J., Cullis, P.R. and Janoff, A.S. (1985) *Biochim. Biophys. Acta* 817, 193-196.

McElhaney, R.N. (1982) *Chem. Phys. Lipids* 30, 229-259.

McElhaney, R.N. (1986) *Biochem. Biophys. Acta* 864, 361-421.

Meier, P., Ohmes, E., Kothe, G., Blume, A., Weidner, J. and Eibl, H. (1983) *J. Phys. Chem.* 87, 4904-4912.

Morris, G.A. and Freeman, R. (1978) *J. Magn. Reson.* 29, 433-462.

Nuhn P., Brezesinski, G., Dobner, B., Förster, G., Gulheil, M. and Dörfler, H. (1986) *Chem. Phys. Lipids* 39, 221-236.

Ortiz, A., Aranda, F.J. and Cómez-Fernandez, J.C. (1987) *Biochim. Biophys. Acta* 898, 214-222.

Parsegian, V.A. (1983) *Biophys. J.* 44, 413-415.

Pauls, K.P., MacKay, A.L. and Bloom, M. (1983) *Biochemistry* 22, 6101-6109.

Pauls, K.P., MacKay, A.L., Söderman, O., Bloom, M., Tanjea, A.K. and Hodges, R.S. (1985) *Eur. Biophys. J.* 12, 1-11.

Phillips, M.C., Williams, R.M. and Chapman, D. (1969) *Chem. Phys. Lipids* 3, 234-244.

Ponpipom, M.M. and Bugianesi, R.L. (1980) *J. Lipid Res.* 21, 136-139.

Pownall, H.J., Pao, Q., Brockman, H.L. and Massey, J.B. (1987) *J. Biol. Chem.* 262, 9033-9036.

Pringle, M.J. and Miller, K.W. (1979) *Biochemistry* 48, 3314-3320.

Rance, M. and Byrd, R. A. (1983) *J. Magn. Reson.* 52, 221-240.

Roux, M., Neuman, J.M., Hodges, R.S., Devaux, P.F. and Bloom,

M. (1989) *Biochemistry* 28, 2213-2221.

Ruocco, M.J. and Shipley, G.G. (1982) *Biochim. Biophys. Acta* 691, 309-320.

Scherer, P.G. and Seelig, J. (1987) *EMBO J.* 6, 2915-2922.

Scott, M.L. (1978) in *The Fat-Soluble Vitamins*, Deluca, H.F. ed., Plenum press, New York, pp 133-210.

Sebrell, W.H. Jr. and Harris, R.S. ed. in *The Vitamins*, 2nd ed., Academic Press, New York, 1972, Vol.5 ch.16, pp 166-317.

Seelig, J. (1977) *Q. Rev. Biophys.* 10, 353-418.

Seelig, J. (1976) in *Spin Labelling: Theory and Application*, Berliner, L.J. ed., Academic press, New York, pp 373-409.

Seelig, J., Borle, F. and Cross, T.A. (1985) *Biochim. Biophys. Acta* 814, 195-198.

Seelig, J. and Browning, M.L. (1978) *FEBS Lett.* 92, 41-44.

Seelig, J., Macdonald, P.M. and Scherer, P.G. (1987) *Biochemistry* 26, 7535-7541.

Seelig, J. and Seelig, A. (1980) *Q. Rev. Biophys.* 13, 19-61.

Sheetz, M.P. and Chan, S.I. (1972) *Biochemsitry* 11, 4573-4581.

Silvius, J.R., Lyons, M., Yeagle, P.L. and O'Leary, T.J. (1985) *Biochemistry* 24, 5388-5395.

Sixl, F. and Watts, A. (1982) *Biochemistry* 21, 6446-6452.

Sixl, F. and Watts, A. (1983) *Proc. Natl. Acad. Sci. USA* 80, 1613-1615.

Slichter, C.P. (1978) in *Principles of Magnetic Resonance*, 2nd ed, Cardona, M., Fulde, P. and Queisser, H.-J. ed., Springer-Verlag Berlin Heidelberg, New York, pp 285-288, 150-158.

Small, D.M., Cabral, D.J., Cistola, D.P., Parks, J.S. and Hamilton, J.A. (1984) *Hepatology* 4, 77S-79S.

Smith, I.C.P. and Ekiel, I.H. (1984) in *Phosphorus-31 NMR, Principle and Applications*, Gorenstein, D.G. ed., Academic, New York, pp 447-475.

Speyer, J.B., Sripada, P.K., Das Gupta, S.K. and Shipley, G.G.

(1987) *Biophys. J.* 51, 687-691.

Spiess, H.W. and Sillescu, H. (1981) *J. Magn. Reson.* 42, 381-389.

Srivastava, S., Phadke, R.S., Govil, G. and Rao, C.N.R. (1983) *Biochim. Biophys. Acta* 734, 353-362.

Sternin, E., Bloom, M. and MacKay, A.L. (1983) *J. Magn. Reson.* 55, 274-282.

Sternin, E. (1982) Depaking of NMR Spectra, M.Sc thesis, University of British Columbia, Vancouver, B.C.

Sternin, E. (1988) Ph.D thesis, Department of Physics, University of British Columbia, Vancouver, B.C. pp 34-42.

Stillwell, W. and Bryant, L. (1983) *Biochim. Biophys. Acta* 731, 483-486.

Stumpel, T., Eibl, H. and Nicksch, A. (1983) *Biochim. Biophys. Acta* 727, 246-254.

Steinberg, D., Herndon, J.H. Jr., Uhlendorf, B.W., Mize, C.E. and Milne, G.W.A. (1967) *Science* 156, 1740-1742.

Tappel, A.L. (1962) *Vitam. Horm.* 20, 493-510.

Taylor, M.G. and Smith, I.C.P. (1983) *Biochim. Biophys. Acta* 733, 256-263.

Thewalt, J.L. and Cushley, R.J. (1987) *Biochim. Biophys. Acta* 905, 329-338.

Thewalt, J.L., Wassall, S.R., Gorrissen, H. and Cushley, R.J. (1985) *Biochim. Biophys. Acta* 817, 355-365.

Tscharner, V.V. and Radda, G.K. (1981) *Biochim. Biophys. Acta* 643, 435-448.

Tsui, F.C., Ojcues, D.M. and Hubbell, W.L. (1986) *Biophys. J.* 49, 459-468.

Urano, S., Iida, M., Otani, I. and Matsuo, M. (1987) *Biochem. Biophys. Res. Comm.* 146, 1413-1418.

van Boeckel, C.A.A., Westerduin, P. and van Boom, J.H. (1984) *Carbohydrate Research* 133, 219-234.

Vega, S. and Pines, A. (1977) *J. Chem. Phys.* 66, 5624-5644.

Vold, R.R. and Vold, R.L. (1977) *J. Chem. Phys.* **66**, 4018-4024.

Volke, F. (1984) *Chem. Phys. Lett.* **112**, 551-554.

Wassall, S.R., Thewalt, J.L., Wong, L., Gorrissen, H. and Cushley, R.J. (1986) *Biochemistry* **25**, 319-326.

Weber, F., Gloor, U. and Miss, O. (1958) *Helv. Chim. Acta* **41**, 1038-1046.

Westerman, P.W., Vaz, M.J., Strenk, L.M. and Doane, J.W. (1982) *Proc. Natl. Acad. Sci. USA* **79**, 2890-2894.

Wittebort, R.J., Schmidt, C.F. and Griffin, R.G. (1981) *Biochemistry* **20**, 4223-4228.

Yellin, N. and Levin I.W. (1977) *Biochim, Biophys. Acta* **489**, 177-190.